

TOGNASOLI, ANA PAULA CARVALHO, Ph.D. Epstein-Barr Virus as a Piece of the Neurodegenerative Disease Mosaic. (2022).
Directed by Dr. Amy Adamson. 111 pp.

Neurodegenerative diseases (ND's) affect approximately 6 million people in the US, and their incidence and severity is linked to genetic and environmental factors. Human herpesviruses such as Epstein-Barr virus (EBV), were recently implicated as potential infectious agents in the etiology of ND's. Over 90% of the world's population has EBV, which initially infects epithelial cells in the nasopharynx to then enter latency in B cells. EBV is a neurotropic virus and can infect astrocytes, neurons, and microglia. In addition, infected B and T cells travel through CNS access areas such as the Glymphatic System and the nasopharynx, where EBV could affect neuronal cell function. Processes such as autophagy, inflammation, and Reactive Oxygen Species (ROS) homeostasis are crucial to ND's and have already been shown to be affected by EBV. While severe neuronal consequences are rare during EBV infection, little is known about its ability to promote neuronal dysfunction that could prime neuronal cells for ND development. We hypothesized that EBV had the potential to affect neuronal cellular processes that are relevant for the development and establishment of ND's. To study these interactions in a practical, more easily accessible cell model than primary neuronal cells, we used retinoic-acid (RA) differentiated SH-SY5Y neuroblastoma cells, which have been widely accepted as a suitable cell line for ND studies. We exposed these cells to EBV virions and demonstrated the presence of intracellular viral genome via qPCR. Thus, we are the first ones to show that RA-differentiated SH-SY5Y neuroblastoma cells are permissive to EBV infection. Interestingly, while we did not detect lytic or latent viral transcripts in these cells, our data suggests that EBV-infected neuroblastoma cells have altered ROS homeostasis and decreased mitochondrial function, increased expression of inflammatory markers and autophagic flux block. Overall, we have established that EBV infection of neuronal cells has the potential to affect the neurodegenerative trifecta: ROS, autophagy, and inflammation. Future studies should focus on

a more in-depth exploration of each of these processes under EBV infection to elucidate if the virus can act as a piece of the neurodegenerative mosaic.

EPSTEIN-BARR VIRUS AS A PIECE OF THE NEURODEGENERATIVE DISEASE MOSAIC

by

Ana Paula Carvalho Tognasoli

A Dissertation

Submitted to

the Faculty of The Graduate School at
The University of North Carolina at Greensboro

in Partial Fulfillment

of the Requirements for the Degree

Doctor of Philosophy

Greensboro

2022

Approved by

Dr. Amy Adamson
Committee Chair

© 2022 Ana Paula Carvalho Tognasoli

DEDICATION

I dedicate this work to the love and support of many. To my dear husband and best friend Bryan, and to my incredible children, Jonas, and Cecilia. They were the light that guided me on the path to reaching my dreams. To my grandmother, Emery Vieira de Carvalho, who only made it up to fourth grade...look at me now! To my amazingly strong mother, Maritza, who allowed me to be my stubborn self, to believe in all things magical and raised me to take on the world. To my loving aunts Rosemary, Shirley, Denise, and Regina. Their strong and wildly different personalities built my character and taught me so much about life. You are all a part of me.

APPROVAL PAGE

This dissertation written by Ana Paula Carvalho Tognasoli has been approved by the following committee of the Faculty of The Graduate School at The University of North Carolina at Greensboro.

Committee Chair

Dr. Amy Adamson

Committee Members

Dr. Paul Steimle

Dr. Zhenquan Jia

Dr. Marta Lipinski

Date of Acceptance by Committee

Date of Final Oral Examination

ACKNOWLEDGEMENTS

I would like to thank the Biology department at UNCG for funding my research.

TABLE OF CONTENTS

LIST OF TABLES.....	viii
LIST OF FIGURES	ix
CHAPTER I: INTRODUCTION.....	1
Epstein-Barr Virus	1
EBV as a neurotropic virus	4
EBV and neurodegenerative diseases.....	6
EBV and Reactive Oxygen Species.....	10
EBV and Autophagy	12
EBV and Inflammation.....	15
CHAPTER II: EPSTEIN-BARR VIRUS INFECTS RETINOIC-ACID DIFFERENTIATED NEUROBLASTOMA CELLS	17
Introduction.....	17
Materials and Methods	20
Cell culture and Differentiation	20
Virus Production, Collection, and Infectivity Assay.....	21
Viral induction/lytic reactivation of infected SH-SY5Y cells.....	22
RNA Collection	22
DNA Collection	23
RGD peptide viral entry assay	24
RT-PCR.....	24
qRT-PCR.....	26
qPCR.....	26
SDS-PAGE Gel Electrophoresis and Western Blotting.....	27
Results	30
Retinoic Acid-differentiated SH-SY5Y neuroblastoma cells are susceptible to EBV infection.	30
RA-differentiated SH-SY5Y cells exhibit GFP signal indicative of lytic EBV infection up to day 2 post- infection.....	33
EBV infection does not alter AKT activation in differentiated SH-SY5Y neuroblastoma cells but appears to promote higher expression of D2DR.....	35
RGD binding motifs are involved in EBV attachment/entry into differentiated SH-SY5Y.....	37

cells.....	37
EBV does not appear to establish known transcriptional programs in RA-differentiated neuroblastoma cells.....	39
EBV infection decreases phosphorylation of p38 and increases that of ERK and STAT3 ..	41
Discussion.....	43
CHAPTER III: EBV INFECTION CAUSES AUTOPHAGIC FLUX BLOCK, CHANGES IN REACTIVE OXYGEN SPECIES HOMEOSTASIS AND INCREASE OF INFLAMMATORY MARKERS IN RETINOIC ACID-DIFFERENTIATED SH-SY5Y NEUROBLASTOMA CELLS....	49
Introduction.....	49
Methods	55
Cell culture and Differentiation	55
Virus Production, Collection, and Infectivity Assay.....	56
RNA Collection	56
DNA Collection	57
qRT-PCR.....	58
Mitochondrial superoxide assay.....	59
Mitochondrial Membrane Potential.....	60
qPCR.....	60
SDS-PAGE Gel Electrophoresis and Western Blotting.....	61
Autophagy flux assay.....	62
Slide Coating with Poly-L-Lysine.....	62
Results	63
RA-differentiated SH-SY5Y cells do not have increased mitochondrial superoxide levels after EBV infection	63
Mitochondrial activity of EBV-infected RA-differentiated cells is significantly lower than that of mock-infected cells	66
RA-differentiated cells infected with EBV show a trend of NF- κ B translocation to the nucleus	69
Inflammatory marker expression increases upon EBV infection of RA-differentiated SH-SY5Y cells	70
Autophagy flux is blocked in EBV-infected cells.....	74
Discussion.....	76
CHAPTER IV: DISCUSSION	82
REFERENCES	93

LIST OF TABLES

Table 2-1. Primer Sequences.....	25
Table 2-2. Antibodies	28
Table 2-3. RA-differentiated SH-SY5Y cells are susceptible to EBV infection but not permissive to viral replication	40
Table 3-1 - Primer Sequences	58
Table 3-2 -Antibodies.....	62

LIST OF FIGURES

Figure 1-1. Epstein-Barr Virus Virion.....	1
Figure 1-2. EBV's Possible Entry Routes into the CNS	6
Figure 1-3. Reactive Oxygen Species Production and Clearance	11
Figure 1-4. The Autophagic Process	13
Figure 2-1. Differentiated SH-SY5Y cells have distinct morphology and increased neuronal marker expression	31
Figure 2-2. Infectious activity of a representative virus preparation collected from EBfaV-GFP cells verified via flow cytometry	32
Figure 2-3. EBV-infected RA-differentiated cells exhibit GFP signal up to day 2 post infection..	34
Figure 2-4. AKT phosphorylation is not altered, but D2DR levels are increased in EBV-infected cells	36
Figure 2-5. EBV infection of RA-differentiated SH-SY5Y cells relies on RGD binding motifs.....	38
Figure 2-6. EBV infection can induce changes in the activation of STAT3, ERK and p38 in the absence of detectable viral transcripts	42
Figure 3-1. Graphical Abstract	49
Figure 3-2. EBV exposed cells do not have increased mitochondrial superoxide levels but have increased expression of antioxidant enzymes SOD1 and SOD2.....	65
Figure 3-3. EBV-infected cells have lower mitochondrial membrane potential than mock-infected cells	67

Figure 3-4. NF- κ B could be activated during EBV infection of RA-differentiated SH-SY5Y neuroblastoma cells70

Figure 3-5. EBV-infected neuroblastoma cells have higher expression of AIM2, NLRP3 and IL-1 β 72

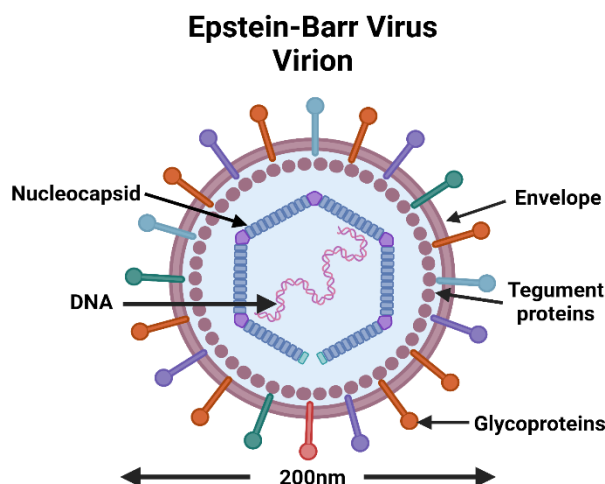
Figure 3-6. RA-differentiated SH-SY5Y cells infected with EBV have obstructed autophagic flux compared to mock-infected cells75

CHAPTER I: INTRODUCTION

Epstein-Barr Virus

Epstein-Barr virus (EBV) is a dsDNA virus that belongs to the order *Herpesvirales*, the family *Herpesviridae*, the *Gammaherpesvirinae* subfamily, and the genus *Lymphocryptovirus*. EBV virions (individual virus particles) are around 200nm in diameter with a glycoprotein-studded envelope used by the virus to enter human host cells (Figure 1-1). Inside the envelope, tegument proteins surround an icosahedral nucleocapsid, which holds the 172Kb genome (*Fields Virology | R2 Digital Library*, n.d.-a).

Figure 1-1. Epstein-Barr Virus Virion



There are 2 types of EBV based upon which variant of EBNA-2 (Epstein-Barr Nuclear Antigen 2) the strain carries, with type 1 being the most common form found in industrialized countries. EBV-2 is prevalent in equatorial regions such as Uganda, the place where Dr. Burkitt first studied the lymphoma that would later take his name (Burkitt's lymphoma). Lymphoma samples from his research sent to Michael Epstein and Yvonne Barr in England enabled the discovery of EBV as the first human oncovirus over 50 years ago (Epstein, 2015).

EBV is well known for infecting epithelial cells of the nasopharynx and B cells, and as the causative agent of Infectious Mononucleosis (IM), which is characterized by fever, pharyngitis, and lymphadenopathy (enlargement of lymph nodes) (*Fields Virology | R2 Digital Library*, n.d.-a). The manifestation of IM symptoms usually occurs in adolescents and adults around week 5 of viral infection, when germinal centers are filled with infected B cells and the adaptive immune system creates havoc in the body trying to clear the virus. In general, however, the disease is believed to be acquired early in life, but it is asymptomatic, evading the immune system completely thus very little is known about the initial infection (Thorley-Lawson, 2015).

EBV uses the viral fusion complex gB - gH/gL to infect epithelial cells of the nasopharynx, particularly the lymphoid tissue lining the area that comprises the adenoids and tonsils named the Waldeyer's Ring (Epstein, 2015; *Fields Virology | R2 Digital Library*, n.d.-a; Thorley-Lawson, 2015). Epithelial cell infection with EBV is accomplished via the viral protein BMRF2 interaction with host's cell surface receptors. $\beta 1$, $\beta 8$ and $\alpha 5$ integrins have been implicated in viral entry and fusion at the plasma membrane, but their interaction with gB and gH/gL has not been established as the sole pathway for initiation of infection (Chesnokova et al., 2009). EBV-infected epithelial cells covering the Waldeyer's ring (which can be as thin as single cell layer) are able to produce viral progeny that when shed, can enter the underlying lymphatic tissue and infect naïve B cells. This infection begins by the interaction of the B cell surface receptor CD21 with the viral proteins gp350/220, allowing the virus to attach to the host's cell surface, facilitating its endocytosis. Lytic plasma cells present in the tissue surrounding the lymphatic follicle can also shed virus and infect incoming naïve B cells. Once the virus is inside the cell, release of the viral genome into the cytoplasm will occur after fusion of viral and endosomal membranes, which is mediated by interactions between viral proteins

(gB, gp42 and gH/gL) and MHC class II (major histocompatibility complex) receptors on B cells (Chesnokova et al., 2015; *Fields Virology | R2 Digital Library*, n.d.-a; Thorley-Lawson, 2015).

In a demonstration of formidable viral exploitation of normal B cell biology, EBV then uses viral proteins LMP1 and LMP2 (Latent Membrane Protein 1 and 2) to mimic signals that would normally be sent by T helper cells and would require B cell receptor involvement. These cues are for cell survival and differentiation, and they will allow these infected B cells to move through lymphatic germinal centers, proceeding with normal events for B cell development, culminating with the creation of infected Plasma cells. Finally, these cells become resting B memory cells, holding the viral genome in episome form (circular DNA), tethered to the cell's own genome via the viral protein EBNA1 (Epstein-Barr Nuclear Antigen 1). This stage is considered as one of EBV's latency programs (Thorley-Lawson, 2015).

EBV infection can result in different fates for the infected cells, which can be immediately driven to the dormant or latent stage and can undergo lytic reactivation later in the host's life. Additionally, cells can undergo cell transformation (tumorigenesis), or enter the lytic cycle when virions are produced and can infect other cells, leading them to death by necrosis and apoptosis (Jha et al., 2016). EBV's lytic phase is a temporal cascade of events that begin with the immediate-early phase when the viral gene products BZLF1 (Z) and BRLF1 (R) are simultaneously produced. Z can activate its own transcription and both Z and R bind to EBV promoters to initiate the early phase of transcription. The early replication phase proteins produced are responsible for assisting in the viral DNA replication and triggering the late phase of the lytic cascade, when viral structural proteins are produced, and the assembly of viral progeny is completed (Young et al., 2007).

There are 4 types of latency for EBV (0, I, II, III) characterized by disease association and type of cell infected. These were based on epithelial, B, T and NK cell infection patterns, which are not the only cell types infected by EBV, but are the most well studied (Dugan et al.,

2019). Non-dividing memory B cells are associated with type 0 latency, in which viral transcripts are not produced, yet there is persistence of the viral genome. Latency I is characterized by the expression of EBNA1, and this latency type is associated with Burkitt's Lymphoma and gastric carcinoma. The expression of EBNA1, LMP2A and B, and LMP1 often occur in association with Nasopharyngeal carcinoma, Natural Killer and T-cell lymphoma as well as Hodgkin's lymphoma and are part of type II latency. The latency III program expresses the most viral proteins of all latency programs, and it is associated with immune suppressed patients, such as those with post-transplant lymphoproliferative diseases or AIDS (Dugan et al., 2019).

EBV is widely known as a cancer-causing virus. All cases of undifferentiated Nasopharyngeal carcinoma are EBV positive. Several immunodeficiencies such as X-Linked Lymphoproliferative Disease 1 (XLP1) and XLP2, 10% of gastric carcinomas, 30-40% of Hodgkin's lymphomas, and over 90% of endemic Burkitt's lymphomas in Africa are also associated with EBV (Cohen, 2015; Dugan et al., 2019; Raab-Traub, 2015). Most recently, EBV has been associated with neurological diseases such as Multiple Sclerosis and Alzheimer's disease, but most interactions between EBV and the CNS have yet to be investigated (Hassani et al., 2018; Shim et al., 2017).

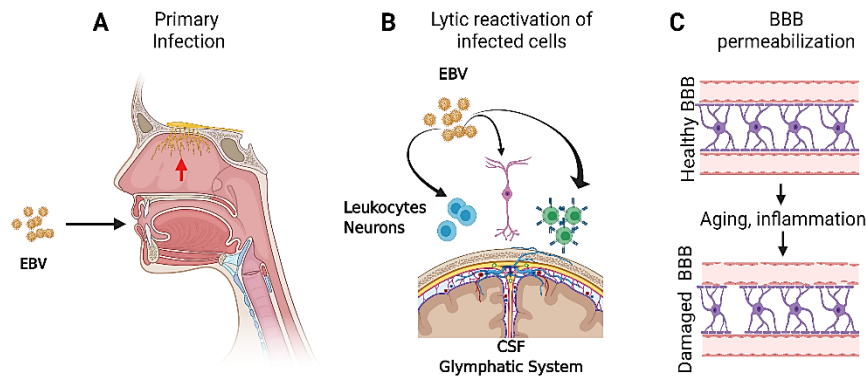
EBV as a neurotropic virus

EBV is an important neurotropic virus (can infect neural tissue), but much research is still needed to fully comprehend its interactions with the nervous system. EBV has been shown to infect a variety of neuronal cells, including astrocytes, endothelial cells, microglia, neurons and undifferentiated neuroblastoma cells (Casiraghi et al., 2011; Hassani et al., 2018; Jha et al., 2015; Menet et al., 1999). EBV infection can lead to encephalitis, meningitis, acute disseminated encephalomyelitis, and in rare cases it has been shown to be involved in Guillain-Barre syndrome and reversible Parkinsonism (Dimova et al., 2006; Guan et al., 2012; S. Y. Kim et al., 2016; Roselli et al., 2006; Soldan & Lieberman, 2020).

EBV has multiple possible routes to enter or modulate the nervous system (Figure 1-2). For example, the olfactory epithelium in the nasal cavity encompasses bipolar olfactory receptor neurons (ORNs) with dendrites that have ciliary projections containing odor molecule receptors, and axons extending through the lamina propria that eventually join to form the olfactory nerve with direct contact to the CNS. These neuronal projections provide a pathway to the CNS, and viral entry through this route via anterograde transport by the axons to the brain has been established for multiple viruses, including Human Herpesvirus I, Murine Cytomegalovirus, Murine Herpesvirus 4 (a gamma herpesvirus) and Influenza A (Durrant et al., 2016a; H. E. Farrell et al., 2016; P. J. Farrell, 2015; Jha et al., 2015; Koyuncu et al., 2013; Menet et al., 1999; Riel et al., 2015).

Besides B cells, T-cells, monocytes and macrophages can be infected by EBV *in vitro* and *in vivo* and contain EBV DNA while circulating in asymptomatic EBV carriers (Coleman et al., 2014; Hassani et al., 2018; Tugizov et al., 2007). EBV-infected leukocytes in the blood have access to cerebrospinal fluid (CSF) and the waste clearing system of vessels that travels through the CNS (Glymphatic System), where virion and pro-inflammatory cytokine release could prime an aging neuroimmune axis for further injury (Erickson & Banks, 2019; Gate, Saligrama, Leventhal, Yang, Unger, Middeldorp, Chen, Lehallier, Channappa, De Los Santos, et al., 2020; Louveau et al., 2015, 2018). Furthermore, the natural aging process itself disturbs the efficacy of the Blood Brain Barrier (BBB) and can compromise its structure by creating areas of permeability allowing for pathogen entry. Cytokines and chemokines such as TNF- α freely cross the BBB and can be produced in response to viruses to further disrupt the brain's immune privilege (Barral & Croibier, 2009; Erickson & Banks, 2019; Riel et al., 2015).

Figure 1-2. EBV's Possible Entry Routes into the CNS



A. EBV has access to the CNS via primary infection of nasopharyngeal epithelial cells that shed virions into the nasopharynx cavity where the exposed olfactory nerve (**A**, red arrow) provides a direct route to the brain. **B.** Lytic reactivation of lymphocytes and other EBV permissive cells that travel through the Glymphatic system can expose several types of neuronal cells to EBV infection. **C.** The low levels of inflammation brought on by natural aging processes can disrupt the BBB.

EBV and neurodegenerative diseases

In recent years, literature has supported the importance of the human microbiome, which includes the human virome, to overall human health. Viruses are capable of influencing immune processes and their interactions with genetic backgrounds and the environment could modulate disease development (Cadwell, 2015; Delwart, 2013). In this context, viruses that establish lifelong infections (such as EBV does) are given a long-term opportunity to affect host health. Through random lytic reactivation events, infected B cells (albeit in small quantities) can directly traffic into the brain during immune surveillance bringing virus in close contact with neurons. Microvasculature endothelial cells under direct EBV infection or exposure to pro-inflammatory molecules of other infected cells can add to a neurotoxic environment. EBV's mimicry of host peptides can cause autoreactive T and B cells to damage neurons (Soldan & Lieberman, 2020).

EBV and Alzheimer's Disease

Alzheimer's Disease (AD) is the most common form of dementia and is the sixth leading cause of death in the United States (Kramarow & Tejada-Vera, 2019). Dementia is defined as an acquired, progressive cognitive impairment that can impact quality of life, leading to disabilities and possible death (Lane et al., 2018). AD patients have memory loss, and later in the disease may exhibit behavioral changes, loss of mobility, hallucinations, and seizures. Death from this disease occurs an average of 8.5 years after initial presentation. It is estimated that 44 million people worldwide suffer from AD, and this figure is expected to triple by the year 2050 (Lane et al., 2018).

Most cases of AD are sporadic, as opposed to purely genetic, and are thought to arise due to an interplay between genetic and environmental factors. At the cellular level, the hallmarks of AD present as amyloid plaques and neurofibrillary tangles. Amyloid plaques are composed of abnormally folded beta-amyloid (A β), while neurofibrillary tangles (NFTs) are made up of hyperphosphorylated tau protein. The pathogenic accumulation of these proteins results in neurodegeneration, neuroinflammation, and eventual loss of the associated neurons and synapses. Complexity increases when mixed pathologies occur, such as the presence of Lewy bodies (LB's), which are aggregations of the protein alpha-synuclein and are a result of faulty autophagic processes among others (Lane et al., 2018).

NFTs and A β are the notable hallmarks of AD, but they are also present in chronic viral infections (Sochocka et al., 2017). Researchers found that A β is produced in response to HSV-1 infection and may act in an anti-viral capacity against HSV-1 and Influenza A infection (Bourgade et al., 2016; White et al., 2014). Recent studies also report increased immune response to EBV antigens in patients with AD in tandem with cognitive decline, in further support of herpesvirus involvement in AD (Shim et al., 2017). EBV has a lifetime of access to the CNS and the tools to promote NFTs and A β . EBV-infected lymphocytes can act as "Trojan

horses” in the Glymphatic system, releasing viral products or virus to induce cytokine release and permeability changes in the BBB (Singh et al., 2021; Soldan & Lieberman, 2020). This process can be facilitated in aging via the low, yet constant inflammatory state known as “inflammaging” to further disrupt the protective barrier in the CNS (Stephenson et al., 2018). EBV readily takes advantage of immunosenescence and low immune surveillance, case in point are EBV’s involvement in Posttransplant lymphoproliferative (Martinez, 2010). Lastly, CNS viral infection (caused by EBV reactivation in lymphocytes, for example) followed by proper immune response and viral clearance can be asymptomatic but not inconsequential. Each such episode can prompt localized changes in BBB permeability and adhesion molecule expression to further enable neuroinflammation. Under this scenario, EBV’s ability to manipulate autophagy can lead to A β accumulation via similar mechanisms as described for HSV-1 (Cirone, 2018; Harris & Harris, 2015).

EBV and Parkinson’s Disease

Parkinson’s disease (PD) affects over 1 million people in the United States with at least 60,000 people expected to be diagnosed every year, and most of them are likely to be men (Bhandari, 2017; *Statistics*, 2017). The disease can have an early onset at 20 years of age, but most cases are diagnosed around 60 years of age (*Statistics*, 2017). The disease is characterized by loss of dopaminergic neurons in the Substantia nigra, and the presence of LB’s, which possess a heterogenous composition that includes phosphorylated Tau, Amyloid β and Alpha-synuclein (Asyn) proteins (Maiti et al., 2017). Diagnosis is usually possible after the onset of motor symptoms, such as rigidity and involuntary movement, when most of neuronal death has already occurred. PD can be Familial (genetic), but most cases are Sporadic and are believed to be induced by an environmental agent, in individuals with some genetic predisposition for the disease (Langston, n.d.).

A possible mechanism of pathology progression for PD was suggested by Braak et al., wherein an environmental pathogen such as a virus could enter neurons in the nasal passages and the gut. This would trigger changes in neurons of the peripheral nervous system (PNS), commencing a pre-clinical PD stage, with subsequent slow dispersion of pathology to the CNS (Rietdijk et al., 2017). Development of the disease in this case could be mediated by the interplay between a genetic predisposition and a ubiquitous environmental agent, such as EBV (Braak et al., 2003). EBV has been associated with 10% of gastric carcinomas and nasopharyngeal carcinomas, making it a good candidate for the PD initiation scenario proposed by Braak, as the virus has a long residence time in the gut and nasopharyngeal tract (Iizasa et al., 2012; Rietdijk et al., 2017). Cross-reactivity between endogenous host antibodies for EBV's viral protein LMP1 and Asyn is known as a potential pathway for oligomerization of the protein (Lan et al., 2017; J. Woulfe et al., 2016).

EBV and Multiple Sclerosis

Multiple Sclerosis (MS) is a demyelinating chronic inflammatory disease affecting the CNS. MS leads to progressive and severe disability especially in young people, and over 2.5 million people have the disease worldwide (Casiraghi et al., 2011; Hassani et al., 2018). Women are disproportionately affected by the disease, which is characterized by plaque formations, injury and disruption of the BBB, in addition to the activation of autoreactive T-cells. Similar to the other neurodegenerative diseases listed previously, MS is thought to be the result of a mosaic of factors that include genetic predisposition and environmental agents (such as viruses) that can lead to inflammation (Casiraghi et al., 2011).

EBV has been proposed as an environmental risk factor for the disease. Individuals that have had Infectious Mononucleosis (caused by EBV) are 20 times more likely to develop MS, and EBV has been shown to be present in the autopsied brains of MS patients (Hassani et al., 2018). Animal models of EBV infection have demonstrated that EBV can enter the CNS and this

was associated with cellular aggregates composed of cells such as macrophages, B and T lymphocytes and reactive astrocytes in the CNS, suggesting the formation of an inflammatory environment post-infection (Hassani et al., 2021). Literature also reports that brain endothelial cells infected with EBV have upregulated expression of inflammatory markers, which are crucial for the development of all neurodegenerative diseases (Casiraghi et al., 2011).

Most recently, a study conducted on military personnel (10 million subjects) over the course of 20 years detailed those individuals that had EBV, but not other viruses, were actually 35 times more likely to develop MS. Additionally, only after EBV antibodies were produced by infected individuals (seroconversion) there were increases in the levels of a biomarker for axonal degeneration (Bjornevik et al., 2022). These findings have solidified EBV as the prime infectious agent involved in MS pathogenesis.

In summary, the ability of Herpesviruses to remain in the body indefinitely seems to predispose their hosts to disease later in life. As EBV can sporadically reactivate in many cells it infects in addition to B cells, which have access to nearly the entire body, EBV has the potential to affect many types of tissues, including the CNS. While not everyone that has EBV will develop disease later on, neuroimmune toxicity from EBV reactivation events could predispose individuals by initiating early changes in neuronal cells, or by driving the disease altogether as it seems to be the case with MS (Bjornevik et al., 2022; *Fields Virology* | R2 Digital Library, n.d.-a; Ringheim & Conant, 2004).

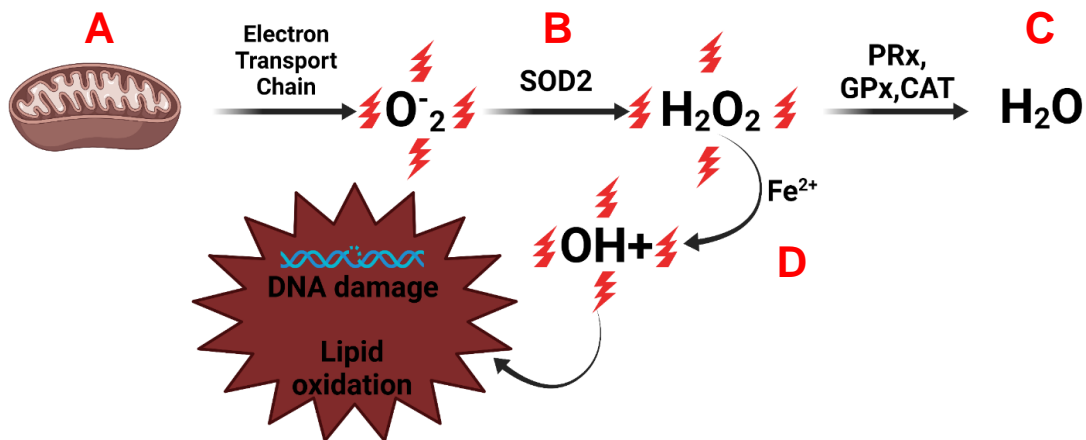
EBV and Reactive Oxygen Species

Reactive Oxygen Species (ROS) are the result of the partial chemical reduction of oxygen and are comprised of molecules such as superoxide anion (O_2^-), nitric oxide (NO) and hydrogen peroxide (H_2O_2) (Figure 3). ROS are generated during oxidative phosphorylation in the mitochondria or may originate from outside the cells (Ray et al., 2012). ROS are important participants in cellular signaling that involves cell survival, cell cycle regulation, elimination of

unwanted cells, immune responses and more. The excess of ROS, also known as oxidative stress, which can be due to overproduction of ROS or reduced antioxidant availability, is associated with cancer, aging, diabetes, and neurodegeneration. Therefore, maintaining homeostatic levels of these species by balancing the production of ROS and their neutralization by antioxidants, is crucial for cellular health (Zorov et al., 2014).

Neuronal cells require high levels of energy and are extremely sensitive to ROS, as noted by the presence of oxidative stress in most neurodegenerative diseases (G. H. Kim et al., 2015; MacAskill & Kittler, 2010). Thus, mitochondria are a major player in neuronal health as they produce energy and ROS (Zorov et al., 2014). Notably, mitochondrial quantity, membrane function, organelle size and antioxidant levels have been linked to neurodegenerative diseases (Yan et al., 2013).

Figure 1-3. Reactive Oxygen Species Production and Clearance



A/B. Superoxide produced in the mitochondria during cellular respiration is converted to Hydrogen peroxide, a potent oxidizing agent, by Superoxide Dismutase 2 (SOD2). **C.** Hydrogen peroxide can then be converted to water by PRx (peroxiredoxins), GPx (glutathione peroxidase) and CAT (catalase) (Schieber & Chandel, 2014), or **D.** it can be converted by ferrous ion to hydroxyl cations that can lead to DNA damage and lipid oxidation.

ROS homeostasis has been reported to be impaired in EBV-infected cells, resulting in oxidative stress, likely due to decreased antioxidant activity (Gargouri et al., 2009). This combination of increased ROS and decreased antioxidant activity are observed in the brains of patients with neurodegenerative diseases (Sherer et al., 2002; Yan et al., 2013). Moreover, changing mitochondrial localization can affect pre- and post-synaptic signaling, intracellular signaling, and many other functions in highly energy-dependent neuronal cells (MacAskill & Kittler, 2010).

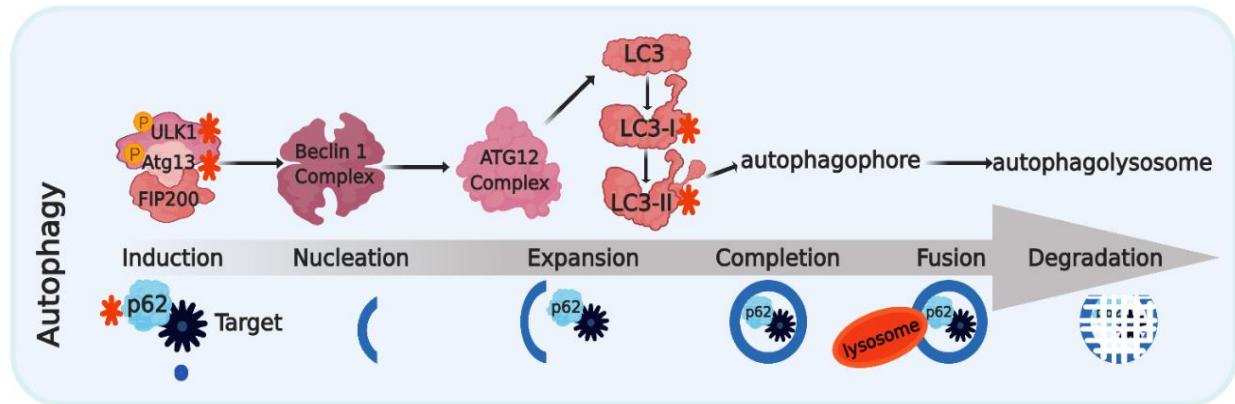
EBV and Autophagy

Autophagy is an essential process for all cells, as it allows for degradation of cellular organelles and proteins to maintain cellular homeostasis and overall cell health. Over-expression accompanied by improper clearance of pathogenic protein is associated with many diseases, notably, neurological conditions such as LB's and Alzheimer's disease (Shintani & Klionsky, 2004). Autophagy can be grouped into 3 main categories: chaperone-mediated autophagy, micro-autophagy, and macro-autophagy. Chaperone-mediated autophagy requires the activity of a chaperone complex that brings the target to the lysosome (Cuervo & Wong, 2014). In micro-autophagy cellular debris or other cytoplasmic components are engulfed via invagination of the lysosomal membrane. Lastly, and most relevant for this study, is macro-autophagy which has the *de novo* formation of autophagosomes as a hallmark. This text will refer to macro-autophagy as simply autophagy from this point on (Parzych & Klionsky, 2014).

The autophagic process begins with the formation of a phagophore that initiates sequestration of the contents to be degraded. This is followed by their full encapsulation in the autophagosome, which then fuses with lysosomes to form an autolysosome. This fusion event provides enzymes to perform the degradation of the encapsulated contents. Successful completion of autophagy has many steps, so the evaluation of its completion (autophagic flux) requires several approaches, each directed at a specific point of the pathway. Furthermore,

coordinated effort and involvement of many proteins is needed (Figure 4), and this can be monitored for assessment of autophagic flux (Klionsky et al., 2016).

Figure 1-4. The Autophagic Process



In Figure 1-4 , upon induction of the ULK complex, nucleation occurs, followed by phagophore expansion in coordination with the lipidation of LC3B and assistance from the Beclin1 and ATG12 complexes. LC3II is cleaved from the fully formed autophagosome which fuses with the lysosome, producing the autolysosome. Degradation of the lysosomal contents and release into the cytoplasm then follow (Parzych & Klionsky, 2014).

One important player in this process is LC3 (microtubule-associated protein 1A/1B-light chain 3), which is cleaved by ATG4B protease, giving rise to LC3-I, then subsequently lipidated by a ubiquitin-like system, producing LC3-II. This version of the protein associates with autophagic membranes, and it is degraded after lysosomal-autophagosome fusion (*CST - LC3B Antibody*, n.d.). Treatment of cells with the vacuolar proton pump inhibitor Bafilomycin can suppress this degradation by blocking proton movement into the lysosomal compartment, and thus its complete acidification, which is needed for proper function. The use of inhibitors of LC3-II degradation can assist in determining if autophagic flux is being blocked and if the upstream or downstream pathways from fusion are the ones likely to be involved.

Other proteins can also be targeted to assess autophagic flux. NBR1 and p62 are selectively degraded during the final step in autophagy, being subject to degradation inside the

autolysosome. NRB1 and p62 are adaptor proteins for ubiquitinated targets of autophagy, and their levels in the cell are maintained by autophagic degradation (Cirone, 2018).

The manipulation of autophagy by EBV in B cells was demonstrated by Granato and colleagues using an inhibitor specific for PI3KC3 (PI3K class 3) known as 3-MA (3-methyladenine), to block the initial steps in autophagy (Granato et al., 2014). While this resulted in reduced expression of immediate-early viral proteins, allowing the induction of EBV's entire lytic replication cycle, it blocked autophagic flux and promoted lytic replication.

As EBV hijacks cellular machinery for its own viral production, it packages virions inside the autophagosome and prevents their fusion with lysosomes to maintain viral progeny integrity. These autophagic vesicles are then able to traffic virions to the cell membrane, from where they are released to infect other cells. This process has been observed in B cells, but we have no knowledge if the same is true for neuronal or neuronal like cells (Granato et al., 2014).

In the context of autophagic processes that are relevant for virus-host interactions and inflammatory processes alike, Precision autophagy could have more influence in the development of neurodegenerative diseases than currently known (Kimura et al., 2016). Precision autophagy relies on the dual function of molecules such as TRIMs or Tripartite motif proteins. TRIMs can act as a receptors and regulators of autophagy by recognizing even untagged molecular targets and serving as a physical stage and coordinator for the assembly of the autophagic machinery. TRIMs have been reported to be involved in the autophagy of viral particles and of inflammasome components such as NLRP3 and pro-caspase 1, thus TRIM mediated Precision autophagy could have an effect in age-related disease processes, such as inflammatory responses (Kimura et al., 2016). Examining autophagic flux in EBV-infected neuronal cells is crucial to assess the consequences of virus-host interactions for neurological diseases and cell health.

EBV and Inflammation

Viral infections are associated with inflammation and activation of the innate and adaptive immune defenses. The attachment of the CD21 cell surface receptor to EBV's gp350 (envelope glycoprotein 350) of B lymphocytes triggers the stimulation of STAT3 and NF- κ B via the JAK/STAT and PI3K-AKT respectively, and both molecules are involved in the initiation of inflammation and oncogenic processes (Ew & N, 2020). In addition, STAT3 is known to be swiftly activated during lytic EBV infection, and it prevents signaling of the DNA damage response, thus participating in the latency process (Li & Bhaduri-McIntosh, 2016). Notably, EBV infection is reported to initiate inflammation in other types of cells, such as monocytes, which suggests that the process likely occurs in most cells that are EBV-infected.(Torii et al., 2017).

The first step in the activation of the inflammatory response is triggered by Pattern recognition receptors or PRRs which are molecules that, upon recognizing a pathogen, will initiate antiviral responses within the cell. Toll-like receptors, such as TLR3 that senses EBV, can recognize DAMPs (damage-associated molecular patterns) and PAMPs (pathogen-associated molecular patterns) which are of viral origin and trigger inflammatory pathways (Singh et al., 2021; C. Zhao & Zhao, 2020, p. 3).

Once viral infection is detected in this manner, the inflammatory response is led by the formation of inflammasomes, a multiprotein aggregate that will orchestrate the cell responses, including cell death (C. Zhao & Zhao, 2020). Inflammasome activation is a two-step process characterized by the priming step (signal 1) and the activation signal (signal 2). One of the most characterized inflammasome complexes, NLRP3, is deeply involved in cellular responses to viral infection. In this complex, signal 1 is initiated by sensing the presence of a pathogen with subsequent activation and nuclear translocation of NF- κ B, which will trigger the transcription and translation of pro-caspase 1, pro-IL-1 β , and NLRP3, the main protein of the inflammasome.

Signal 2 occurs when additional signals, such as mitochondrial injury, ROS, lysosomal injury, and protein aggregation are received by DAMP's and PAMP's, triggering the assembly and subsequent activation of the NLRP3 inflammasome (C. Zhao & Zhao, 2020, p. 3). Excessive ROS and the immune system, independent cytokine production, can notably prime NLRP3 without NF- κ B's translocation to the nucleus (Gros Lambert & Py, 2018).

Inflammation is part of the complex etiology of neurodegenerative diseases. Normal aging processes such as "inflammaging" (a low-grade inflammatory state that can be induced by latent infections) and immune senescence are intrinsically linked to most neurodegenerative diseases (Erickson & Banks, 2019). Thus, it is no surprise that long term viral infections, such as EBV, which can lead to inflammation throughout the host's life, have been added to the mosaic of environmental triggers for sporadic neurological disease (Koyuncu et al., 2013). Our research can help bring about answers to the extent of EBV's involvement in age related neurological diseases.

CHAPTER II: EPSTEIN-BARR VIRUS INFECTS RETINOIC-ACID DIFFERENTIATED NEUROBLASTOMA CELLS

Introduction

Epstein-Barr virus (EBV) is a human Herpesvirus that persists in over 90% of the world's human population (*Fields Virology | R2 Digital Library*, n.d.-a; Thorley-Lawson, 2015). One commonality amongst all Herpesviruses is their life cycle duplexity: they initially enter one cell type and undergo lytic (productive) replication then enter a second cell type and enter latency (dormancy). EBV infects epithelial cells of the oropharynx in its lytic cycle using the viral fusion complex gB - gH/gL to interact with CR2 (Complement Receptor 2 or CD21), $\beta 1$, $\beta 8$ and $\alpha 5$ integrins during viral entry and fusion at the host-cell plasma membrane (Chesnokova et al., 2009; Thorley-Lawson, 2015). B cells can be infected during EBV's lytic and latent cycles via the interaction of the B cell surface receptor CD21 with the viral proteins gp350/220, permitting viral attachment to the host's cell surface, facilitating its endocytosis (Thorley-Lawson, 2015). Infection of other cells, such as astrocytes and microglia, has been reported, but little is understood about these infection mechanisms (Hassani et al., 2018; Menet et al., 1999).

During latency, EBV-infected cells undergo limited gene expression of viral transcripts such as EBERs (Epstein-Barr encoded small RNAs) and EBNA 1 (Epstein-Barr nuclear antigen 1) and the infection persists indefinitely. EBV can randomly reactivate back into its lytic cycle under certain circumstances, such as immune suppression or senescence, producing viral transcripts in a lytic cascade that is initiated by the BZLF1 (Zebra) viral transcript (Dugan et al., 2019). The ability of EBV to establish a lifelong infection predisposes their hosts to disease later in life. In fact, persistent infection with Herpesviruses is currently under investigation by many groups for their potential to cause, affect, or exacerbate Alzheimer's Disease (AD), Multiple Sclerosis (MS), and Parkinson's Disease (PD) (Bourgade et al., 2016; Harris & Harris, 2015; Hassani et al., 2018; Mangold & Szpara, 2019; Moreno et al., 2018; Pender, 2011; J. Woulfe et

al., 2016; J. M. Woulfe et al., 2014). EBV has four types of latency (0, I, II, III) characterized by disease association and type of cell infected. The most common transcript during lytic replication is BZLF1 and during latent infection EBERs and EBNA1 are consistently detected (Dugan et al., 2019)

EBV can sporadically reactivate in B cells (enter lytic replication), which have access to nearly the entire body, therefore EBV has the potential to affect many types of tissues (*Fields Virology | R2 Digital Library*, n.d.-a). While not everyone that has EBV will develop age-related diseases such as MS or AD, neuroimmune toxicity from EBV reactivation events could predispose individuals by initiating early changes in neuronal cell function (Ringheim & Conant, 2004). Current data has conflicting reports of EBV's presence in autopsied brains at the late stages of neurodegenerative diseases, but these data do not account for viral involvement in early disease stages, and do not reject sporadic viral interference in neuronal cell health during these lifelong infections (Allnutt et al., 2020; Moreno et al., 2018).

EBV has multiple possible routes to enter or modulate the nervous system. For example, infection of the oropharynx is in proximity to bipolar olfactory receptor neurons with axons extending through the lamina propria. These axons join to form the olfactory nerve with direct access to the brain. Viral entry through this route via anterograde transport by the axons to the brain has been established for multiple viruses, including HSV1, murine CMV, and murine Herpesvirus (a gamma herpesvirus) (Durrant et al., 2016a; H. E. Farrell et al., 2016; P. J. Farrell, 2015; *Fields Virology | R2 Digital Library*, n.d.-a; Koyuncu et al., 2013; Menet et al., 1999; Riel et al., 2015). In addition, the natural aging process itself disturbs the efficacy of the Blood Brain Barrier (BBB) and can compromise its structure by creating areas of permeability allowing for pathogen entry. Cytokines and chemokines such as TNF- α freely cross the BBB and can be produced in response to viruses to further disrupt the brain's immune privilege (Barral & Croibier, 2009; Erickson & Banks, 2019; Riel et al., 2015). Monocytes and

macrophages can be infected by EBV *in vitro* and *in vivo* and contain EBV DNA while circulating in asymptomatic EBV carriers. Therefore, B cells are not alone carrying the virus (Hassani et al., 2018; Tugizov et al., 2007). These data suggest that EBV can have access to the CNS via various routes.

Our aging population is growing and neurodegenerative diseases are a looming threat (*Neurodegenerative Diseases*, n.d.). AD is the most common form of dementia and is the sixth leading cause of death in the United States. Alzheimer's patients present with loss of memory, and later in the disease may exhibit behavioral changes, loss of mobility, hallucinations, and seizures. Death from this disease occurs an average of 8.5 years after initial presentation. It is estimated that 44 million people worldwide suffer from this disease, and this figure is expected to triple by the year 2050 (Lane et al., 2018). PD affects over 1 million people in the United States with at least 60,000 people expected to be diagnosed every year (*Statistics*, 2017). Most cases are diagnosed around 60 years of age and the disease is typified by loss of dopaminergic neurons (DAs) in the Substantia nigra, and the presence of protein aggregates known as Lewy bodies (LB's) (Maiti et al., 2017). This disease is progressive and is characterized by tremors, stiffness, and difficulty walking. Most recently, clinical studies have implicated EBV as a possible causative agent of MS amidst an already existing call by prominent scientists in the field of Herpes virology to further explore EBV's neurotropism in relevant neuronal models (Bjornevik et al., 2022; Shim et al., 2017; Shipley et al., 2017; Soldan & Lieberman, 2020).

To this extent, we decided to investigate the potential of Retinoic-Acid (RA) differentiated SH-SY5Y neuroblastoma cells as a suitable model for studying EBV's effects in neuronal cells. SH-SY5Y cells are derived from a subclone of the SK-N-SH neuroblastoma cell line that was obtained from a biopsy of bone marrow in 1970. SH-SY5Y cells present as a mixed population of epithelial and neuroblast like cells, some adherent and some suspension cells. Treating SH-SY5Y cells with certain chemicals, such as phorbol esters and Retinoic acid, has been shown to

induce differentiation into mature human neurons, and the cells display neuronal morphology and increased neuronal marker expression (Shiple et al., 2016). RA-differentiated SH-SY5Y cells have been widely used as a reliable cell model to study neurological diseases (Deng et al., 2005; Rcom-H'cheo-Gauthier et al., 2017; Shipley et al., 2017; Storch et al., 2000; van der Merwe et al., 2017). RA-differentiated SH-SY5Y cells thus can provide a relevant and affordable model to study EBV-neuron interactions (Shiple et al., 2017). Cells such as induced pluripotent stem cells (iPSCs) or primary cells can be cost-prohibitive and difficult to grow for virologists who have the necessary expertise and understanding of viral dynamics and wish to perform exploratory yet neurologically-relevant studies of EBV's interactions with neuronal cells.

Here, we exposed RA-differentiated SH-SY5Y cells to infectious EBV virions and revealed that these cells are susceptible to EBV infection. Furthermore, we demonstrated that RGD binding motifs found in integrins, such as integrin $\beta 1$ and $\beta 8$, are likely involved in viral attachment and entry of EBV in these differentiated SH-SY5Y neuroblastoma cells. Furthermore, we found that infection of these cells with EBV led to an increase in Dopamine Receptor 2 (D2DR) levels, a neural differentiation marker. Intriguingly, we could not detect any of the common viral transcripts found in during EBV's lytic or latent cycles, but we did detect the EBV genome within infected cells, as well as the activation of STAT3 and ERK, and a trend of phosphorylated p38 migrating into the nucleus. Together these data suggest that EBV is capable of infecting differentiated neuronal cells, and that infection of RA-differentiated cells leads to changes in molecules important for inflammatory cellular responses.

Materials and Methods

Cell culture and Differentiation

The EBfaV-GFP cell line is derived from the EBV-positive B958 cell line and contains a GFP marker to denote infected cells (Speck & Longnecker, 1999). Raji cells are EBV-positive B

cells derived from a patient with Burkitt's lymphoma (ATCC). Both were grown in RPMI medium supplemented with 10% fetal bovine serum, antibiotics and antimycotics. SH-SY5Y neuroblastoma cells are a thrice cloned subline of the SK-N-SH neuroblastoma cell line obtained from a 4-year-old cancer patient with metastatic bone tumor (ATCC). Undifferentiated SH-SY5Y were grown in 1:1 DME-F12 with 10% fetal bovine serum, antibiotics and antimycotics. Differentiation was performed by culturing cells in serum-reduced medium (1% fetal bovine serum-FBS) with the addition of 5 μ M Retinoic Acid for 5-7 days, changing the medium every other day and splitting as needed. All cells were kept in incubators with 5% CO₂ levels at 37°C. Differentiation status was confirmed via observation of cell morphology changes under light microscope and Dopamine Receptor 2 levels via Western blotting. SH-SY5Y neuroblastoma cells were a kind gift from Dr. Zhenquan Jia.

Virus Production, Collection, and Infectivity Assay

EBfaV-GFP cells were cultured in 100mL of RPMI with 3mM sodium butyrate and 20ng/ml of 12-O-tetradecanoylphorbol-13-acetate (TPA), to allow for virus production and shedding into the medium (also called induction). Visual inspection of GFP fluorescence via microscopy was performed 3 days post-induction to ensure cells were lytic. At day 6, cells and medium were centrifuged to pellet and remove the cells and the supernatant was filtered with a Corning sterilized 0.25 μ m filter to separate the virus from the cells. The supernatant was then ultracentrifuged in a Beckman Coulter Optima L-80 Floor Digital Ultracentrifuge using a fixed angle rotor type 70i at 24,000 rpm at 4°C for 90 minutes. The supernatant was discarded, and the remaining virus pellet was resuspended in either 1:1 DME/F12 or RPMI and stored at -80°C. Virus batches collected from EBfaV-GFP cells were tested to ensure they produced infectious virus. Briefly, Raji cells were induced in 5ml of RPMI with 3mM sodium butyrate and 20ng/ml of TPA in addition to 200-400 μ l of virus stock, while control cells only had fresh medium added.

Cells were centrifuged to remove medium and GFP was detected via flow cytometry 2 days post-infection, using Guava easyCyte 6-2L and Guava easyCyte software both by Luminex corporation. Only virus batches that were shown to be infectious were used for experiments. For a few experiments (as noted), we used virus stock purchased from ATCC VR-1492 (HHV4), this stock also infected the differentiated SH-SY5Y cells.

Viral induction/lytic reactivation of infected SH-SY5Y cells

SH-SY5Y cells were differentiated and either treated with 200-400 μ l of EBV stock produced in the lab or purchased from ATCC or vehicle (control). Infected cells were treated with 20ng/ml of TPA and 3mM of sodium butyrate 2 days prior to collection times, unless otherwise noted. To assess lytic reactivation via qRT-PCR, cells were collected at 3, 5, and 9 days post-infection.

RNA Collection

RNA samples were collected using Trizol (Invitrogen) according to manufacturer's instructions. Cells were rinsed with 1XPBS (137mM NaCl, 2.7mM KCl, 10mM Na₂HPO₄, 1.8mM KH₂PO₄) and 300-400 μ L of Trizol was added to the sample to lyse the cells followed by trituration with a pipette to homogenize the lysate, followed by 5 minutes incubation at room temperature to dissociate nucleoproteins. Next, 80 μ l of chloroform was added and the lysate was gently vortexed and incubated at room temperature for 3 minutes. The lysate was then centrifuged in an Eppendorf Centrifuge 5417R using rotor FA45-24-11 at 12,000rpm for 15 minutes at 4°C, which allowed the formation of 3 layers composed of an upper aqueous phase (which contains the RNA), and an interphase and lower phenol-red phase. The aqueous phase was gently removed by tilting the tube at a 45° angle, and placed in a new tube to which 200 μ L of isopropanol was added for a 10-minute incubation period at room temperature to precipitate

the RNA. Centrifugation at 12,000rpm for 10 minutes at 4°C followed, to pellet the RNA. The supernatant was discarded, and the pellet was resuspended in 400µL of 75% ethanol to wash the RNA, and vortexed and centrifuged at 4°C for 5 minutes at 7,500 rpm. The wash was discarded, and tubes were placed upside down to air dry for 5-10 minutes, before resuspension with 20-50µL of RNase free water. To ensure solubilization of the RNA, samples were immediately incubated for 15 min in a heat block at 55-60°C. Samples were stored at -80°C. RNA was quantified using NanoDrop One/One^C Microvolume UV-Vis Spectrophotometer.

DNA Collection

Viral DNA was collected using an Adamson lab modification of the HIRT protocol (*Modified Hirt Procedure for Rapid Purification of Extrachromosomal DNA from Mammalian Cells*, n.d.). Briefly, cells were scraped and centrifuged to remove media, and pellet was resuspended and incubated with 50mM pH 7.5 Tris, 10mM pH 8.0 EDTA and 1.2% SDS for 5 minutes at room temperature. This was followed by the addition of 350µL of precipitation buffer with 3M cesium chloride, 1M potassium acetate and 0.67M acetic acid and further incubation on ice for 15 minutes. Cells were then centrifuged at 4°C in an Eppendorf Centrifuge 5417R using rotor FA45-24-11 at 14,000 rpm for 15 minutes to pellet cellular debris. The supernatant was then loaded in a silica gel membrane spin tube and centrifuged for 30 seconds in an Eppendorf centrifuge Mini Spin at 7,000rpm. The flow-through was discarded and 750µL of wash buffer composed of 80mM potassium acetate, 10mM Tris, 40µM EDTA and 60% ethanol was added. Tubes were centrifuged and the wash discarded, followed by elution of DNA with 20-50µL of TE. Quantification of the DNA was performed within a NanoDrop One/One^C Microvolume UV-Vis Spectrophotometer.

RGD peptide viral entry assay

RGD peptides (Arg-Gly-Asp, catalog: A8052-5MG) were purchased from Millipore Sigma and diluted according to manufacturer's instructions. SH-SY5Y cells were differentiated and incubated with either 0.5 or 0.3mM of RGD peptides or vehicle (sterile diH₂O) for 30 minutes at 37°C in differentiation medium. Cells were then rinsed with 1XPBS and treated with 200-400µl of EBV stock or vehicle and collected 2 days post-infection. qPCR was performed to assess viral DNA content using a Raji cell EBV DNA Standard Curve.

RT-PCR

Access RT-PCR System (Promega) was used with primer sets for the viral transcripts Z, LMP1, LMP2A, EBNA1 and EBNA2. The master mix for reactions of 25µl total volume were composed of 10µl AMV/Tfl 5X reaction buffer per reaction, 0.2mM of dNTP Mix (at 10mM each dNTP), downstream and upstream primers at 20pmol each, 1mM of 25mM of magnesium sulfate, and RNase free water to 25µl final volume. AMV Reverse Transcriptase and Tfl DNA Polymerase at a final concentration of 0.1µ/µl were added and tube was gently vortexed. Negative controls received RNase free water instead of RNA template, and samples were amplified in an MJ Mini Personal Thermal Cycler (Bio-Rad). The following program was used: 1 cycle at 45°C for 45 minutes for reverse transcription, 1 cycle of 2 minutes at 95°C for RT inactivation/denaturation, and 40 cycles of 30 seconds at 94°C, 1 minute at 60°C, 2 minutes at 68°C for annealing, extension, and final extension respectively. Reactions were performed in triplicates. All primers were purchased from Eurofins unless listed otherwise.

Table 2-1. Primer Sequences

Target	Sequence	Specificity
Z (X. Liu et al., 2013)	F: 5'-AGAATCGCTGGAGGAATGC-3'	HHV4
	R: 5'-CTTAAACTTGGCCCGGCATT-3'	
LIR	F: 5'-CCGAAATCTGACACTTTAGAGC-3'	HHV4
	R: 5'-CCCTGACCTTTGGTGAAGTC-3'	
EBNA 1 (X. Liu et al., 2013)	F: 5'-GAGCCTGACCTGTGATCGTC-3'	HHV4
	R: 5'-TAGGCCATTTCCAGGTCCTGTA-3'	
LMP2A (X. Liu et al., 2013)	F: 5'-GCAACACGACGGGAATGAC-3'	HHV4
	R: 5'-TTCCTCTGCCCGCTTCTTC-3'	
LMP1 (X. Liu et al., 2013)	F: 5'-CTTTGTCTACTCCTACTGATGATCAC-3'	HHV4
	R: 5'-CCGAAGATGAACAGCACAATTC-3'	
EBER 1 (Aromseree et al., 2017)	F: 5'-AGGACCTACGCTGCCCTAGA-3'	HHV4
	R: 5'-ATTCAGTTGAGAAAACATGCGG-3'	

EBER	F:	5'-	HHV4
2 (Aromseree et al., 2017)	AGGACAGCCGTTGCCCTAGTGGTTTC -3'		
	R: 5'-ATTCAGTTGAGAAAAATAGCGG -3'		

Numbers listed by "Target" are references for the sequences. *Kind gifts from Dr. Zhenquan Jia.

qRT-PCR

RNA at concentrations of 20-50ng/ μ L was amplified in a StepOne Real-Time PCR System (Applied Biosciences) using Power SYBR Green RNA-to-CT 1-Step Kit. Reactions were each prepared using 10 μ L of Power SYBR Green RT-PCR 2X mix, 20pmol each of forward and reverse primers, 0.16 μ L of RT enzyme Mix (125X), and RNase free water to 20 μ L total volume. Amplification was performed using the recommended setting of 30 minutes at 48°C for the RT step, 95°C for 10 minutes for polymerase activation, followed by 40 cycles of 95°C for 15 seconds (denaturation) and 60°C for 1 minute (annealing and extending). Primers used were the same listed under RT-PCR methods, and reactions were performed in technical triplicates and biological triplicates.

qPCR

PowerUp SYBR green master mix (Applied Biosciences) was used according to manufacturer specifications for primers with $T_m > 60^\circ\text{C}$. Each 20 μ L reaction was prepared using 10 μ L of PowerUp SYBR Green Master Mix (2X), 20pmol of forward and reverse primers for EBV's LIR sequence [(Long-Internal Repeat) with an expected product of 214bp - from bp 799-1042 in the 3072bp BamHI-W repeat fragment of EBV DNA], 1 μ L of DNA template and nuclease free water to the final volume. The cycling mode began at 50°C for 2 minutes for UDG (Uracil-DNA Glycosylase for PCR product stabilization for 72 hrs), 95°C for 2 minutes to activate the

DNA polymerase followed by 40 cycles of 15 seconds at 95°C and 1 minute at 60°C. A standard curve with 5, 0.5, 0.05, and 0.005ng of EBV DNA collected from Raji cells using the modified HIRT protocol was performed with every run, and reactions were completed once with 2 technical replicates for the standard curve and experimental samples. Absolute quantification was performed, and the following equation was used to determine the viral copy number:

$$\text{Number of copies (molecules)} = \frac{X \text{ ng} * 6.0221 * 10^3 \text{ molecules/mole}}{\left(N * \frac{660 \text{ g}}{\text{mole}}\right) * 1 * 10^9 \frac{\text{ng}}{\text{g}}}$$

Where X= amount of amplicon in nanograms

N= length of dsDNA amplicon

600g/mole = average mass of 1 bp of dsDNA

SDS-PAGE Gel Electrophoresis and Western Blotting

Cells were collected by scraping and centrifuging (for adherent cells) or centrifuging alone (for suspension cells). Cells were rinsed once with 1XPBS and resuspended in 20-50µL of ELB lysis buffer (0.25M NaCl, 0.1% NP40 alternative detergent, 50mM HEPES pH 7.5, 5nM EDTA, protease inhibitors), then subjected to 2 freeze/thaw cycles of 5 minutes in the -80°C freezer and 1 minute in a 37°C water bath respectively, to crack the cells open. This was followed by centrifugation at 4°C to concentrate the protein in the supernatant. Proteins were stored at -80°C until use. Quantification was performed by Bradford Assay. Equal amounts of proteins (20-50µg) were separated with 10-12% SDS gels at 90V through stacking wells then at 125V through a separating gel submersed in Running Buffer (25mM Tris, 192 mM glycine, 0.1% SDS). Transfer to 0.45µm PVDF membrane was performed overnight in Electroblothing Buffer (25mM Tris, 192 mM glycine, 0.1% SDS, 10% methanol, pH 8.3) at 100mA, and membranes were blocked with 0.25% milk block (0.25% of powdered whole milk, 0.1% Tween in 1XPBS) and activated with 100% methanol prior to immunostaining. Incubation with primary antibodies

was performed on a rocker for 1-3 hours at room temperature or overnight at 4^oC using manufacturer's recommended concentrations. Subsequent washes in Wash Buffer (1XPBS, 0.1% Tween) and 10-15 minute secondary antibody incubations were carried out in a SNAP i.d. Protein Detection System by Millipore Sigma. Visualization and quantification of chemiluminescent protein bands were performed with WesternBright ECL HRP substrate (Advansta, catalog: K-12045-D20) in a C-DiGit Blot Scanner and Image Studio™ both by Li-Cor.

Table 2-2. Antibodies

<i>Antibody</i>	<i>Specificity</i>	<i>Manufacturer</i>
D2DR	Human	Santa Cruz Biotechnology, sc-5303
BIII tubulin-	Mammalian and Chicken	R&D Systems, MAB1195-SP
pERK	Human, mouse, and others	Cell Signaling, #9101
ERK	Human, mouse, and others	Cell Signaling, #9102
pAKT 1/2/3 (B-5)	Human, mouse, rat	Santa Cruz Biotechnology, sc-271966
AKT 1/2/3 (5C10)	Human	Santa Cruz Biotechnology, sc-81434
p-STAT3 (B-7)	Human, mouse, rat	Santa Cruz Biotechnology, sc-8059
STAT3 (F-2)	Human	Santa Cruz Biotechnology, sc-8019
Beta Actin (C-4)	Human, mouse, and others	Santa Cruz Biotechnology, sc-47778

Lamin B1 (D9V6H)	Human, mouse, rat	Cell Signaling, #13435
p-P38 (E-1)	Human	Santa Cruz Biotechnology, sc-166182
P38 (A-12)	Human	Santa Cruz Biotechnology, sc-7972
Beta Integrin 1(A-4)	Human	Santa Cruz Biotechnology, sc-374429
EBV Zebra (BZ1)	HHV-4	Santa Cruz Biotechnology, sc-53904

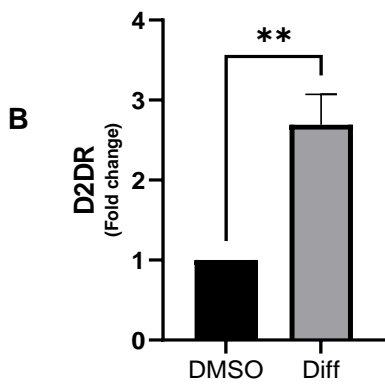
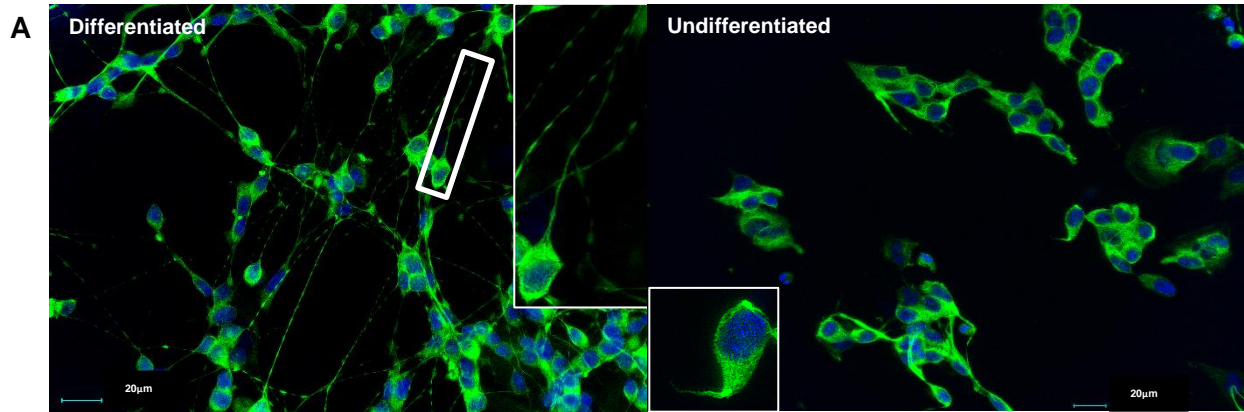
Results

Retinoic Acid-differentiated SH-SY5Y neuroblastoma cells are susceptible to EBV infection.

To investigate the consequences of EBV infection on neuronal cell processes that can influence the development of neurodegenerative diseases, we endeavored to first establish if a simple and more cost-effective cell model than induced pluripotent stem cells (iPSCs) would be susceptible to EBV infection. Previous researchers have shown that EBV and its murine counterpart (MHV-68) could infect and establish transcriptional programs – including latency – in undifferentiated SH-SY5Y cells (Cho & Song, 2014; Jha et al., 2015). However, undifferentiated and Retinoic Acid (RA) differentiated SH-SY5Y cells have distinct transcriptional profiles, and the latter is much closer to that of neuronal cells (Korecka et al., 2013; Lopes et al., 2010). We made use of an already established differentiation protocol consisting of a 5-7 day serum starvation (with 1% FBS) combined with 5 μ M of Retinoic Acid to differentiate cells prior to infection (Lopes et al., 2010). Our differentiated SH-SY5Y cells, as shown in Figure 2-1A, presented longer neurites that extended and connected to other cells, and less clustering than undifferentiated cells, akin to a differentiated cell phenotype. Furthermore, the cells expressed significantly higher levels of the dopaminergic marker Dopamine 2 receptor (Figure 2-1B), indicating that our RA treatment protocol was sufficient to change the morphology and expression profiles of the cells to more closely resemble neuronal cells.

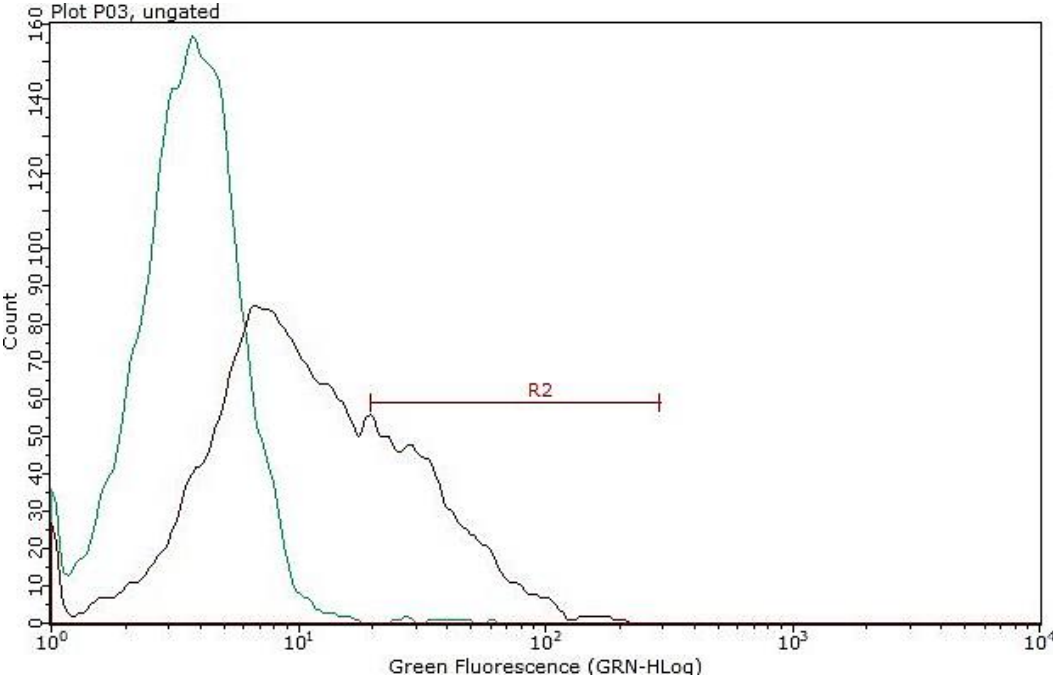
Our main source of EBV virus particles was the EBfaV-GFP cell line. This line was chosen to simplify viral infection characterization, as infected cells will have a green fluorescent signal, due to the GFP gene inserted into the virus' genome within EBfaV-GFP cells (Speck & Longnecker, 1999). As shown in Figure 2-2, we were able to infect Raji cells and detect a GFP signal by flow cytometry, indicating that we had collected and concentrated infectious virus stocks that could be used to infect our SH-SY5Y cells.

Figure 2-1. Differentiated SH-SY5Y cells have distinct morphology and increased neuronal marker expression



A- Differentiated SH-SY5Y cells (left panel) exhibited a neuronal-like morphology with neurites and less cell body clustering as compared to undifferentiated cells (right panel). Magnification 40X. **B-** Dopamine receptor protein levels in RA-differentiated SH-SY5Y cells. Differentiated cells expressed significantly higher levels of Dopamine 2 Receptor expression, a neuronal marker, in comparison to undifferentiated cells. Results are from Western Blots, N=3 shown as SEM. Statistical analysis was performed using the Student's T-test. P- value $** < 0.005$.

Figure 2-2. Infectious activity of a representative virus preparation collected from EBfaV-GFP cells verified via flow cytometry

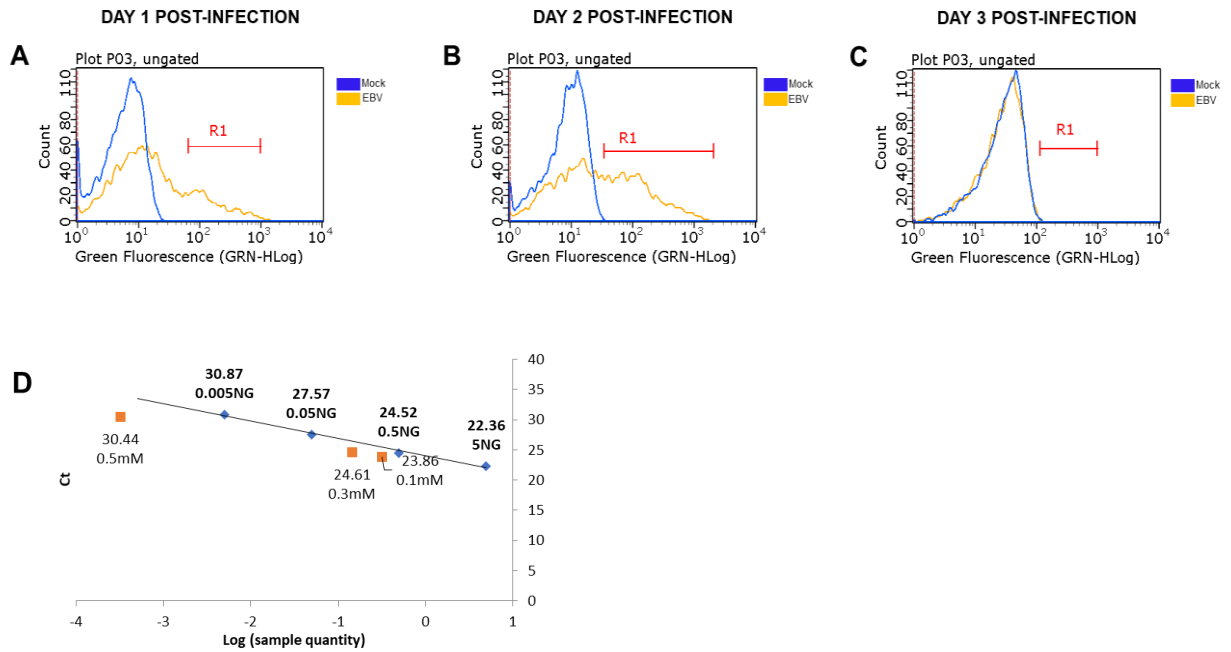


Virus preparations were tested before being added to experimental conditions to ensure virus was present and infectious. Raji cells were infected with virus collected from EBfaV-GFP cells and chemically induced with TPA and sodium butyrate. GFP was detected 48hrs post-infection by flow cytometry.

RA-differentiated SH-SY5Y cells exhibit GFP signal indicative of lytic EBV infection up to day 2 post- infection.

We then proceeded to infect RA-differentiated SH-SY5Y cells with our EBV preparation and measure their GFP fluorescence at days 1-3 post-infection(p.i).As shown in Figure 2-3 A, B, and C, the infected cells produced a GFP signal up to day 2 p.i., with none detected on day 3 p.i. To further confirm infection, we employed qPCR to quantify viral genomes within the RA-differentiated SH-SY5Y cells. To quantify copy number, we performed qPCR with primers for EBV's long internal repeat (LIR) sequence and compared genome levels to a standard curve of induced Raji cell viral DNA (Figure 2-3D). RA-differentiated SH-SY5Y cells that were GFP-positive also had detectable levels of EBV DNA, indicating that RA-differentiated SH-SY-5Y cells are susceptible to EBV infection

Figure 2-3. EBV-infected RA-differentiated cells exhibit GFP signal up to day 2 post infection

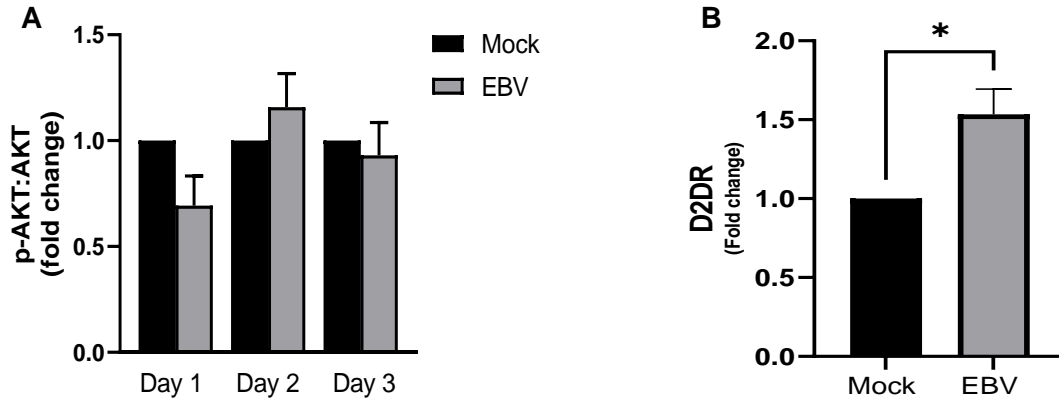


A-B-C- virus collected from the EBV-positive cell line EBfaV-GFP was used to infect RA-differentiated SH-SY5Y cells. Infected cells emit a GFP signal. Detection of green fluorescence via flow cytometry was possible up to day 2 post-infection with EBV. **D-** Absolute quantification of viral genome load in EBV-infected neuronal cells (orange squares) 2 days post-infection via Standard curve (blue diamonds) created using EBV genomic DNA from Raji cells.

EBV infection does not alter AKT activation in differentiated SH-SY5Y neuroblastoma cells but appears to promote higher expression of D2DR.

We wanted to investigate whether EBV infection would alter the differentiation status of SH-SY5Y cells, by assessing changes in the levels of 2 differentiation markers, AKT and D2DR. AKT phosphorylation has been shown to increase during the RA differentiation process and to remain unchanged upon HSV-1 infection (Shiple et al., 2017). We hypothesized that the same would be true during EBV infection. Figure 2-4A shows that AKT phosphorylation levels are not significantly different between EBV and mock-infected cells, confirming our hypothesis. Surprisingly, however, EBV-infected cells had significantly higher levels of D2DR compared to mock-infected cells (Figure 2-4B), a dopaminergic marker that is highly expressed in the Substantia Nigra and olfactory bulb which are areas of importance for neuronal processes that can be severely affected by infirmities such as Parkinson's Disease (Ayano, 2016). Combined, these results indicate that EBV infection does not alter cell survival and overall differentiation but can change the expression of receptors in neurodegenerative disease susceptible cells.

Figure 2-4. AKT phosphorylation is not altered, but D2DR levels are increased in EBV-infected cells

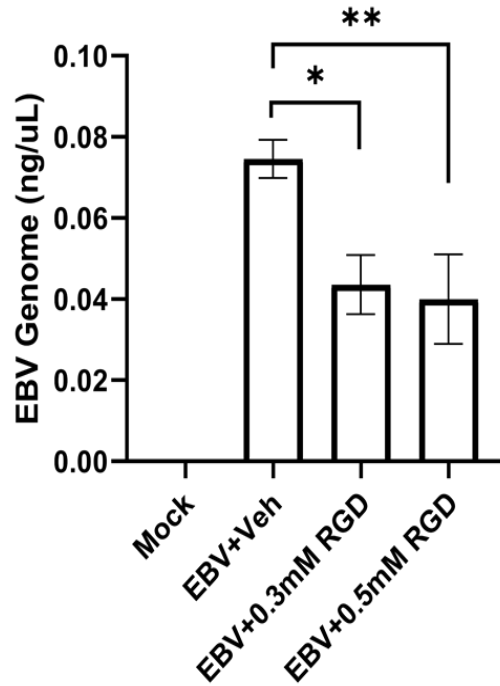


A- EBV-infected cells do not have significantly different levels of AKT phosphorylation in comparison to Mock-infected cells. **B-** At day 3 post infection, EBV-infected cells have significantly higher levels of Dopamine D2 receptor, a differentiation marker. Data shown is from cells infected with EBV and then gathered at 3 days post-infection for protein collection and assayed by Western blots SEM, N=3. Statistical analysis was done with Student's T-test, P-value * <0.05 , ** <0.005 .

RGD binding motifs are involved in EBV attachment/entry into differentiated SH-SY5Y cells.

Once we determined that RA-differentiated SH-SY5Y cells were susceptible to EBV infection, we wanted to investigate possible attachment and entry receptors for the virus. EBV is known to bind to CD21/CR2 to enter B cells and to the RGD binding motifs of integrins to enter epithelial cells (*Fields Virology | R2 Digital Library*, n.d.-a). Importantly, integrins such as β_1 have also been shown to increase infection susceptibility of a variety of B cells, despite not being the primary receptor, thus highlighting the importance of these molecules for EBV attachment and entry (Dorner et al., 2010). RGD binding motifs are expressed in the cell membrane of microglia, astrocytes, neurons, and many other central nervous system (CNS) cells (Peluffo et al., 2007). Therefore, we examined whether RGD binding motifs were also involved in EBV entry into RA-differentiated SH-SY5Y cells, by incubating the cells with either vehicle (diH₂O), 0.3mM or 0.5mM of RGD peptides for 30 minutes prior to EBV exposure. Our data, presented in Figure 2-5, shows a statistically significant dose-dependent decrease in the quantity of EBV genome in cells pre-incubated with increasing concentrations of RGD peptides, compared to those incubated with the vehicle only. This data suggests that EBV attachment and entry in RA-differentiated SH-SY5Y cells also involves integrin RGD binding motifs in cell surface receptors.

Figure 2-5. EBV infection of RA-differentiated SH-SY5Y cells relies on RGD motifs



RGD binding motifs are involved in the EBV infection of SH-SY5Y cells, demonstrating similarities to EBV's entry route into epithelial cells of the nasopharynx. Cells were pre-treated with increasing concentrations of RGD peptides to block integrin RGD motif binding domains. qPCR results show a statistically significant dose-dependent decrease in viral genome presence in the EBV+RGD exposed cells compared to EBV+ vehicle (Veh) alone. Data shown is SEM, N=3. Statistical analysis was done with Student's T-test, P-value $* < 0.05$, $** < 0.005$.

EBV does not appear to establish known transcriptional programs in RA-differentiated neuroblastoma cells

We wanted to determine which EBV transcriptional program was being established by EBV upon infecting differentiated SH-SY5Y cells. EBV has four latency types in addition to a lytic transcriptional program, each with hallmark transcripts. During the lytic replication stage, BZLF1 or “Z” is the first viral transcript produced by the infected cells in all cell types known to be susceptible to EBV infection. Of the latency programs, EBERs and EBNA1 transcripts are produced in 4 out of 4 and in 3 of 4 programs, respectively (Dugan et al., 2019). Therefore, we performed qRT-PCR to look for the transcripts listed in table 2-3, using previously verified primers(X. Liu et al., 2013) Cells were tested up to day 10 post-infection, and some were treated and incubated for 24hrs prior to collection with the chemical induction cocktail (TPA and sodium butyrate) to promote lytic reactivation at days 5, 7 and 9 post infection. Furthermore, we used 20, 30, and 50ng of RNA template to test the possibility that we were not picking up any transcripts due to low transcript levels. Ultimately, we did not detect any of the main EBV transcripts in neuroblastoma cells infected with EBV. Collectively, these data suggest that while the RA-differentiated cells are susceptible to EBV infection, they are not permissive to viral replication or latency.

Table 2-3. RA-differentiated SH-SY5Y cells are susceptible to EBV infection but not permissive to viral replication

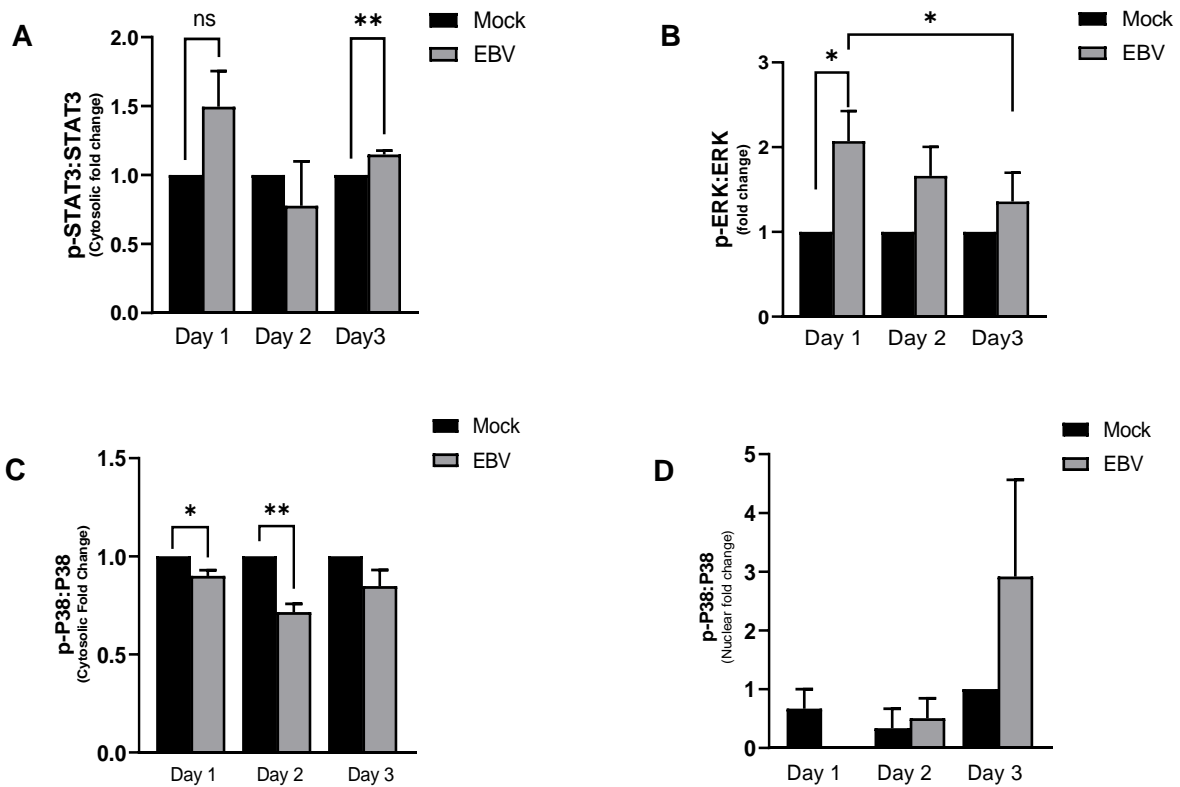
Cell Type	Program	Viral Genes	Transcripts Investigated	Transcript Status in SH-SY5Y cells infected with EBV
Plasma	Lytic	All lytic genes	BZLF1	Not detected
Naïve B cells and <i>in vitro</i> infected	Latency III (Growth)	All latent genes	EBNA-1, LMP2, EBERs	Not detected
NPC, germinal center and memory	Latency II (Default)	EBNA-1, LMP1, LMP2, EBERs	EBNA-1, LMP2, EBERs 1 and 2	Not detected
Memory B cells in peripheral blood	Latency 0 (Latency)	EBERs	EBERs 1 and 2	Not detected
Memory B cells (dividing) in peripheral blood, Burkitt's lymphoma	EBNA-1 only	EBNA-1, EBERs	EBNA-1, EBERs 1 and 2	Not detected

qRT-PCR was performed for the transcripts above to determine viral infection patterns. EBV genes listed on the table are those present in every currently known transcriptional program for the virus. None were detected in our EBV-infected SH-SY5Y cells. Experiments were performed in at least triplicate with multiple samples and template/primer concentrations for up to day 10 post-infection and using lytic reactivation chemical induction.

EBV infection decreases phosphorylation of p38 and increases that of ERK and STAT3

It has been reported that EBV alters the phosphorylation patterns of STAT3, ERK and p38 proteins, as they are important cellular pathways to promote its lytic and latent cycles in B lymphocytes and epithelial cells (Li & Bhaduri-McIntosh, 2016, p. 3; Y. Luo et al., 2021). Thus, we aimed to investigate if changes in the phosphorylation status of these proteins still occurred despite the RA-differentiated SH-SY5Y cells not being permissive to viral replication. We infected differentiated cells with 200-400 μ l of EBV stock and collected cells at day 3 post-infection for Western blot analysis to detect total and phosphorylated levels of STAT3, ERK and p38. As shown in Figure 2-6A, STAT3 had increased phosphorylation at day 1 post-infection, and a statistically significant increase at day 3 post-infection compared to mock-infected cells. In Figure 2-6B, we show that ERK had a statistically significant increase in phosphorylation at day 1 post-infection in comparison to mock-infected cells. Additionally, there was a gradual decrease in the phosphorylation levels of ERK between infected cells as the infection progresses to day 3, with ERK phosphorylation levels just slightly above that of mock-infected cells. Conversely, the data in Figure 2-6C show that p38 phosphorylation levels were significantly lower at days 1 and 2 post-infection compared to mock-infected cells, and although not statistically significant, they remained lower than control at day 3 post-infection. To further investigate this difference in p38's response to EBV infection, we decided to examine nuclear levels of phosphorylated p38. As shown in Figure 2-6D, phosphorylated p38 levels were virtually absent from the nucleus at day 1 post-infection but showed a steady increasing trend towards day 3 post-infection compared to mock-infected cells. Overall, these data suggest that mere viral attachment and entry and the presence of viral genome to at least day 3 post-infection are sufficient to engage cellular responses in major cellular signaling pathways.

Figure 2-6. EBV infection can induce changes in the activation of STAT3, ERK and p38 in the absence of detectable viral transcripts



A: STAT 3 phosphorylation, as analyzed via Western Blot, was significantly higher in EBV-infected cells in relation to mock cells at day 3 post infection **B:** EBV-infected cells had significantly higher levels of ERK activation at day 1 post-infection in comparison to mock-infected, than EBV-infected cells at day 3 post-infection. Overall higher levels of phosphorylation were seen in EBV-infected cells in relation to mock-infected. **C:** p38 activation in the cytosol was significantly lower at days 1 and 2 post-infection in EBV-infected cells in relation to mock cells. **D:** However, nuclear levels of phosphorylation showed an increase at days 2 and 3 post-infection. For all experiments above, cellular proteins were collected at day 3 post-infection for Western blot analysis. Statistical analysis was performed using Student's T-test, SEM of N=3; P-value* <0.05, **<0.005.

Discussion

Recently, EBV has been linked to several neurological diseases and the need for affordable, practical, and relevant cell models to study virus-host interactions has risen (Bjornevik et al., 2022; Shim et al., 2017; J. M. Woulfe et al., 2014). We aimed to investigate the suitability of RA-differentiated SH-SY5Y neuroblastoma cells to study the effects of EBV infection in neuronal cells because they have been widely used to investigate neuronal diseases (Deng et al., 2005; Murakami et al., 2017; Shipley et al., 2017). This provides a plethora of data that can be used to compare cellular responses to viral infection and neurological disease in the same system. First, we demonstrated that our RA-differentiated cells had the morphology and increased D2DR neuronal marker expression noted in differentiated cells. Undifferentiated SH-SY5Y cells have been shown to be permissive to EBV infection with the aid of a transfection reagent (Polybrene), but had not been previously demonstrated in their RA-differentiated state where much of their transcriptional profile is changed, thus we had to first establish if they could become infected by EBV (Jha et al., 2015; Korecka et al., 2013; Pezzini et al., 2017). Our results show that RA-differentiated cells are susceptible to EBV infection without the use of a transfection reagent, and that we were able to detect a GFP signal up to day 2 post-infection using flow cytometry. This seemed to suggest a transient infection state or the establishment of latency, as the GFP signal would only be present during the lytic replication stage of EBV infection (Speck & Longnecker, 1999, p. 958).

Notably, when we checked the phosphorylation levels of the serine-threonine protein kinase Akt, which have been reported to be upregulated in RA-differentiated SH-SY5Y cells, there were no significant differences between mock and EBV-infected cells. Akt regulates cell growth and differentiation amongst other cellular functions, therefore this seemed to indicate that cell differentiation was not affected during EBV infection (Cheung et al., 2009; J. Luo et al., 2003). Concordant with this result, we did not see any visual indication of cell death in the EBV-

infected cultures, similar to EBV infection in B cells when the virus enters B lymphocytes and maintains latency in the cells without much disruption of regular cellular function (Thorley-Lawson, 2015). Similarly, the widely neurotropic Herpes Simplex I (HSV-1) Infection of RA-differentiated SH-SY5Y cells did not promote change in the phosphorylation levels of Akt, thus this may be a commonality between EBV and HSV-1 infection of these cells (Shiple et al., 2016).

Interestingly, we observed that the expression of D2DR was significantly higher in EBV-infected cells in comparison to mock-infected cells. EBV's viral protein Z has been shown to bind directly to retinoic acid receptors RAR (Retinoic Acid Receptors) and RXR (Retinoic X Receptors), which are active in the RA differentiation process (Dreyfus et al., 1999). RA binds to RARs, which further heterodimerize with RXRs then bind to RARE (RA Response Element) to regulate transcription of differentiation genes (Xie et al., 2010). Thus, it is possible that the increased levels of D2DR are due to increased activation of the RA pathway by EBV's viral protein Z. Notably and of great importance is the function of D2DR as an auto-receptor and regulator of dopamine synthesis, release and uptake, which if dysregulated could have significant effects on neuronal function (Ayano, 2016; Ford, 2014; Pan et al., 2019).

An important aspect of EBV biology is that the virus seems to follow specific patterns of infection depending of the cell type infected, as noted by the classification of the latency states (Thorley-Lawson, 2015). Understanding the patterns of viral entry and attachment may reveal aspects of viral infection that follow an already known pattern. We were able to demonstrate that blocking the RGD epitope of RA-differentiated cells prior to EBV exposure resulted in a dose-dependent decrease in viral genome in the infected cells, suggesting that RGD binding motifs play a role in viral attachment and entry in these cells. RGD binding motifs are composed of the Arginine-Glycine-Aspartate tripartite amino acid that is present in multiple integrins, such as $\alpha 5\beta 1$, $\alpha 8\beta 1$, $\alpha v\beta 1$ and others. Integrins are highly expressed in the CNS and the cell membrane

of astrocytes, microglia, neurons and other neuronal cell types express many different integrins (Peluffo et al., 2007). The ability of EBV to use this motif to enter RA-differentiated cells supports that the virus could also enter other neuronal cells by the same mechanism, thus giving EBV the chance to interact with cells in the CNS.

We examined viral transcript expression of BZLF1, the viral lytic cascade initiator, and of two transcripts that are observed in all known latent programs, EBNA1 and EBERs 1/2 (Thorley-Lawson, 2015). We collected RNA from infected cells at 24-, 48-, and 72-hours post infection. To investigate entry into latency, we also treated EBV-infected cells with a lytic induction cocktail of TPA and sodium butyrate two days prior to collecting them at days 5, 7 and 9 post infection. Surprisingly, we were unable to detect any of the three viral transcripts in any of the above-described conditions, despite having infection status confirmed by qPCR (data not shown). We had hypothesized that viral transcripts would peak starting at 24hrs post infection, as this is a common time point seen in other cell types and even in undifferentiated SH-SY5Y cells (Jha et al., 2015; X. Liu et al., 2013). Our results suggest that viral expression may have peaked and subsided prior to our earliest time point of 24hrs, and the GFP expression seen up to day 2 post-infection may be residual, and only possible due to the GFP protein half-life and fluorescence signal strength combined with the high sensitivity of flow cytometry. EBV has been reported to express the lytic transcript Z in B cells as early as 2hrs post lytic reactivation and EBERs were shown to peak at 12 hrs. post-reactivation (Yuan et al., 2006). Therefore, future studies where EBV's viral transcript production is examined in the first 24hrs post infection are needed.

Despite our inability to detect EBV's viral products, we report that STAT3 and ERK are significantly activated upon EBV infection of RA-differentiated SH-SY5Y cells. STAT3 (signal transducer and activator of transcription), once phosphorylated translocates to the nucleus and can activate the transcription of genes related to immunity, apoptosis and embryogenesis. In

fact, suppression of STAT3 can promote inflammasome activation (Bai, n.d.). EBV entry alone can activate STAT3 via JAK (Janus Kinase) pathway as can EBV's viral protein LMP1. Notably for our results, high levels of STAT3 have been shown to impede the cell's ability to enter or remain in the lytic state (Koganti et al., 2015; Li & Bhaduri-McIntosh, 2016, p. 3). Our data shows that STAT3 is significantly upregulated at day 3 post infection, at the same time we can no longer detect the GFP signal indicative of EBV's lytic cycle. It is possible that EBV entry or LMP1 activated the phosphorylation of STAT3, which in turn undermined the lytic cycle leaving the cells with undetectable levels of viral transcripts. To further support this hypothesis future experiments should investigate STAT3 levels after day 3 post infection and should include a broader assessment of latent transcripts that includes all of EBV's latent products. This could elucidate if these cells did enter latency but failed to reactivate upon chemical induction due to consistent high levels of phosphorylated STAT3. ERK (extracellular signal-regulated kinase) phosphorylation during EBV infection has been shown to induce autophagy and to activate the transcription of Z lytic viral protein (Hung et al., 2014; Lee et al., n.d.). ERK activation occurs as a response to environmental stress, including viral infection (Canovas & Nebreda, 2021). Our results show that ERK significantly increased in phosphorylation at day 1 post infection, and its activation decreases at day 2, with day 3 post infection being significantly lower than EBV-infected cells at day 1 post infection. These data underline the possibility that RA-differentiated SH-SY5Y cells experience a brief burst of viral transcription (as noted by GFP signals up to day 2 post infection) perhaps followed by entry into latency, as suggested by our data showing the increase in STAT3 phosphorylation at day 3 post infection.

As one of the MAPKs (mitogen-activated protein kinases), p38 phosphorylation can have many cellular consequences, including the stimulation of activator protein 1 (AP-1), which can initiate inflammatory cytokine production, like STAT3, and the regulation of autophagy (Canovas & Nebreda, 2021). Downregulation of p38 has been shown to decrease the expression of EBV's

viral latent protein LMP1, and the activation of p38 via external stress stimuli or cytokines has been linked to EBV's evasion of apoptosis (Johansson et al., 2010; Singh et al., 2021). In relation to neuronal cells, the activation of p38 has also been associated with Tau protein hyperphosphorylation in AD and neuroinflammation in PD (Canovas & Nebreda, 2021; Corrêa & Eales, 2012). Our results we show that cytosolic p38 has significantly lower levels at days 1 and 2 post infection in relation to mock-infected cells, implying that EBV infection could have hindered p38 activity. When we investigated the nuclear levels of p38 activation however, we observed a steady increase of phosphorylated p38's translocation to the nucleus from day 1 to day 3 post infection. In the context of EBV infection, the increase in p38 activation which in turn can upregulate LMP1 is consistent with our hypothesis of a brief lytic burst followed by entry into latency. Importantly, we cannot discount the dual nature of p38 as it can regulate pro and anti-inflammatory processes, thus further research is needed to determine the downstream consequences of p38 modulation during EBV infection in these cells (Canovas & Nebreda, 2021).

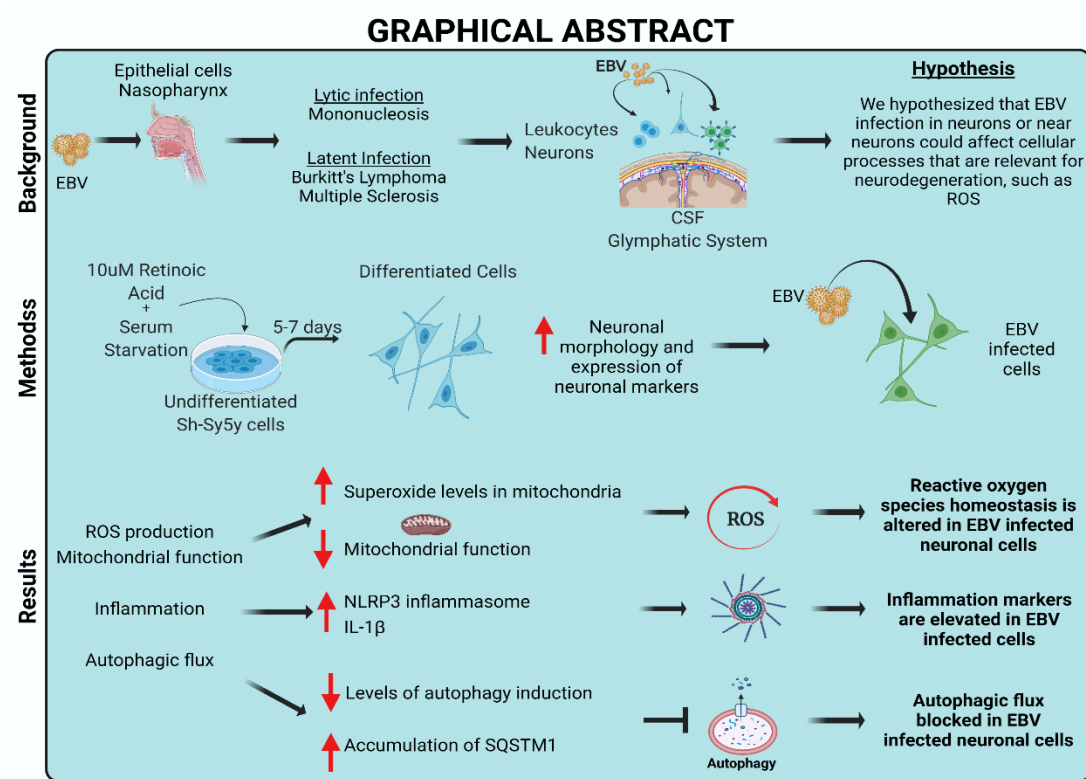
In summary, we demonstrated that RA-differentiated SH-SY5Y neuroblastoma are susceptible to EBV infection, and that viral entry is associated with RGD binding motifs that can be found in integrins, which are highly expressed in a variety of neuronal cells. We were able to detect GFP signals, indicative of lytic infection, up to day 2 post infection, and while we were unable to detect viral transcripts in the infected cells, we did observe differences between mock and EBV-infected cells suggesting that EBV can affect cellular processes that are important for neurodegenerative diseases. The dopaminergic neuronal marker D2DR had increased levels in EBV-infected cells in comparison to mock-infected cells. Activation of regulators of inflammation and autophagy, STAT3 and ERK respectively, were increased thus further research is needed to assert the effects of EBV infection on those cellular processes. The modulation of p38 also requires further investigation, but the mere fact that changes were seen indicates that EBV

infection could affect this important pathway. Overall, RA-differentiated cells present an unexplored and suitable cell model for further investigation of virus-host interactions of EBV in the CNS as they could be relevant to neurodegenerative diseases.

CHAPTER III: EBV INFECTION CAUSES AUTOPHAGIC FLUX BLOCK, CHANGES IN REACTIVE OXYGEN SPECIES HOMEOSTASIS AND INCREASE OF INFLAMMATORY MARKERS IN RETINOIC ACID-DIFFERENTIATED SH-SY5Y NEUROBLASTOMA CELLS

Introduction

Figure 3-1. Graphical Abstract



Epstein-Barr virus (EBV) is an enveloped, double-stranded DNA virus of the family *Herpesviridae* and virions possess a glycoprotein-studded envelope used by the virus to enter host cells (*Fields Virology | R2 Digital Library*, n.d.-a; Thorley-Lawson, 2015). EBV exists in over 90% of the world's human population, by infecting epithelial cells of the nasopharynx during its lytic cycle (productive), and B lymphocytes in its lytic and latent (dormant) cycles. The virus is associated with mononucleosis, and cancers such as Burkitt's lymphoma, nasopharyngeal carcinoma, and gastric carcinoma. Initial infection occurs in the tissue lining the area that contains the adenoids and tonsils, named the Waldeyer's Ring (*Fields Virology | R2 Digital*

Library, n.d.-b; Iizasa et al., 2012; Raab-Traub, 2015; Thorley-Lawson, 2015). EBV uses the viral glycoproteins gB and gH/gL to interact with cell surface proteins such as CD21, β 1, β 8, or α 5 integrins and initiate attachment to host cells, although this has not been established as the sole pathway for initiation of infection (Chesnokova et al., 2009; *Fields Virology | R2 Digital Library*, n.d.-b). EBV-infected epithelial and lytic B cells are able to shed virus and infect other cells such as astrocytes and microglia, via poorly understood mechanisms (*Fields Virology | R2 Digital Library*, n.d.-b; Hassani et al., 2018; Menet et al., 1999; Tugizov et al., 2007). EBV has been found in the cerebrospinal fluid, and in the brains of Parkinsonism patients, Parkinson's Disease (PD) symptoms caused by EBV encephalitis, and Multiple Sclerosis (MS) patients. Furthermore, *in vitro* studies and clinical data have provided evidence hinting to EBV's ability to abet CNS diseases (Bjornevik et al., 2022; Dimova et al., 2006; Gate, Saligrama, Leventhal, Yang, Unger, Middeldorp, Chen, Lehallier, Channappa, De Los Santos, et al., 2020; Guan et al., 2012; Hassani et al., 2018; Pedneault et al., 1992).

Initial EBV infection occurs in the Waldeyer's Ring near the olfactory epithelium in the nasal cavity, which encompasses bipolar olfactory receptor neurons (ORNs). These neurons have dendrites with ciliary projections containing odor molecule receptors, and axons extending through the lamina propria that eventually join to form the olfactory nerve with direct contact to the CNS (Barral & Croibier, 2009; Riel et al., 2015). Even if the Blood Brain Barrier (BBB) and uninfected immune cells shield the brain from viral insult, it is possible that molecular changes occur before effective clearance of the pathogen, or that viral infection can occur despite these mechanisms. ORNs projections provide a pathway to the CNS, and viral entry through this route via anterograde transport by the axons to the brain has been established for multiple viruses, including HSV1, Murine CMV, Murine Herpesvirus 4 (a gamma herpesvirus) and others (Durrant et al., 2016b; H. E. Farrell et al., 2016; P. J. Farrell, 2015; Koyuncu et al., 2013; Riel et al., 2015). Other viral sources are monocytes, macrophages and T-cells which can be infected by

EBV *in vitro* and *in vivo*, and contain EBV DNA while circulating in healthy, asymptomatic EBV carriers, thus B cells are not the only pathway to infection (Coleman et al., 2014, p. 2; Hassani et al., 2018; Tugizov et al., 2007). The Glymphatic system also provides an access point to the CNS for EBV-infected lymphocytes, which can sporadically reactivate into a lytic infection, or release molecular products such as cytokines or even EBERs that can be exported from cells via exosomes (Ahmed et al., 2014; Louveau et al., 2018; Soldan & Lieberman, 2020).

Recently, we showed that Retinoic-Acid (RA) differentiated SH-SY5Y neuroblastoma cells of human origin can be infected by EBV (manuscript in preparation). RA-differentiated SH-SY5Y cells have elevated expression of neuronal markers and present neuronal morphology (Shiple et al., 2016). They have been used consistently to study neurodegeneration and thus provide a way to compare those results to the ones obtained under viral infection, in the same cell model (Shiple et al., 2017). EBV infection of RA-differentiated SH-SY5Y cells led to lower cytosolic levels of p38 in EBV-infected cells compared to mock-infected, and a trend of increased nuclear translocation of p38, despite the fact that we could not detect any viral transcripts at 24-, 48-, and 72-hours post infection. Moreover, EBV-infected cells had significant increases the activation of STAT3 and ERK, molecular pathways that regulate a variety of cellular functions, including autophagy, Reactive Oxygen Species (ROS) homeostasis and inflammation responses (Cirone, 2018; Hung et al., 2014; Li & Bhaduri-McIntosh, 2016, p. 3). The research we present here aimed to answer whether EBV infection could alter autophagic flux, ROS homeostasis and mitochondrial function, and trigger inflammatory responses within RA-differentiated SH-SY5Y cells.

Autophagy allows for the degradation of cellular organelles and proteins to maintain cellular homeostasis and cell health. Over-expression and improper clearance of pathogenic protein is linked to neurological conditions such as Lewy Bodies (LB) and Alzheimer's disease (AD) (*Lewy Body - an Overview | ScienceDirect Topics*, n.d.; Volpicelli-Daley et al., 2011). EBV

can manipulate autophagy by packaging virions inside the autophagosome, and by preventing autophagosome fusion with lysosomes; this maintains viral progeny integrity. These autophagic vesicles traffic virions to the cell membrane to be released and infect other cells. This process occurs in B cells, yet we have no knowledge if the same is true for neuronal cells, or if this dysregulation of vesicle trafficking can lead to LB formation or other pathogenic protein aggregation (Granato et al., 2014).

Rigorous assessment of autophagic flux involves monitoring of LC3. This protein is altered by cleavage and lipidation, to give rise to LC3-II, which associates with autophagic membranes and it is degraded after autolysosome formation. (*CST - LC3B Antibody*, n.d.) Treating cells with the vacuolar proton pump inhibitor Bafilomycin can be used to determine if autophagic flux is being blocked and if the upstream or downstream pathways from fusion are the ones likely to be perturbed. In addition, SQSTM1 (p62), which is selectively degraded by autophagy, can be examined, as p62 is an adaptor protein for ubiquitinated targets, and its levels in the cell are maintained by autophagic degradation (Johansen & Lamark, 2011; Klionsky et al., 2016). Monitoring the levels of activated LC3 I/II and p62 can provide a robust picture of autophagic flux in the context of EBV infection. Examining autophagy in EBV-infected RA differentiated SH-SY5Y cells is crucial to assess the consequences of virus-host interactions in relation to neurological diseases as pathogenic protein accumulation is known to occur in several neurodegenerative diseases (Stephenson et al., 2018).

ROS such as superoxide anion (O_2^-) and hydrogen peroxide (H_2O_2) are produced intracellularly mainly by mitochondria and enzymes such as oxidase (Nox) during oxygen's partial reduction. Ultra violet light and certain drugs that rely on ROS production as part of their mechanism of action are some examples of extracellular ROS sources (G. H. Kim et al., 2015). ROS levels are tightly controlled by antioxidant enzymes like Superoxide Dismutase 1 (SOD1) in the cytosol and Superoxide Dismutase 2 (SOD2) in the mitochondria, which catalyze the

conversion of the superoxide anion into hydrogen peroxide and oxygen (Wang et al., 2018). ROS works in cellular pathways that regulate cell survival and cellular proliferation, thus are necessary to maintain cell health (G. H. Kim et al., 2015). Conversely, the overproduction of ROS and the inability of the cell to produce enough antioxidants in response, can alter ROS homeostasis and result in oxidative stress, leading to DNA and protein damage in addition to lipid oxidation (Ray et al., 2012). Oxidative stress and mitochondrial dysfunction are common hallmarks of neurodegenerative diseases (G. H. Kim et al., 2015).

EBV can alter ROS production and homeostatic regulation in infected cell, and could potentially disrupt the electron transport chain Complex 1 (ETC-C1), a system known to often malfunction in PD (Cirone, 2018; Y. Zhao et al., 2017). EBV's viral protein BZLF1 can power lytic replication by the activation of mTORC1 and enhance ROS production via the promotion of protein synthesis and oxidative metabolism. EBV was shown to decrease SOD1 activity and alter mitochondrial location in B cells. This combination of increased ROS and decreased antioxidant activity are observed in the brains of patients with neurodegenerative diseases (Gargouri et al., 2009; LaJeunesse et al., 2005; Y. Zhao et al., 2017). Moreover, changing mitochondrial localization can affect pre- and post-synaptic signaling, intracellular signaling, and many other functions in highly energy-dependent neuronal cells (MacAskill & Kittler, 2010). The maintenance of the mitochondrial membrane potential created by the electron transport chain is crucial for proper cellular functioning, and dysfunction of mitochondria is linked to AD, PD, MS, and other neurological disorders (G. H. Kim et al., 2015). In summary, EBV has been shown to manipulate ROS production, antioxidant activity and mitochondrial location in the cells it infects, and these are all mechanisms that are altered in neurodegenerative diseases. Recent studies that looked for EBV in deceased Alzheimer's or dementia patients' brains have conflicting reports: some had a viral presence, while others did not. These results are not conclusive to determine if viral interference was a factor at the late stages of disease, and cannot discount the

possibility that viral interference was of consequence in early disease stages, thus the necessity for this study (Gate, Saligrama, Leventhal, Yang, Unger, Middeldorp, Chen, Lehallier, Channappa, Santos, et al., 2020; Warren-Gash et al., 2019).

Imbalances in ROS homeostasis, mitochondrial dysfunction and autophagy disruption are commonly seen in neurodegenerative diseases and their occurrence is connected with inflammatory responses (Kelley et al., 2019; Kimura et al., 2016; Shintani & Klionsky, 2004; Stephenson et al., 2018). Natural ageing processes trigger the steady state of low inflammation, known as “inflammaging” which can be further exacerbated by additional inflammation caused by viral infections for example, and contribute to neurodegeneration (Stephenson et al., 2018). Innate immune responses to pathogens are initiated by PRRs, or pathogen-recognition receptors, upon sensing of pathogen-molecular patterns (PAMPs) and damage-associated molecular patterns (DAMPs) (Kelley et al., 2019). Responses to these stimuli are characterized by a two-step signaling process. The first step where the pathogen sensing by Toll-like receptors (TLR), which are included in the PRRs, induces the activation of NF- κ B and the subsequent translocation of its p65 subunit to the nucleus, it is known as the priming step. During the priming step the transcription of NLRP3 is induced as well as that of pro-IL-1 β , and pro-caspase-1 (C. Zhao & Zhao, 2020). The second event, also known as the activation signal, is triggered by a variety of PAMPs and DAMPs, such as ROS, mitochondrial injury, and protein aggregates, and it will lead to the formation and activation of the inflammasome complex (C. Zhao & Zhao, 2020).

Inflammasome complexes are formed by a multi-protein intracellular structure that once active will start the cleavage of pro-caspase-1, which will then coordinate the cleavage of IL-1 β (Kelley et al., 2019). In these complexes, there are several proteins known as sensor proteins, including the protein absent in melanoma 2 (AIM2) and NLR-family pyrin-domain containing proteins 1, 3 and 4, or NLRP1, NLRP3 and NLRP4 (Kelley et al., 2019; Kimura et al., 2015).

NLRP3 is particularly known to be active during viral infection and EBV has been shown to inhibit NLRP3 using the viral microRNA miR-BART15, and EBV-infected monocytes had increased transcript levels of AIM2 (Torii et al., 2017; C. Zhao & Zhao, 2020). The overlap between viral manipulation of processes that are hallmarks in neurodegeneration, in addition to increased evidence of EBV neurotropism warrant our preliminary investigations (Bjornevik et al., 2022; Roselli et al., 2006; Shim et al., 2017; Soldan & Lieberman, 2020). Furthermore, any insight into the cell biology associated with EBV infection of RA-differentiated SH-SY5Y neuroblastoma cells can be used to assess the need and possible efficacy of antiviral treatment to ameliorate the effects of neurodegenerative disease.

Methods

Cell culture and Differentiation

The EBfaV-GFP cell line is derived from the EBV-positive B958 cell line and contains a GFP marker to denote infected cells (Speck & Longnecker, 1999). Raji cells are EBV-positive B cells derived from a patient with Burkitt's lymphoma (ATCC). Both were grown in RPMI medium supplemented with 10% fetal bovine serum, antibiotics and antimycotics. SH-SY5Y neuroblastoma cells are a thrice cloned subline of the SK-N-SH neuroblastoma cell line obtained from a 4-year-old cancer patient with metastatic bone tumor (ATCC). Undifferentiated SH-SY5Y were grown in 1:1 DME-F12 with 10% fetal bovine serum, antibiotics and antimycotics. Differentiation was performed by culturing cells in serum reduced medium (1% fetal bovine serum-FBS) with the addition of 5 μ M Retinoic Acid for 5-7 days, changing the medium every other day and splitting as needed. All cells were kept in incubators with 5% CO₂ levels at 37°C. Differentiation status was confirmed via observation of cell morphology changes under light microscope and Dopamine Receptor 2 levels via Western blotting. SH-SY5Y neuroblastoma cells were a kind gift from Dr. Zhenquan Jia.

Virus Production, Collection, and Infectivity Assay

EBfaV-GFP cells were cultured in 100mL of RPMI with 3mM sodium butyrate and 20ng/ml of 12-O-tetradecanoylphorbol-13-acetate (TPA), to allow for virus production and shedding into the medium (also called induction). Visual inspection of GFP fluorescence via microscopy was performed 3 days post-induction to ensure cells were lytic. At day 6, cells and medium were centrifuged to pellet and remove the cells and the supernatant was filtered with a Corning sterilized 0.25µm filter to separate the virus from the cells. The supernatant was then ultracentrifuged in a Beckman Coulter Optima L-80 Floor Digital Ultracentrifuge using a fixed angle rotor type 70i at 24,000 rpm at 4°C for 90 minutes. The supernatant was discarded, and the remaining virus pellet was resuspended in either 1:1 DME/F12 or RPMI and stored at -80°C. Virus batches collected from EBfaV-GFP cells were tested to ensure they produced infectious virus. Briefly, Raji cells were induced in 5ml of RPMI with 3mM sodium butyrate and 20ng/ml of TPA in addition to 200-400µl of virus stock, while control cells only had fresh medium added. Cells were centrifuged to remove medium and GFP was detected via flow cytometry 2 days post-infection, using Guava easyCyte 6-2L and Guava easyCyte software both by Luminex corporation. Only virus batches that were shown to be infectious were used for experiments. For a few experiments (as noted), we used virus stock purchased from ATCC VR-1492 (HHV-4), this stock also infected the differentiated SH-SY5Y cells.

RNA Collection

RNA samples were collected using Trizol (Invitrogen) according to manufacturer's instructions. Cells were rinsed with 1XPBS (137mM NaCl, 2.7mM KCl, 10mM Na₂HPO₄, 1.8mM KH₂PO₄) and 300-400µL of Trizol was added to the sample to lyse the cells followed by trituration with a pipette to homogenize the lysate, followed by 5 minutes incubation at room temperature to dissociate nucleoproteins. Next, 80µl of chloroform was added and the lysate

was gently vortexed and incubated at room temperature for 3 minutes. The lysate was then centrifuged in an Eppendorf Centrifuge 5417R using rotor FA45-24-11 at 12,000rpm for 15 minutes at 4°C, which allowed the formation of 3 layers composed of an upper aqueous phase (which contains the RNA), and an interphase and lower phenol-red phase. The aqueous phase was gently removed by tilting the tube at a 45° angle and placed in a new tube to which 200µL of isopropanol was added for a 10-minute incubation period at room temperature to precipitate the RNA. Centrifugation at 12,000rpm for 10- minutes at 4°C followed, to pellet the RNA. The supernatant was discarded, and the pellet was resuspended in 400µL of 75% ethanol to wash the RNA, and vortexed and centrifuged at 4°C for 5 minutes at 7,500 rpm. The wash was discarded, and tubes were placed upside down to air dry for 5-10 minutes, before resuspension with 20-50µL of RNase free water. To ensure solubilization of the RNA, samples were immediately incubated for 15 min in a heat block at 55-60°C. Samples were stored at -80°C. RNA was quantified using NanoDrop One/One^C Microvolume UV-Vis Spectrophotometer.

DNA Collection

Viral DNA was collected using an Adamson lab modification of the HIRT protocol (*Modified Hirt Procedure for Rapid Purification of Extrachromosomal DNA from Mammalian Cells*, n.d.). Briefly, cells were scraped and centrifuged to remove media, and pellet was resuspended and incubated with 50mM pH 7.5 Tris, 10mM pH 8.0 EDTA and 1.2% SDS for 5 minutes at room temperature. This was followed by the addition of 350µL of precipitation buffer with 3M cesium chloride, 1M potassium acetate and 0.67M acetic acid and further incubation on ice for 15 minutes. Cells were then centrifuged at 4°C in an Eppendorf Centrifuge 5417R using rotor FA45-24-11 at 14,000 rpm for 15 minutes to pellet cellular debris. The supernatant was then loaded in a silica gel membrane spin tube and centrifuged for 30 seconds in an Eppendorf centrifuge Mini Spin at 7,000rpm. The flow-through was discarded and 750µL of wash buffer

composed of 80mM potassium acetate, 10mM Tris, 40μM EDTA and 60% ethanol was added. Tubes were centrifuged and the wash discarded, followed by elution of DNA with 20-50μL of TE. Quantification of the DNA was performed within a NanoDrop One/One^C Microvolume UV-Vis Spectrophotometer.

qRT-PCR

RNA at concentrations of 20-50ng/μL was amplified in a StepOne Real-Time PCR System (Applied Biosciences) using Power SYBR Green RNA-to-CT 1-Step Kit. Reactions were each prepared using 10μl of Power SYBR Green RT-PCR 2X mix, 20pmol each of forward and reverse primers, 0.16μL of RT enzyme Mix (125X), and RNase free water to 20μl total volume. Amplification was performed using the recommended setting of 30 minutes at 48°C for the RT step, 95°C for 10 minutes for polymerase activation, followed by 40 cycles of 95°C for 15 seconds (denaturation) and 60°C for 1 minute (annealing and extending). Primers used are listed below, and reactions were performed in technical triplicates and biological triplicates.

Table 3-1. Primer sequences

Target	Sequence	Specificity
SOD 1*	F: 5'-AGGGCATCATCAATTTTCGAG-3'	Human
	R: 5'- ACATTGCCCAAGTCTCCAAC-3'	
SOD 2*	F: 5'-TTGGCCAAGGGAGATGTTAC-3'	Human
	R: 5'-AGTCACGTTTGATGGCTTCC-3'	
IL-1 Beta (Liang et al., 2020)	F: 5'-CTGAGCTCGCCAGTGAAATG-3'	Human

	R: 5'-TGTCCATGGCCACAACAACACT-3'	
NLRP3 (Bai, n.d.)	F: 5'-GATCTTCGCTGCGATCAACAG-3'	Human
	R: 5'-CGTGCATTATCTGAACCCAC-3'	
AIM2 (X. Liu et al., 2013)	F: 5'-TTGAGACCCAAGAAGGCAAG-3'	Human
	R: 5'-CGTGAGGCGCTATTTACCTC-3'	
IL-18 (X. Liu et al., 2013)	F: 5'-TGGCTGCTGAACCAGTAGAA-3'	Human
	R: 5'-ATAGAGGCCGATTTCTTGG-3'	
GAPDH	F: 5' -AGA ACG GGA AGCTTGTCATC-3'	Human
	R: 5'-GGAGGC ATTGCTGATGATCT-3'	

*These primers were a kind gift of Dr. Zhenquan Jia.

Mitochondrial superoxide assay

Retinoic Acid differentiated SH-SY5Y cells were rinsed with 1X phosphate-buffered saline (PBS) and incubated for 10 minutes at 37°C in the dark with 5µM of MitoSOX™ Red Mitochondrial Superoxide Indicator dissolved in differentiation medium (Invitrogen-ThermoFisher catalog number:M36008). Control cells were treated with vehicle (DMSO) only. Immediately after incubation, experimental conditions either received 200µl of EBV stock, 1µM of Rotenone, or 1µM of PNQ (9,10-Phenanthrenequinone, Sigma-Aldrich catalog: 275034). Cells were incubated for 3 days, rinsed with 1X PBS and fluorescence emission at 580 nm was measured via flow cytometry with Guava easyCyte 6-2L and Guava easyCyte software by Luminex corporation.

Mitochondrial Membrane Potential

Differentiated SH-SY5Y cells were plated in Poly-L-Lysine coated coverslips and infected with 200 μ l of EBV stock or fresh medium only. At day 3 post-infection cells were either loaded with vehicle (DMSO) or 500nM of MitoTracker™ Red CMXRos (ThermoFisher, catalog:M7512), and incubated at 37°C in the dark for 30 minutes. Cells were then rinsed with 1XPBS and kept in the dark for remaining processing. The coverslips were incubated for 15 min at room temperature with 4% Paraformaldehyde, rinsed with 1XPBS and subsequently incubated in the dark with 1:2000 dilution of Hoechst stain for 5 minutes. Coverslips were then rinsed again with 1XPBS and mounted on slides. All Images were captured with a CY5 filter in a Keyence BZ-X170 All-in-One Fluorescence microscope at 20X and 40X magnification, and the acquisition settings were the same for all conditions in an individual trial. Fluorescence quantification was done using Image J software by NIH, using the control condition in each trial to threshold the images.

qPCR

PowerUp SYBR green master mix (Applied Biosciences) was used according to manufacturer specifications for primers with $T_m > 60^\circ\text{C}$. Each 20 μ l reaction was prepared using 10 μ l of PowerUp SYBR Green Master Mix (2X), 20pmol of forward and reverse primers for EBV's LIR sequence [(Long-Internal Repeat) with an expected product of 214bp - from bp 799-1042 in the 3072bp BamHI-W repeat fragment of EBV DNA], 1 μ l of DNA template and nuclease free water to the final volume. The cycling mode began at 50° C for 2 minutes for UDG (Uracil-DNA Glycosylase for PCR product stabilization for 72 hrs), 95° C for 2 minutes to activate the DNA polymerase followed by 40 cycles of 15 seconds at 95° C and 1 minute at 60° C. A standard curve with 5, 0.5, 0.05, and 0.005ng of EBV DNA collected from Raji cells using the modified HIRT protocol was performed with every run, and reactions were completed once with 2

technical replicates for the standard curve and experimental samples. Absolute quantification was performed, and the following equation was used to determine the viral copy number:

$$\text{Number of copies (molecules)} = \frac{X \text{ ng} * 6.0221 * 10^3 \text{ molecules/mole}}{\left(N * \frac{660\text{g}}{\text{mole}}\right) * 1 * 10^9 \frac{\text{ng}}{\text{g}}}$$

Where X= amount of amplicon in nanograms

N= length of dsDNA amplicon

600g/mole = average mass of 1 bp of dsDNA

SDS-PAGE Gel Electrophoresis and Western Blotting

Cells were collected by scraping and centrifuging (for adherent cells) or centrifuging alone (for suspension cells). Cells were rinsed once with 1XPBS and resuspended in 20-50 μ L of ELB lysis buffer (0.25M NaCl, 0.1% NP40 alternative detergent, 50mM HEPES pH 7.5, 5nM EDTA, protease inhibitors), then subjected to 2 freeze/thaw cycles of 5 minutes in the -80 $^{\circ}$ C freezer and 1 minute in a 37 $^{\circ}$ C water bath respectively, to crack the cells open. This was followed by centrifugation at 4 $^{\circ}$ C to concentrate the protein in the supernatant. Proteins were stored at -80 $^{\circ}$ C until use. Quantification was performed by Bradford Assay. Equal amounts of proteins (20-50 μ g) were separated with 10-12% SDS gels at 90V through stacking wells then at 125V through a separating gel submersed in Running Buffer (25mM Tris, 192 mM glycine, 0.1% SDS). Transfer to 0.45 μ m PVDF membrane was performed overnight in Electroblothing Buffer (25mM Tris, 192 mM glycine, 0.1% SDS, 10% methanol, pH 8.3) at 100mA, and membranes were blocked with 0.25% milk block (0.25% of powdered whole milk, 0.1% Tween in 1XPBS) and activated with 100% methanol prior to immunostaining. Incubation with primary antibodies was performed on a rocker for 1-3 hours at room temperature or overnight at 4 $^{\circ}$ C using manufacturer's recommended concentrations. Subsequent washes in Wash Buffer (1XPBS, 0.1% Tween) and 10–15-minute secondary antibody incubations were carried out in a SNAP i.d.

Protein Detection System by Millipore Sigma. Visualization and quantification of chemiluminescent protein bands were performed with WesternBright ECL HRP substrate (Advansta, catalog: K-12045-D20) in a C-DiGit Blot Scanner and Image Studio™ both by Li-Cor.

Table 3-2. Antibodies

<i>Antibody</i>	<i>Specificity</i>	<i>Manufacturer</i>
LC3 B	Human, mouse, rat	Cell Signaling, #2775S
SQSTM1	Human, mouse, and others	Cell Signaling, #5114
NF-κB	Human, mouse, and others	Cell Signaling, #3034
Histone (96C10)	Human, mouse, and others	Cell Signaling, #3638
Beta Actin (C-4)	Beta Actin (C-4)	Beta Actin (C-4)

Autophagy flux assay

Western blotting: SH-SY5Y neuroblastoma cells were differentiated and then treated with 200-400µl of EBV stock or vehicle (cell medium). On day 3 post-infection, relevant conditions were incubated with 50nM of Bafilomycin for 1 hour at 37°C. Cells for all conditions were rinsed with 1XPBS and ¼ of the sample was used for DNA collection and qPCR to confirm infectious status, and ¾ were used for SDS-PAGE Electrophoresis and Western Blotting.

Slide Coating with Poly-L-Lysine

Poly-L-Lysine 0.1% solution (w/v, catalog: P4707-50ml) was purchased from Millipore Sigma and diluted 1:10 in sterile diH₂O. Glass coverslips were rinsed with 1% HCl in 70% ethanol,

then rinsed with 1XPBS and incubated in the Poly-L-Lysine solution for 5 minutes at room temperature under sterile conditions. Coverslips were allowed to dry under UV light at room temperature overnight before being stored at room temperature for up to 3 months. Coverslips were rinsed 3 times with 1XPBS prior to use.

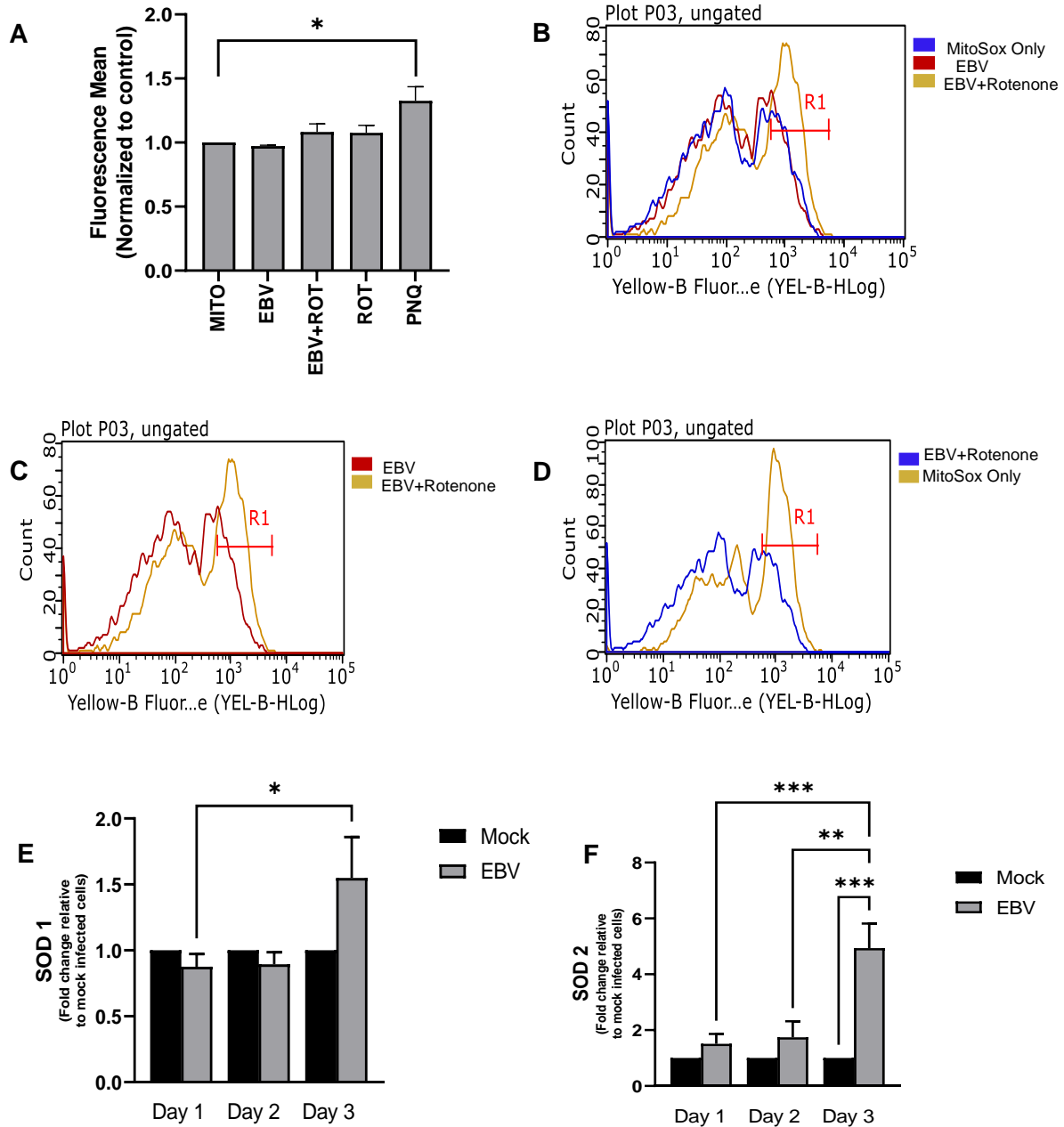
Results

RA-differentiated SH-SY5Y cells do not have increased mitochondrial superoxide levels after EBV infection

We had previously shown that EBV infection of RA-differentiated SH-SY5Y cells caused increases in activation of P38 and ERK, two central proteins of the MAPK pathway, and in STAT3, a main protein in the JAK/STAT pathway. These pathways are deeply connected to Reactive Oxygen Species (ROS) homeostasis and they have been shown to be involved in the increases in ROS noted during lytic reactivation of Raji cells (Gargouri et al., 2011). Notably, ROS homeostasis dysregulation, and particularly mitochondrial ROS, are factors in most neurodegenerative diseases (G. H. Kim et al., 2015). Thus, we hypothesized that mitochondrial superoxide levels could be affected in EBV-infected neuroblastoma cells. To investigate this hypothesis, cells were incubated with MitoSox Red Mitochondrial Superoxide indicator prior to infection with EBV (as described in Materials and Methods). We collected the cells at day 3 post-infection for flow cytometry analysis. As shown in Figure 3.2A-D, there are no significant differences in mitochondrial superoxide levels in EBV-infected cells in relation to mock-infected cells, contrary to our initial hypothesis. We then decided to assess the transcript levels of the two enzymes that function as catalysts to break down superoxide in the mitochondria and cytosol, SOD2 (Superoxide Dismutase 2) and SOD1 (Superoxide Dismutase 1). EBV-infected cells were collected at days 1, 2 and 3 post-infection for qRT-PCR. Figure 3-2E shows that EBV-infected cells had significantly higher levels of SOD1 at day 3 post-infection compared to

EBV-infected cells at day 1 post-infection. Most importantly, in Figure 3-2F, SOD2 levels increased consistently over days 1-3 and were significantly increased at day 3 post-infection in comparison to day 3 mock-infected as well as days 1 and 2 EBV-infected cells. Together these data imply that the lack of significant levels of superoxide detected in the mitochondria of EBV-infected cells at day 3 post-infection may have been due to the adequate homeostatic response of increasing SOD2 levels. Moreover, the increase in SOD1 at day 3 may be suggestive of superoxide production or leakage into the cytosol. The latter could be indicative of a problem often seen in neurodegenerative diseases: mitochondrial membrane malfunction.

Figure 3-2. EBV exposed cells do not have increased mitochondrial superoxide levels but have increased expression of antioxidant enzymes SOD1 and SOD2



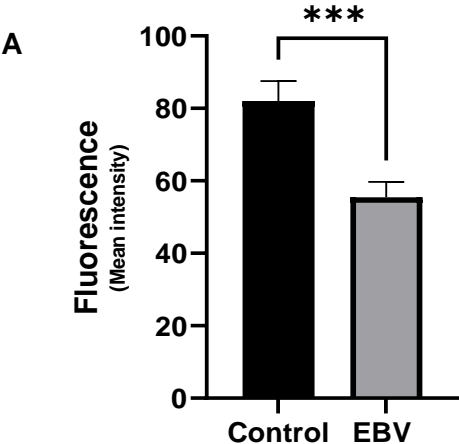
EBV exposed cells do not have significant changes in mitochondrial superoxide levels at day 3 post-infection in comparison to mock-infected cells. **A-** Cells were pre-loaded with

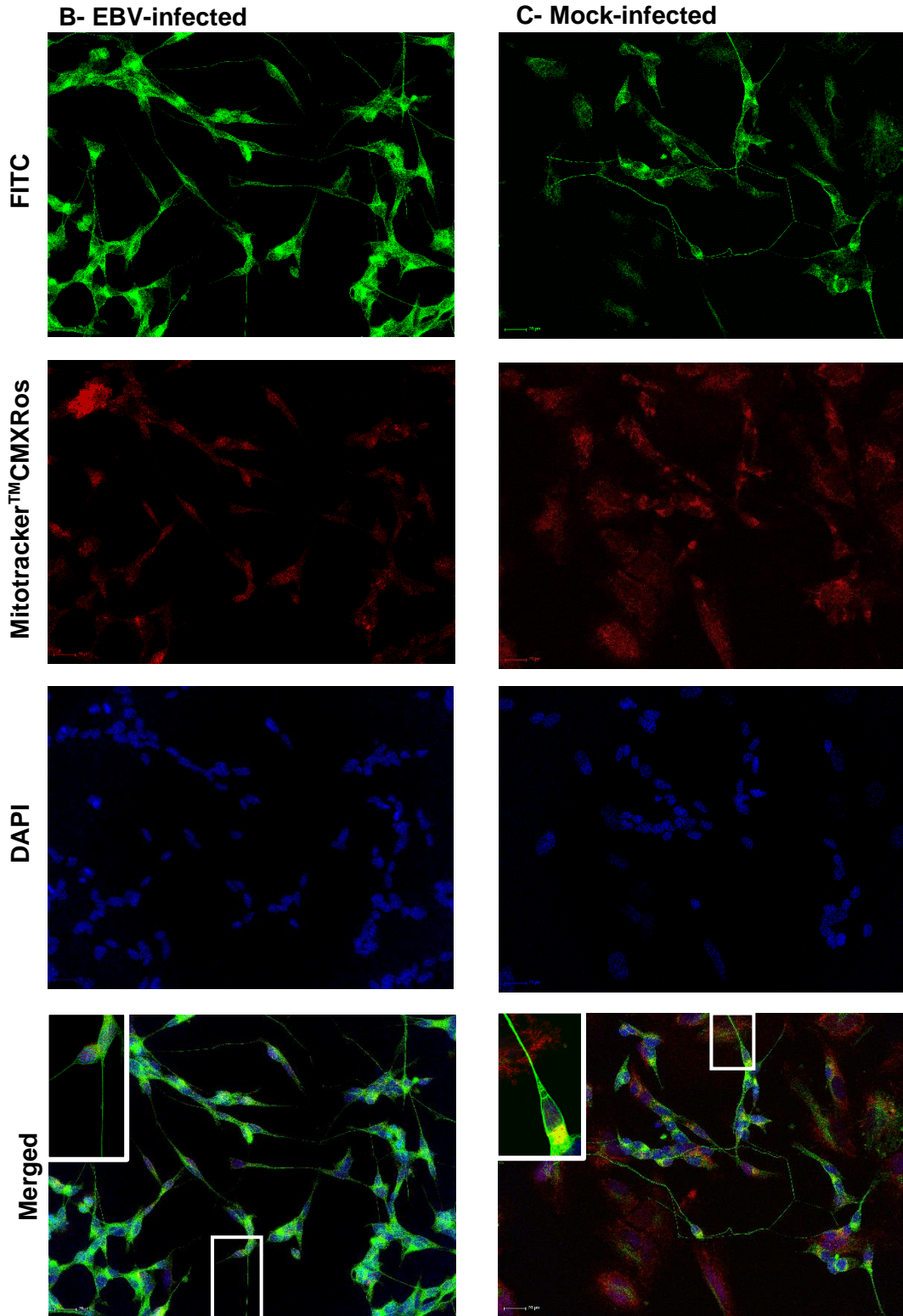
MitoSox RED before infection and were then collected 3 days post infection for flow cytometry analysis. **B-D-** Flow cytometry histograms representative of results. P-value * <0.05, data show is SEM of N=4 . One-way ANOVA, Tukey multiple comparisons. **E-** At day 3 post-infection, EBV exposed cells presented a significant increase in the expression of SOD 1 in relation to day 1 post infection. P-value * < 0.05. **F-** On day 3 post infection EBV exposed cells had a significant increase in SOD 2 in relation to days 1 and 2 post infection. P-value **<0.005, ***<0.0005. Student's T-Test. Data shown is SEM of N=3.

Mitochondrial activity of EBV-infected RA-differentiated cells is significantly lower than that of mock-infected cells

Next, we wanted to explore the consequences of EBV infection for mitochondrial function. Neuronal cells require high amounts of energy, and the quantity, localization and activity of mitochondria are crucial to maintain healthy neuronal cell health (Sherer et al., 2002). We measured mitochondrial membrane potential by incubating EBV-infected cells 3 days post-infection with MitoTracker™ Red CMXRos for 30 minutes and measuring fluorescence via microscopy (as described in Materials and Methods). As shown in Figure 3-A, EBV-infected cells had significantly lower fluorescence emission than mock-infected cells. Figure 3-3B and C show representative microscopy images of EBV-infected and mock-infected cells, respectively. These data suggest that EBV infection can reduce mitochondrial membrane potential thus change mitochondrial function and possibly disrupt ROS homeostasis in the process.

Figure 3-3. EBV-infected cells have lower mitochondrial membrane potential than mock-infected cells



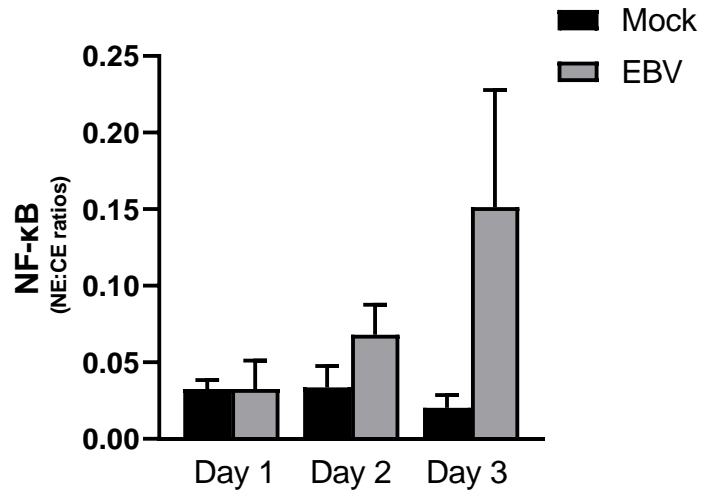


A- At 3 days post infection neuronal cells were incubated with 0.5 μ M of MitoTracker™ Red CMXRos, and Image J software was used to measure fluorescence intensity. **B,C-** Sample microscopy images of EBV-infected and Mock-infected cells, respectively. Statistical analysis used Student's T-test, SEM shown of N=3. P-value ***<0.0005.

RA-differentiated cells infected with EBV show a trend of NF- κ B translocation to the nucleus

Next, as we observed increases in molecules that also affect inflammatory pathways, we decided to investigate whether EBV infection would also activate the translocation of NF- κ B to the nucleus, as this is considered a hallmark, although not the only pathway, for the priming step of the inflammatory process. Cells were collected at days 1, 2 and 3 post-infection and cytosolic and nuclear extracts were used for Western blot analysis to quantify the translocation of the p65 subunit of NF- κ B to the nucleus. Figure 3 shows the trend in EBV-infected cells having higher p65 subunit translocation to the nucleus compared to EBV negative cells, despite the lack of statistical significance. This data suggests that NF- κ B could be involved in the priming step of inflammasome activation in EBV-infected neuroblastoma cells, although more experiments will be required to assert this.

Figure 3-4. NF- κ B could be activated during EBV infection of RA-differentiated SH-SY5Y neuroblastoma cells



EBV-infected cells were collected and the levels of NF- κ B's p65 subunit were measured via Western blotting. A trend of increased translocation to the nucleus is visible for the EBV-infected cells in comparison to mock-infected cells.

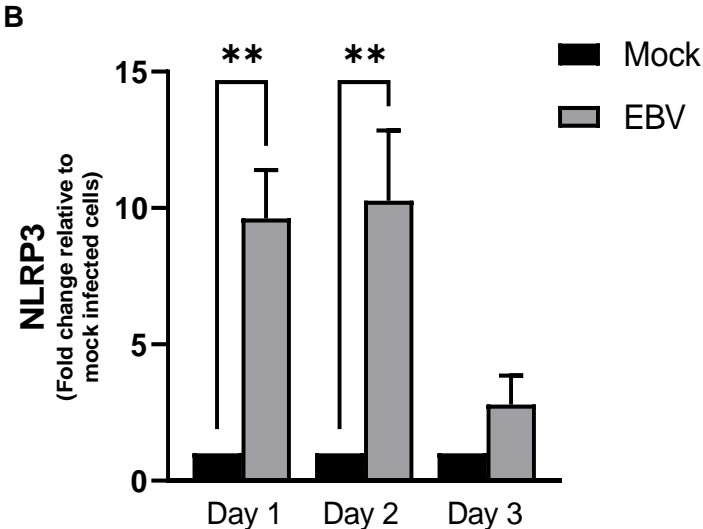
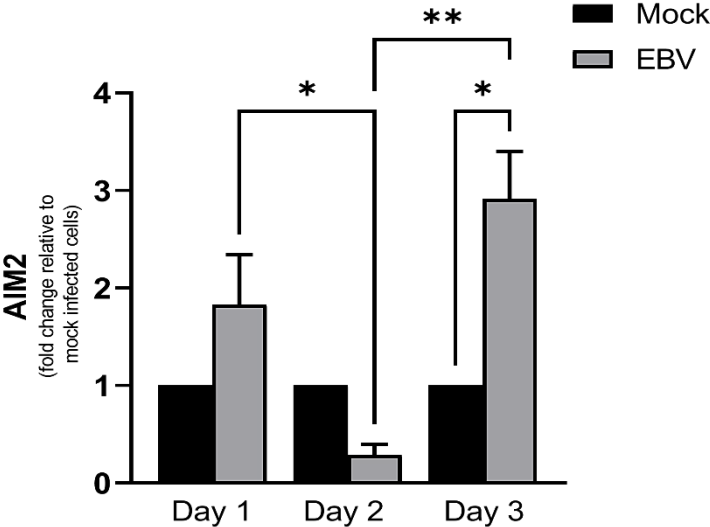
Inflammatory marker expression increases upon EBV infection of RA-differentiated SH-SY5Y cells

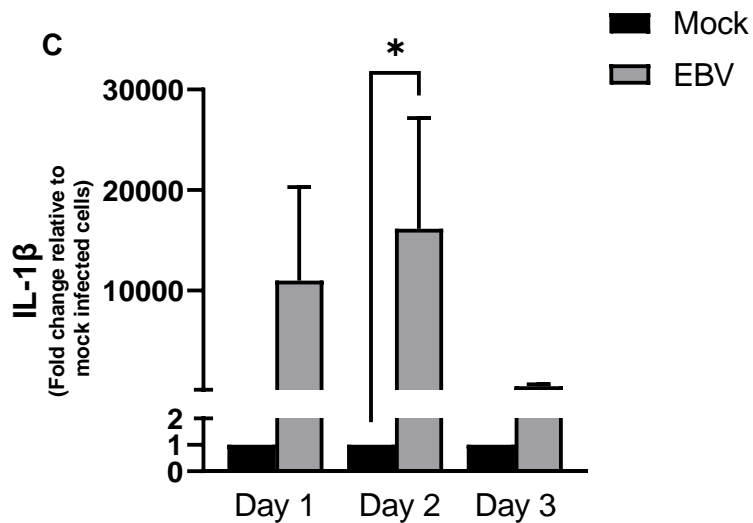
As ROS homeostasis appeared to be perturbed during EBV infection, we decided to check inflammatory marker levels, as they are another important aspect of neurodegenerative disease development and are known to be activated during viral infection(Stephenson et al., 2018; Torii et al., 2017). We collected RNA from EBV-infected cells at days 1, 2 and 3 post-infection and examined AIM2 (absent in melanoma 2), NLRP3 (NLR family pyrin domain containing 3), and IL-1 β (Interleukin 1 Beta) and transcript levels. Figures 3-5A, B, and C show our results for AIM2, NLRP3 and IL-1 β , respectively. AIM2 at day 2 post infection had

significantly lower levels than EBV-infected cells at day 1 post infection but presented a statistically significant increase at day 3 post infection compared to EBV-infected cells at day 2 post infection, and mock-infected cells at day 3 post infection. NLRP3 had significantly higher levels of expression at days 1 and 2 post-infection compared to mock-infected cells, suggesting the activation of the NLRP3 inflammasome complex. IL-1 β follows the same pattern by having considerably higher levels at day 1 post-infection and significantly higher levels at day 2 post-infection in relation to the uninfected cells. These data suggest that EBV infection of differentiated neuroblastoma cells resulted in the activation of NLRP3, which is a main component of the NLRP3 inflammasome complex, where the rate-limiting step of IL-1 β 's processing and secretion occurs.

A

Figure 3-5. EBV-infected neuroblastoma cells have higher expression of AIM2, NLRP3 and IL-1 β



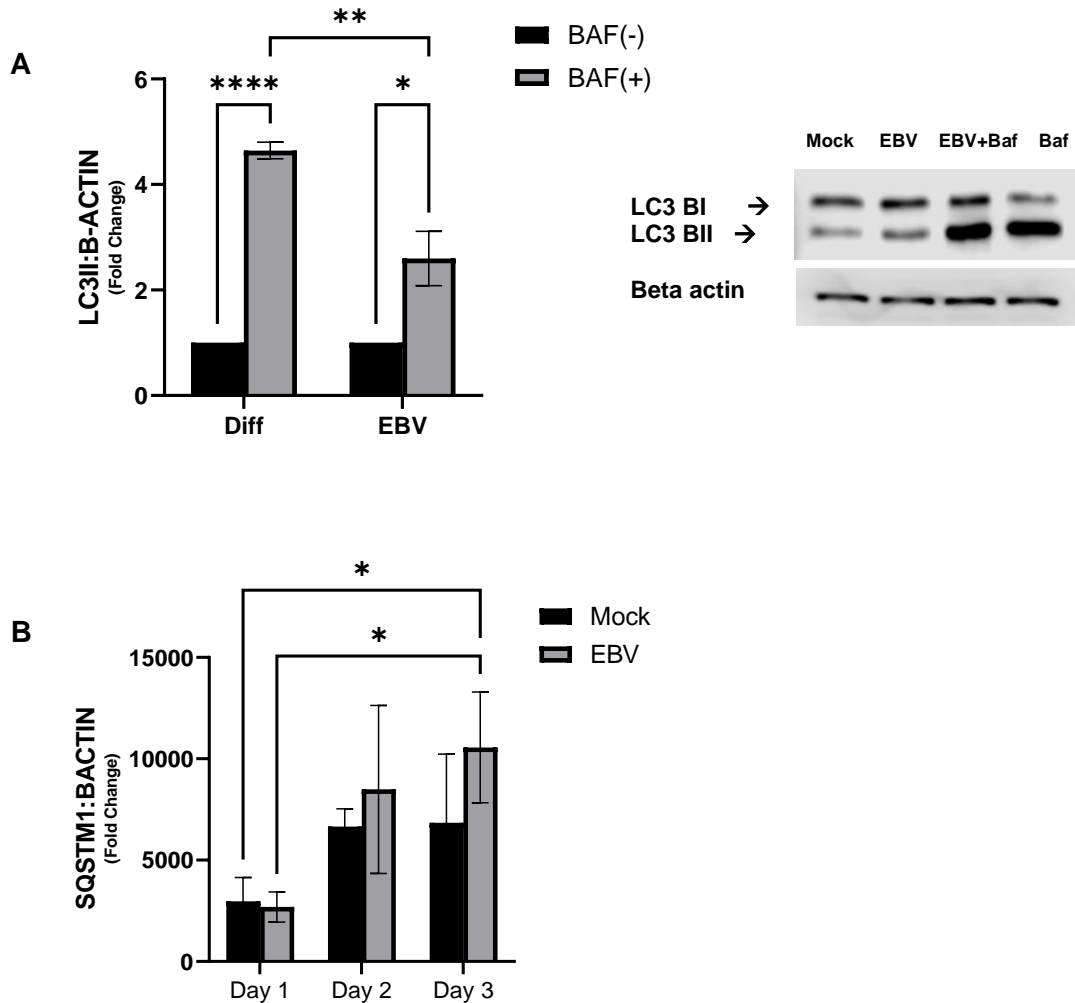


A- EBV-infected cells have significantly higher levels of AIM2 transcripts than mock-infected cells at day 3 post infection. Furthermore, AIM2 levels decrease significantly in EBV-infected cells from day 1 to day 2 post infection, followed by a significant increase from day 2 to day 3 post-infection. Data is from qRT-PCR, N=2. One-Way ANOVA with Sidak's multiple comparisons. **B-** Cells infected with EBV have significantly higher levels of NLRP3 expression in relation to mock-infected cells at days 1 and 2 post-infection. Data shown is qRT-PCR, N=3. ANOVA with Sidak's correction. P-value $** < 0.005$. **C-** At all 3 days post-infection, EBV-infected cells have higher levels of IL-1 β , an inflammatory marker, than mock-infected cells. On day 2 post-infection the increase is statistically significant in comparison to mock-infected cells. Data shown is qRT-PCR, N=3. ANOVA with Friedman's multiple comparisons, P-value $* < 0.05$.

Autophagy flux is blocked in EBV-infected cells

Another crucial cellular process in the development of neurodegenerative disease that is also manipulated by most viruses, including EBV, is autophagy. Viruses will hijack autophagic vesicles to export virions to the extracellular matrix or to prevent the degradation of viral products being produced in the cell upon infection (Cirone, 2018; De Leo et al., 2015). Therefore, we aimed to look at the levels of LC3B (Microtubule-associated protein light chain 3) and SQSTM1/p62, which are early and late indicators of autophagic flux function, respectively. Cells were infected with EBV as previously described. Cells being used for LC3B assessment were treated with 50 μ M of Bafilomycin for 1 hour prior to collection to inhibit the vacuolar type H⁺-ATPase, thus preventing acidification of autophagosomes. Cells being used to assess p62 levels were infected with EBV and collected at days 1, 2 and 3 post-infection. Figure 3-6A shows that EBV-infected cells have significantly lower levels of autophagy compared to control cells. In Figure 3-6B our data shows that p62 levels consistently increase as the infection progresses and that day 3 post-infection has significantly higher levels of p62 compared to day 1 EBV-infected and control cells. Together, these data suggest that despite the absence of viral products, autophagic flux is blocked in EBV-infected cells. This could potentially promote toxic protein accumulation and prime neuronal cells for further injury.

Figure 3-6. RA-differentiated SH-SY5Y cells infected with EBV have obstructed autophagic flux compared to mock-infected cells



A- Late stages of autophagy are blocked in EBV-infected cells. EBV-infected cells present lower levels of LC3BII/B-Actin than mock-infected cells. Cells were infected or mock-infected with EBV, and relevant conditions were incubated for 1 hour with 50µM of Bafilomycin or vehicle at day 3 post-infection. Data shown from Western blots, N=3. ANOVA with Tukey post-hoc. P-value * <0.05, **< 0.005, ****< 0.0005. **B-** Late stages of autophagy are blocked in EBV exposed cells. During days 1-3 post-infection SQSTM1 levels increase and are

significantly higher at day 3 in EBV-infected cells. Data shown from Western blots, N=3. Two-way ANOVA with Tukey post-hoc. P-value * <0.05.

Discussion

We recently demonstrated that EBV can infect RA-differentiated SH-SY5Y neuroblastoma cells (manuscript in preparation), which are a suitable model for neurodegenerative disease studies as they have been extensively used to understand neurological disease (Kovalevich & Langford, 2013; Rcom-H'cheo-Gauthier et al., 2017; Shipley et al., 2016). We also noted that EBV-infected cells had elevated phosphorylation levels of STAT3 and ERK and increased levels of p38 translocation to the nucleus. These molecules are in pathways that control ROS, autophagy and inflammation, processes that are often found dysregulated in PD, AD, MS (Kelley et al., 2019; G. H. Kim et al., 2015; Rivero-Ríos et al., 2016; Yan et al., 2013). Based on these observations we wanted to investigate if EBV infection could alter ROS homeostasis, mitochondrial function, autophagic flux and inflammation.

To achieve this goal, we assayed mitochondrial superoxide levels in EBV-infected RA-differentiated neuroblastoma cells at 3 days post infection, as we had previously established this to be a relevant time point due to the increases in STAT3, ERK and p38. Using MitoSOX Red mitochondrial superoxide indicator levels, our data showed that at day 3 post-infection EBV-infected cells and mock-infected cells had similar levels of mitochondrial superoxide, suggesting that EBV infection did not increase superoxide in the mitochondria. To build upon these results, we also performed qRT-PCR in EBV-infected cells at days 1, 2, and 3 post infection to assess the progression of the expression of SOD1 and SOD2. We demonstrated that EBV-infected cells at day 3 have significantly higher levels of SOD1 than EBV-infected cells at day 1 post infection, and overall SOD1 expression is higher in EBV-infected cell at day 3 post infection compared to mock-infected cells. Importantly, we showed that at day 3 post infection SOD2

expression is significantly higher in EBV-infected cells compared to that of mock-infected cells. Furthermore, there is a significant increase in SOD2 expression of EBV-infected cells between days 1 and 2 post infection in relation to day 3 post infection. These data reveal that the absence of excess superoxide in the mitochondria of EBV-infected cells compared to mock-infected cells may be the result of effective homeostatic regulation of ROS levels in RA-differentiated SH-SY5Y cells. This hints at EBV's ability to interfere in the ROS pathway to cause the production of additional superoxide, not observed under mock-infected conditions. Aging neuronal cells may not be able to respond as promptly to these ROS insults as they already have higher levels of ROS and Reactive Nitrogen Species (RNS), and EBV infection could tip the ROS homeostasis scale to the pathogenic side (Erickson & Banks, 2019). Even if EBV infection is transient, repeated induction of high superoxide levels can prime neuronal cells to further damage. Moreover, superoxide originates mostly in the mitochondria and this organelle's function is crucial for highly energy dependent neuronal cells with reduced ability to perform glycolysis, and thus rely heavily on mitochondria for its energetic needs (Yan et al., 2013). Other organelles such as the endoplasmic reticulum can also produce ROS, thus could contribute to its homeostasis, and EBV infection effects should be investigated under this scenario (Zorov et al., 2014). Finally, other ROS levels such as H_2O_2 should also be explored in future studies. Hydrogen peroxide is the product of superoxide's dismutation and as a non-charged molecule, it can freely travel to the cytoplasm where it could also affect ROS homeostasis (Schieber & Chandel, 2014).

Considering the suggested increases in superoxide seen in EBV cells, we then questioned whether EBV infection could alter mitochondrial membrane function in RA-differentiated SH-SY5Y cells. We demonstrated here that mitochondrial membrane potential is significantly lower in EBV-infected cells in relation to mock-infected cells at day 3 post infection, which indicate the presence of malfunctioning mitochondria. Mitochondrial dysfunction is

present in neurodegenerative diseases such as AD and PD and increases in cellular ROS can damage mitochondrial DNA (mtDNA). These events can further perpetuate the mitochondrial dysfunction, creating a cycle of insult where damage to mtDNA leads to mitochondrial dysfunction, leading to more ROS production, which in turn can cause more mtDNA damage (Yan et al., 2013). Conversely, decreased mitochondrial potential can impair the cell's ability to produce ATP and thus cause ROS levels below those required for homeostasis, a state which is also harmful to the cells known as reductive stress (Zorova et al., 2018). It should also be considered that EBV infection could have an effect in mitochondrial dynamics – fusion and fission – which could have altered ROS homeostasis and induced the lower mitochondrial membrane potential seen in the infected cells (MacAskill & Kittler, 2010). Either scenario suggests potential harmful effects for EBV infection of neuronal cells.

Inflammatory pathways can be triggered by excessive ROS and mitochondrial damage, and inflammation is present in neurodegenerative disease states and in viral infections (Gros Lambert & Py, 2018; Q. Liu et al., 2018; C. Zhao & Zhao, 2020, p. 3). Thus, we wanted to explore the effects of EBV infection on inflammasome activation, particularly AIM2 and NLRP3 which had been previously shown to be manipulated by the virus (Torii et al., 2017; C. Zhao & Zhao, 2020). We began by analyzing the main player on inflammasome priming, NF- κ B, as its activation and subsequent translocation to the nucleus are required for this step. NF- κ B stimulation can occur during viral infection and detection of pathogens by PRRs, and this in turn can activate TNF- α and IFN- β , leading to additional NF- κ B activation and NLRP3 activation (C. Zhao & Zhao, 2020). In fact, EBV virions and the viral glycoprotein gp350's interaction with cell host receptors (TLRs) activate NF- κ B, using a signaling pathway dependent on MyD88. Interestingly, viral sensing responses that go through the MyD88 pathway regulate the induction of NLRP3 (Kelley et al., 2019). As we had hypothesized, NF- κ B's p65 subunit demonstrated a consistent increase in translocation to the nucleus. This trend, while not statistically significant,

led us hypothesize that inflammasome activation could have taken place, being potentiated by PAMPs and DAMPs such as the ROS and mitochondrial dysfunction seen in our previous results.

To assess inflammasome activation we performed qRT-PCR to determine the levels of expression of three crucial inflammatory molecules that had been previously implicated in EBV infection: AIM2, NLRP3 and IL-1 β (Torii et al., 2017). We demonstrated that AIM2 and NLRP3 transcripts were upregulated in EBV-infected RA-differentiated neuroblastoma cells. While AIM2 transcript levels only showed a modest increase at day 1 post infection and a decrease at day 2, at day 3 post infection there is a significant increase in relation to day 3 mock-infected cells and in relation to EBV-infected cells at days 1 and 3 post infection, indicating that AIM2 activation occurred. EBV infection has been shown to increase the expression of AIM2 in human monocytes, and this resulted in the cleavage of pro-caspase-1 and the activation of caspase-1, thus the AIM2 inflammasome is implicated in the inflammatory reaction to EBV infection (Torii et al., 2017). NLRP3 was significantly upregulated immediately, at days 1 and 2 post infection, indicating that the virus was quickly sensed by innate responses in RA-differentiated SH-SY5Y cells. Our data suggests that EBV infection could have led to NLRP3 activation either by direct EBV activation of PRRs or indirectly through the production of ROS and mitochondrial dysfunction (C. Zhao & Zhao, 2020). Previous research also reports that EBV's viral protein LMP1 and viral RNAs mir-BHRFs and miR-BARTs can activate and modulate NLRP3, and EBV DNA can activate AIM2 and NLRP3 (Jangra et al., 2019). Remarkably, exosomes from EBV-infected B cells can carry miR-BART15, which upon entering an uninfected cell can inhibit NLRP3 activation (Jangra et al., 2019). Our data in conjunction with these previous reports provide multiple pathways by which EBV infection could modulate the inflammatory response and severely abet neurological disease. These results led us to question whether another process that is relevant for neurodegeneration and can be manipulated by EBV was perturbed

in RA-differentiated cells infected with EBV: autophagy (Cirone, 2018; Shintani & Klionsky, 2004).

To investigate the effects of EBV infection in RA-differentiated SH-SY5Y cells, we treated them for one hour prior to collection with the vacuolar-type H⁺-ATPase [V-ATPase] enzyme inhibitor, Bafilomycin (Baf). The use of this inhibitor blocks the fusion of autophagosomes with lysosomes, thus preventing the formation of autophagolysosomes. Comparing the levels of LC3BII protein between treatment plus Baf in relation to treatment alone, to those of untreated in relation to untreated with Baf, will indicate whether autophagic flux block at this step has occurred (Klionsky et al., 2016). What we would expect to see in the case of autophagic block then, are lower levels of LC3BII in EBV-infected cells that were also treated with Baf in comparison to LC3BII levels of cells with Baf alone. EBV has been reported to inhibit and induce autophagy depending on the circumstances of infection. During lytic replication, the virus induces autophagy to make use of autophagic vesicles for viral assembly and transport. Conversely, EBV inhibits autophagy during latency to avoid the recognition of viral particles by the immune system, thus evading host defenses (Cirone, 2018). EBV's viral proteins LMP1, EBNA3C, Z, LMP2A and others have been reported to block autophagy in the early steps during *de novo* infection, and to inhibit late steps during viral reactivation from latency (Cirone, 2018). Here we demonstrate EBV-infected RA-differentiated SH-SY5Y have autophagic block at the late stages of autophagy, as seen by the lower levels of LC3BII accumulation seen in the EBV+Baf condition in relation to the Baf alone condition. These results suggest that EBV may have disrupted autophagy either to use vesicles to promote lytic replication or to prevent immune system detection.

To further evaluate autophagic block we assayed the levels of the protein sequestosome1 (p62) via Western blot, as this protein is selectively degraded during autophagy and its accumulation indicates blockade in the final steps of the process (Klionsky et al., 2016).

We and others have previously reported that EBV infection can activate the STAT3 pathway which is known to also regulate autophagy. In addition, EBV infection has been reported to block the degradation of p62 (Montani et al., 2019). Our data shows that p62 levels are significantly higher in EBV-infected cells at day 3 post infection compared to mock and EBV-infected cells at day 1 post infection. Together, these data indicate that autophagic flux is blocked in EBV-infected RA-differentiated cells. This blockade can promote the accumulation of pathogenic proteins and organelles such as mitochondria which in turn would increase levels of ROS and inflammation in the cell, which are all represented in our data (Kelley et al., 2019). Furthermore, dysregulation of autophagy could specifically affect the process of precision autophagy by which inflammatory molecules such as NLRP3 and pro-caspase 1, are degraded to prevent excessive inflammation (Kimura et al., 2015). Further studies should be done to assess the direct involvement of EBV in these processes.

In summary, we demonstrated that EBV infection of RA-differentiated SH-SY5Y cells likely increased superoxide levels in the mitochondria that were met with increases in SOD1 and 2 production, and mitochondrial activity was reduced. We also showed that AIM2, NLRP3 and IL-1 β transcript expressions were significantly higher, and that autophagic flux was blocked in EBV-infected cells in comparison to mock-infected. Together, these data indicate that EBV has the potential to alter cellular processes that are crucial for the development of neurodegenerative diseases, thus further in-depth studies of each process should be conducted to further elucidate EBV's involvement.

CHAPTER IV: DISCUSSION

Recently, EBV has been linked to several neurological diseases and the need for affordable, practical, and relevant cell models to study virus-host interactions has risen (Bjornevik et al., 2022; Shim et al., 2017; J. M. Woulfe et al., 2014). We aimed to investigate the suitability of RA-differentiated SH-SY5Y neuroblastoma cells to study the effects of EBV infection in neuronal cells because they have been widely used to investigate neuronal diseases (Deng et al., 2005; Murakami et al., 2017; Shipley et al., 2017). This provides a plethora of data that can be used to compare cellular responses to viral infection and neurological disease in the same system. First, we demonstrated that our RA-differentiated cells had the morphology and increased D2DR neuronal marker expression noted in differentiated cells. Undifferentiated SH-SY5Y cells have been shown to be permissive to EBV infection with the aid of a transfection reagent (Polybrene), but had not been previously demonstrated in their RA-differentiated state where much of their transcriptional profile is changed, thus we had to first establish if they could become infected by EBV (Jha et al., 2015; Korecka et al., 2013; Pezzini et al., 2017). Our results showed that RA-differentiated cells are susceptible to EBV infection without the use of a transfection reagent, and that we were able to detect a GFP signal up to day 2 post-infection using flow cytometry. This seemed to suggest a transient infection state or the establishment of latency, as the GFP signal would only be present during the lytic replication stage of EBV infection (Speck & Longnecker, 1999, p. 958).

Notably, when we checked the phosphorylation levels of the serine-threonine protein kinase Akt, which have been reported to be upregulated in RA-differentiated SH-SY5Y cells, there were no significant differences between mock and EBV-infected cells. Akt regulates cell growth and differentiation amongst other cellular functions, therefore this seemed to indicate that cell differentiation was not affected during EBV infection (Cheung et al., 2009; J. Luo et al., 2003). Concordant with this result, we did not see any visual indication of cell death in the EBV-

infected cultures, similar to EBV infection in B cells when the virus enters B lymphocytes and maintains latency in the cells without much disruption of regular cellular function (Thorley-Lawson, 2015). Similarly, the widely neurotropic Herpes Simplex I (HSV-1) Infection of RA-differentiated SH-SY5Y cells did not promote change in the phosphorylation levels of Akt, thus this may be a commonality between EBV and HSV-1 infection of these cells (Shiple et al., 2016).

Interestingly, we observed that the expression of D2DR was significantly higher in EBV-infected cells in comparison to mock-infected cells. EBV's viral protein Z has been shown to bind directly to retinoic acid receptors RAR (Retinoic Acid Receptors) and RXR (Retinoic X Receptors), which are active in the RA differentiation process (Dreyfus et al., 1999). RA binds to RARs, which further heterodimerize with RXRs then bind to RARE (RA Response Element) to regulate transcription of differentiation genes (Xie et al., 2010). Thus, it is possible that the increased levels of D2DR are due to increased activation of the RA pathway by EBV viral protein Z. Notably and of great importance is the function of D2DR as an auto-receptor and regulator of dopamine synthesis, release and uptake, which if dysregulated could have significant effects on neuronal function (Ayano, 2016; Ford, 2014; Pan et al., 2019).

An important aspect of EBV biology is that the virus seems to follow specific patterns of infection depending of the cell type infected, as noted by the classification of the latency states (Thorley-Lawson, 2015). Understanding the patterns of viral entry and attachment may reveal aspects of viral infection that follow an already known pattern. We were able to demonstrate that blocking the RGD epitope of RA-differentiated cells prior to EBV exposure resulted in a dose-dependent decrease in viral genome in the infected cells, suggesting that RGD binding motifs play a role in viral entry and attachment in these cells. RGD binding motifs are composed of the Arginine-Glycine-Aspartate tripartite amino acid that is present in multiple integrins, such as $\alpha 5\beta 1$, $\alpha 8\beta 1$, $\alpha v\beta 1$ and others. Integrins are highly expressed in the CNS and the cell membrane

of astrocytes, microglia, neurons and other neuronal cell types express many different integrins (Peluffo et al., 2007). The ability of EBV to use this motif to enter RA-differentiated cells supports that the virus could also enter other neuronal cells by the same mechanism, thus giving EBV the chance to interact with cells in the CNS.

We examined viral transcript expression of BZLF1, the viral lytic cascade initiator, and of two transcripts that are observed in all known latent programs, EBNA1 and EBERs 1/2 (Thorley-Lawson, 2015). We collected RNA from infected cells at 24-, 48-, and 72-hours post infection. To investigate entry into latency, we also treated EBV-infected cells with a lytic induction cocktail of TPA and sodium butyrate two days prior to collecting them at days 5, 7 and 9 post infection. Surprisingly, we were unable to detect any of the three viral transcripts in any of the above-described conditions, despite having infection status confirmed by qPCR (data not shown). We had hypothesized that viral transcripts would peak starting at 24hrs post infection, as this is a common time point seen in other cell types and even in undifferentiated SH-SY5Y cells (Jha et al., 2015; X. Liu et al., 2013). Our results suggest that viral expression may have peaked and subsided prior to our earliest time point of 24hrs, and the GFP expression seen up to day 2 post-infection may be residual, and only possible due to the GFP protein half-life and fluorescence signal strength combined with the high sensitivity of flow cytometry. EBV has been reported to express the lytic transcript Z in B cells as early as 2hrs post lytic reactivation and EBERs were shown to peak at 12 hrs post-reactivation (Yuan et al., 2006). Therefore, future studies where EBV's viral transcript production is examined in the first 24hrs post infection are needed.

Despite our inability to detect EBV's viral products, we report that STAT3 and ERK are significantly activated upon EBV infection of RA-differentiated SH-SY5Y cells. STAT3 (signal transducer and activator of transcription), once phosphorylated translocates to the nucleus and can activate the transcription of genes related to immunity, apoptosis and embryogenesis. In

fact, suppression of STAT3 can promote inflammasome activation (Bai, n.d.). EBV entry alone can activate STAT3 via JAK (Janus Kinase) pathway as can EBV's viral protein LMP1. Notably for our results, high levels of STAT3 have been shown to impede the cell's ability to enter or remain in the lytic state (Koganti et al., 2015; Li & Bhaduri-McIntosh, 2016, p. 3). Our data shows that STAT3 is significantly upregulated at day 3 post infection, at the same time we can no longer detect the GFP signal indicative of EBV's lytic cycle. It is possible that EBV entry or LMP1 activated the phosphorylation of STAT3, which in turn undermined the lytic cycle leaving the cells with undetectable levels of viral transcripts. To further support this hypothesis future experiments should investigate STAT3 levels after day 3 post infection and should include a broader assessment of latent transcripts that includes all of EBV's latent products. This could elucidate if these cells did enter latency but failed to reactivate upon chemical induction due to consistent high levels of phosphorylated STAT3. ERK (extracellular signal-regulated kinase) phosphorylation during EBV infection has been shown to induce autophagy and to activate the transcription of Z lytic viral protein (Hung et al., 2014; Lee et al., n.d.). ERK activation occurs as a response to environmental stress, including viral infection (Canovas & Nebreda, 2021). Our results show that ERK significantly increased in phosphorylation at day 1 post infection, and its activation decreases at day 2, with day 3 post infection being significantly lower than EBV-infected cells at day 1 post infection. These data underline the possibility that RA-differentiated SH-SY5Y cells experience a brief burst of viral transcription (as noted by GFP signals up to day 2 post infection) perhaps followed by entry into latency, as suggested by our data showing the increase in STAT3 phosphorylation at day 3 post infection.

As one of the MAPKs (mitogen-activated protein kinases), p38 phosphorylation can have many cellular consequences, including the stimulation of activator protein 1 (AP-1), which can initiate inflammatory cytokine production, like STAT3, and the regulation of autophagy (Canovas & Nebreda, 2021). Downregulation of p38 has been shown to decrease the expression of EBV's

viral latent protein LMP1, and the activation of p38 via external stress stimuli or cytokines has been linked to EBV's evasion of apoptosis (Johansson et al., 2010; Singh et al., 2021). In relation to neuronal cells, the activation of p38 has also been associated with Tau protein hyperphosphorylation in AD and neuroinflammation in PD (Canovas & Nebreda, 2021; Corrêa & Eales, 2012). Our results we show that cytosolic p38 has significantly lower levels at days 1 and 2 post infection in relation to mock-infected cells, implying that EBV infection could have hindered p38 activity. When we investigated the nuclear levels of p38 activation however, we observed a consistent increase of phosphorylated p38's translocation to the nucleus from day 1 to day 3 post infection. In the context of EBV infection, the increase in p38 activation which in turn can upregulate LMP1 is consistent with our hypothesis of a brief lytic burst followed by entry into latency. Importantly, we cannot discount the dual nature of p38 as it can regulate pro and anti-inflammatory processes, thus further research is needed to determine the downstream consequences of p38 modulation during EBV infection in these cells (Canovas & Nebreda, 2021).

In summary, we demonstrated that RA-differentiated SH-SY5Y neuroblastoma are susceptible to EBV infection, and that viral entry is associated with RGD binding motifs that can be found in integrins, which are highly expressed in a variety of neuronal cells. We were able to detect GFP signals, indicative of lytic infection, up to day 2 post infection, and while we were unable to detect viral transcripts in the infected cells, we did observe differences between mock and EBV-infected cells suggesting that EBV can affect cellular processes that are important for neurodegenerative diseases. The dopaminergic neuronal marker D2DR had increased levels in EBV-infected cells in comparison to mock-infected cells. Activation of regulators of inflammation and autophagy, STAT3 and ERK respectively, were increased thus further research is needed to assert the effects of EBV infection on those cellular processes. The modulation of p38 also requires further investigation, but the mere fact that changes were seen indicates that EBV

infection could affect this important pathway. Overall, RA-differentiated cells present an unexplored and suitable cell model for further investigation of virus-host interactions of EBV in the CNS as they could be relevant to neurodegenerative diseases.

Based on these observations we wanted to investigate if EBV infection could alter ROS homeostasis, mitochondrial function, autophagic flux and inflammation. To achieve this goal, we assayed mitochondrial superoxide levels in EBV-infected RA-differentiated neuroblastoma cells at 3 days post infection, as we had previously established this to be a relevant time point due to the increases in STAT3, ERK and p38. Using MitoSOX Red mitochondrial superoxide indicator levels, our data showed that at day 3 post-infection EBV-infected cells and mock-infected cells had similar levels of mitochondrial superoxide, suggesting that EBV infection did not increase superoxide in the mitochondria.

To build upon these results, we also performed qRT-PCR in EBV-infected cells at days 1, 2, and 3 post infection to assess the progression of the expression of SOD1 and SOD2. We demonstrated that EBV-infected cells at day 3 have significantly higher levels of SOD1 than EBV-infected cells at day 1 post infection, and overall SOD1 expression is higher in EBV-infected cell at day 3 post infection compared to mock-infected cells. Importantly, we showed that at day 3 post infection SOD2 expression is significantly higher in EBV-infected cells compared to that of mock-infected cells. Furthermore, there is a significant increase in SOD2 expression of EBV-infected cells between days 1 and 2 post infection in relation to day 3 post infection. These data reveal that the absence of excess superoxide in the mitochondria of EBV-infected cells compared to mock-infected cells may be the result of effective homeostatic regulation of ROS levels in RA-differentiated SH-SY5Y cells. This hints at EBV's ability to interfere in the ROS pathway to cause the production of additional superoxide, not observed under mock-infected conditions. Aging cells may not be able to respond as promptly to these ROS insults as they already have higher levels of ROS and Reactive Nitrogen Species (RNS),

and EBV infection could tip the ROS homeostasis scale to the pathogenic side (Erickson & Banks, 2019). Even if EBV infection is transient, repeated induction of high superoxide levels can prime neuronal cells to further damage. Moreover, superoxide originates mostly in the mitochondria and this organelle's function is crucial for highly energy dependent neuronal cells with reduced ability to perform glycolysis, and thus rely heavily on mitochondria for its energetic needs (Yan et al., 2013).

Considering the suggested increases in superoxide seen in EBV cells, we then questioned whether EBV infection could alter mitochondrial membrane function in RA-differentiated SH-SY5Y cells. We demonstrated here that mitochondrial membrane potential is significantly lower in EBV-infected cells in relation to mock-infected cells at day 3 post infection, which indicate the presence of malfunctioning mitochondria. Mitochondrial dysfunction is present in neurodegenerative diseases such as AD and PD and increases in cellular ROS can damage mitochondrial DNA (mtDNA). These events can further perpetuate the mitochondrial dysfunction, creating a cycle of insult where damage to mtDNA leads to mitochondrial dysfunction, leading to more ROS production, which in turn can cause more mtDNA damage (Yan et al., 2013). Conversely, decreased mitochondrial potential can impair the cell's ability to produce ATP and thus cause ROS levels below those required for homeostasis, a state which is also harmful to the cells known as reductive stress (Zorova et al., 2018). It should also be considered that EBV infection could have an effect in mitochondrial dynamics – fusion and fission – which could have altered ROS homeostasis and induced the lower mitochondrial membrane potential seen in the infected cells (MacAskill & Kittler, 2010). Either scenario suggests potential harmful effects for EBV infection of neuronal cells.

Inflammatory pathways can be triggered by excessive ROS and mitochondrial damage, and inflammation is present in neurodegenerative disease states and in viral infections

(Gros Lambert & Py, 2018; Q. Liu et al., 2018; C. Zhao & Zhao, 2020, p. 3). Thus, we wanted to explore the effects of EBV infection on inflammasome activation, partic

ularly AIM2 and NLRP3 which had been previously shown to be manipulated by the virus (Torii et al., 2017; C. Zhao & Zhao, 2020). We began by analyzing the main player on inflammasome priming, NF- κ B, as its activation and subsequent translocation to the nucleus are required for this step. NF- κ B stimulation can occur during viral infection and detection of pathogens by PRRs, and this in turn can activate TNF- α and IFN- β , leading to additional NF- κ B activation and NLRP3 activation (C. Zhao & Zhao, 2020). In fact, EBV virions and the viral glycoprotein gp350's interaction with cell host receptors (TLRs) activate NF- κ B, using a signaling pathway dependent on MyD88. Interestingly, viral sensing responses that go through the MyD88 pathway regulate the induction of NLRP3 (Kelley et al., 2019). As we had hypothesized, NF- κ B's p65 subunit demonstrated a consistent increase in translocation to the nucleus. This trend, while not statistically significant, led us hypothesize that inflammasome activation could have taken place, being potentiated by PAMPs and DAMPs such as the ROS and mitochondrial dysfunction seen in our previous results.

To assess inflammasome activation we performed qRT-PCR to determine the levels of expression of three crucial inflammatory molecules that had been previously implicated in EBV infection: AIM2, NLRP3 and IL-1 β (Torii et al., 2017). We demonstrated that AIM2 and NLRP3 transcripts were upregulated in EBV-infected RA-differentiated neuroblastoma cells. While AIM2 transcript levels only showed a modest increase at day 1 post infection and a decrease at day 2, at day 3 post infection there is a significant increase in relation to day 3 mock-infected cells and in relation to EBV-infected cells at days 1 and 3 post infection, indicating that AIM2 activation occurred. EBV infection has been shown to increase the expression of AIM2 in human monocytes, and this resulted in the cleavage of pro-caspase-1 and the activation of caspase-1, thus the AIM2 inflammasome is implicated in the inflammatory reaction to EBV infection (Torii et

al., 2017). NLRP3 was significantly upregulated immediately, at days 1 and 2 post infection, indicating that the virus was quickly sensed by innate responses in RA-differentiated SH-SY5Y cells. Our data suggests that EBV infection could have led to NLRP3 activation either by direct EBV activation of PRRs or indirectly through the production of ROS and mitochondrial dysfunction (C. Zhao & Zhao, 2020). Previous research also reports that EBV's viral protein LMP1 and viral RNAs mir-BHRFs and miR-BARTs can activate and modulate NLRP3, and EBV DNA can activate AIM2 and NLRP3 (Jangra et al., 2019). Remarkably, exosomes from EBV-infected B cells can carry miR-BART15, which upon entering an uninfected cell can inhibit NLRP3 activation (Jangra et al., 2019). Our data in conjunction with these previous reports provide multiple pathways by which EBV infection could modulate the inflammatory response, which can severely abet neurological disease. These results led us to question whether another process that is relevant for neurodegeneration and can be manipulated by EBV was perturbed in RA-differentiated cells infected with EBV: autophagy (Cirone, 2018; Shintani & Klionsky, 2004).

To investigate the effects of EBV infection in RA-differentiated SH-SY5Y cells, we treated them for one hour prior to collection with the vacuolar-type H⁺-ATPase [V-ATPase] enzyme inhibitor, Bafilomycin (Baf). The use of this inhibitor blocks the fusion of autophagosomes with lysosomes, thus preventing the formation of autophagolysosomes. Comparing the levels of LC3BII protein between treatment plus Baf in relation to treatment alone, to those of untreated in relation to untreated with Baf, will indicate whether autophagic flux block at this step has occurred (Klionsky et al., 2016). What we would expect to see in the case of autophagic block then, are lower levels of LC3BII in EBV-infected cells that were also treated with Baf in comparison to LC3BII levels of cells with Baf alone. EBV has been reported to inhibit and induce autophagy depending on the circumstances of infection. During lytic replication, the virus induces autophagy to make use of autophagic vesicles for viral assembly

and transport. Conversely, EBV inhibits autophagy during latency to avoid the recognition of viral particles by the immune system, thus evading host defenses (Cirone, 2018). EBV's viral proteins LMP1, EBNA3C, Z, LMP2A and other have been reported to block autophagy in the early steps during de novo infection, and to inhibit late steps during viral reactivation from latency (Cirone, 2018). Here we demonstrate EBV-infected RA-differentiated SH-SY5Y have autophagic block at the late stages of autophagy, as seen by the lower levels of LC3BII accumulation seen in the EBV+Baf condition in relation to the Baf alone condition. These results suggest that EBV may have disrupted autophagy either to use vesicles to promote lytic replication or to prevent immune system detection.

To further evaluate autophagic block we assayed the levels of the protein sequestosome1 (p62) via Western blot, as this protein is selectively degraded during autophagy and its accumulation indicated blockade in the final steps of the process (Klionsky et al., 2016). We and others have previously reported that EBV infection can activate the STAT3 pathway which is known to also regulate autophagy. In addition, EBV infection has been reported to block the degradation of p62 (Montani et al., 2019). Our data shows that p62 levels are significantly higher in EBV-infected cells at day 3 post infection compared to mock and EBV-infected cells at day 1 post infection. Together, these data indicate that autophagic flux is blocked in EBV-infected RA-differentiated cells. This blockade can promote the accumulation of pathogenic proteins and organelles such as mitochondria which in turn would increase levels of ROS and inflammation in the cell, which are all represented in our data (Kelley et al., 2019). Furthermore, dysregulation of autophagy could specifically affect the process of precision autophagy by which inflammatory molecules such as NLRP3 and pro-caspase 1, are degraded to prevent excessive inflammation (Kimura et al., 2015). Further studies should be done to assess the direct involvement of EBV in these processes. In summary, we demonstrated that EBV infection of RA-differentiated SH-SY5Y cells likely increased superoxide levels in the

mitochondria that were met with increases in SOD1 and 2 production, and mitochondrial activity was reduced. We also showed that AIM2, NLRP3 and IL-1 β transcript expressions were significantly higher, and that autophagic flux was blocked in EBV-infected cells in comparison to mock-infected. Together, these data indicate that EBV has the potential to alter cellular processes that are crucial for the development of neurodegenerative diseases, thus further in-depth studies of each process should be conducted to further elucidate EBV's involvement.

REFERENCES

- Ahmed, W., Philip, P. S., Tariq, S., & Khan, G. (2014). Epstein-Barr Virus-Encoded Small RNAs (EBERs) Are Present in Fractions Related to Exosomes Released by EBV-Transformed Cells. *PLOS ONE*, 9(6), e99163. <https://doi.org/10.1371/journal.pone.0099163>
- Allnutt, M. A., Johnson, K., Bennett, D. A., Connor, S. M., Troncoso, J. C., Pletnikova, O., Albert, M. S., Resnick, S. M., Scholz, S. W., De Jager, P. L., & Jacobson, S. (2020). Human Herpesvirus 6 Detection in Alzheimer's Disease Cases and Controls across Multiple Cohorts. *Neuron*. <https://doi.org/10.1016/j.neuron.2019.12.031>
- Aromseree, S., Middeldorp, J. M., Pientong, C., Eijndhoven, M. van, Ramayanti, O., Lougheed, S. M., Pegtel, D. M., Steenbergen, R. D. M., & Ekalaksananan, T. (2017). High Levels of EBV-Encoded RNA 1 (EBER1) Trigger Interferon and Inflammation-Related Genes in Keratinocytes Expressing HPV16 E6/E7. *PLOS ONE*, 12(1), e0169290. <https://doi.org/10.1371/journal.pone.0169290>
- Ayano, G. (2016). Dopamine: Receptors, Functions, Synthesis, Pathways, Locations and Mental Disorders: Review of Literatures. *Journal of Mental Disorders and Treatment*, 2(2). <https://doi.org/10.4172/2471-271X.1000120>
- Bai. (n.d.). *Downregulation of signal transduction and STAT3 expression exacerbates oxidative stress mediated by NLRP3 inflammasome*. Retrieved January 11, 2022, from <https://www.nrronline.org/article.asp?issn=1673-5374;year=2018;volume=13;issue=12;spage=2147;epage=2155;aulast=Bai>
- Barral, J.-P., & Croibier, A. (2009). Chapter 10—Olfactory nerve. In J.-P. Barral & A. Croibier (Eds.), *Manual Therapy for the Cranial Nerves* (pp. 59–72). Churchill Livingstone. <https://doi.org/10.1016/B978-0-7020-3100-7.50013-6>
- Bhandari, T. (2017, September 14). *Medical history can point to earlier Parkinson's disease diagnosis*. Washington University School of Medicine in St. Louis.

<https://medicine.wustl.edu/news/medical-history-can-point-earlier-parkinsons-disease-diagnosis/>

Bjornevik, K., Cortese, M., Healy, B. C., Kuhle, J., Mina, M. J., Leng, Y., Elledge, S. J., Niebuhr, D. W., Scher, A. I., Munger, K. L., & Ascherio, A. (2022). Longitudinal analysis reveals high prevalence of Epstein-Barr virus associated with multiple sclerosis. *Science (New York, N.Y.)*. <https://doi.org/10.1126/science.abj8222>

Bourgade, K., Le Page, A., Bocti, C., Witkowski, J. M., Dupuis, G., Frost, E. H., & Fülöp, T. (2016). Protective Effect of Amyloid- β Peptides Against Herpes Simplex Virus-1 Infection in a Neuronal Cell Culture Model. *Journal of Alzheimer's Disease: JAD*, *50*(4), 1227–1241. <https://doi.org/10.3233/JAD-150652>

Braak, H., Rüb, U., Gai, W. P., & Del Tredici, K. (2003). Idiopathic Parkinson's disease: Possible routes by which vulnerable neuronal types may be subject to neuroinvasion by an unknown pathogen. *Journal of Neural Transmission*, *110*(5), 517–536. <https://doi.org/10.1007/s00702-002-0808-2>

Cadwell, K. (2015). The virome in host health and disease. *Immunity*, *42*(5), 805–813. <https://doi.org/10.1016/j.immuni.2015.05.003>

Canovas, B., & Nebreda, A. R. (2021). Diversity and versatility of p38 kinase signalling in health and disease. *Nature Reviews Molecular Cell Biology*, *22*(5), 346–366. <https://doi.org/10.1038/s41580-020-00322-w>

Casiraghi, C., Dorovini-Zis, K., & Horwitz, M. S. (2011). Epstein-Barr virus infection of human brain microvessel endothelial cells: A novel role in multiple sclerosis. *Journal of Neuroimmunology*, *230*(1), 173–177. <https://doi.org/10.1016/j.jneuroim.2010.08.003>

Chesnokova, L. S., Jiang, R., & Hutt-Fletcher, L. M. (2015). Viral Entry. In C. Münz (Ed.), *Epstein Barr Virus Volume 2: One Herpes Virus: Many Diseases* (pp. 221–235). Springer International Publishing. https://doi.org/10.1007/978-3-319-22834-1_7

- Chesnokova, L. S., Nishimura, S. L., & Hutt-Fletcher, L. M. (2009). Fusion of epithelial cells by Epstein-Barr virus proteins is triggered by binding of viral glycoproteins gHgL to integrins alphavbeta6 or alphavbeta8. *Proceedings of the National Academy of Sciences of the United States of America*, *106*(48), 20464–20469.
<https://doi.org/10.1073/pnas.0907508106>
- Cheung, Y.-T., Lau, W. K.-W., Yu, M.-S., Lai, C. S.-W., Yeung, S.-C., So, K.-F., & Chang, R. C.-C. (2009). Effects of all-trans-retinoic acid on human SH-SY5Y neuroblastoma as in vitro model in neurotoxicity research. *NeuroToxicology*, *30*(1), 127–135.
<https://doi.org/10.1016/j.neuro.2008.11.001>
- Cho, H.-J., & Song, M. J. (2014). A Gammaherpesvirus Establishes Persistent Infection in Neuroblastoma Cells. *Molecules and Cells*, *37*(7), 518–525.
<https://doi.org/10.14348/molcells.2014.0024>
- Cirone, M. (2018). EBV and KSHV Infection Dysregulates Autophagy to Optimize Viral Replication, Prevent Immune Recognition and Promote Tumorigenesis. *Viruses*, *10*(11).
<https://doi.org/10.3390/v10110599>
- Cohen, J. I. (2015). Primary Immunodeficiencies Associated with EBV Disease. In C. Münz (Ed.), *Epstein Barr Virus Volume 1: One Herpes Virus: Many Diseases* (pp. 241–265). Springer International Publishing. https://doi.org/10.1007/978-3-319-22822-8_10
- Coleman, C. B., Wohlford, E. M., Smith, N. A., King, C. A., Ritchie, J. A., Baresel, P. C., Kimura, H., & Rochford, R. (2014). Epstein-Barr Virus Type 2 Latently Infects T Cells, Inducing an Atypical Activation Characterized by Expression of Lymphotactic Cytokines. *Journal of Virology*. <https://journals.asm.org/doi/abs/10.1128/JVI.03001-14>
- Corrêa, S. A. L., & Eales, K. L. (2012). The Role of p38 MAPK and Its Substrates in Neuronal Plasticity and Neurodegenerative Disease. *Journal of Signal Transduction*, *2012*, 1–12.
<https://doi.org/10.1155/2012/649079>

- CST - LC3B Antibody. (n.d.). Retrieved June 2, 2019, from www.cellsignal.com/products/primary-antibodies/lc3b-antibody/2775&Ntt=lc3bantib&thead=true
- Cuervo, A. M., & Wong, E. (2014). Chaperone-mediated autophagy: Roles in disease and aging. *Cell Research*, *24*(1), 92–104. <https://doi.org/10.1038/cr.2013.153>
- De Leo, A., Colavita, F., Ciccocanti, F., Fimia, G. M., Lieberman, P. M., & Mattia, E. (2015). Inhibition of autophagy in EBV-positive Burkitt's lymphoma cells enhances EBV lytic genes expression and replication. *Cell Death & Disease*, *6*(9), e1876–e1876. <https://doi.org/10.1038/cddis.2015.156>
- Delwart, E. (2013). A Roadmap to the Human Virome. *PLOS Pathogens*, *9*(2), e1003146. <https://doi.org/10.1371/journal.ppat.1003146>
- Deng, H., Jankovic, J., Guo, Y., Xie, W., & Le, W. (2005). Small interfering RNA targeting the PINK1 induces apoptosis in dopaminergic cells SH-SY5Y. *Biochemical and Biophysical Research Communications*, *337*(4), 1133–1138. <https://doi.org/10.1016/j.bbrc.2005.09.178>
- Dimova, P. S., Bojinova, V., Georgiev, D., & Milanov, I. (2006). Acute reversible parkinsonism in Epstein–Barr virus–related encephalitis lethargica-like illness. *Movement Disorders*, *21*(4), 564–566. <https://doi.org/10.1002/mds.20742>
- Dorner, M., Zucol, F., Alessi, D., Haerle, S. K., Bossart, W., Weber, M., Byland, R., Bernasconi, M., Berger, C., Tugizov, S., Speck, R. F., & Nadal, D. (2010). B1 Integrin Expression Increases Susceptibility of Memory B Cells to Epstein-Barr Virus Infection. *Journal of Virology*, *84*(13), 6667–6677. <https://doi.org/10.1128/JVI.02675-09>
- Dreyfus, D. H., Nagasawa, M., Pratt, J. C., Kelleher, C. A., & Gelfand, E. W. (1999). Inactivation of NF- κ B by EBV BZLF-1-Encoded ZEBRA Protein in Human T Cells. *The Journal of Immunology*, *163*(11), 6261–6268.

- Dugan, J. P., Coleman, C. B., & Haverkos, B. (2019). Opportunities to Target the Life Cycle of Epstein-Barr Virus (EBV) in EBV-Associated Lymphoproliferative Disorders. *Frontiers in Oncology*, 9. <https://www.frontiersin.org/article/10.3389/fonc.2019.00127>
- Durrant, D. M., Ghosh, S., & Klein, R. S. (2016a). The Olfactory Bulb: An Immunosensory Effector Organ during Neurotropic Viral Infections. *ACS Chemical Neuroscience*, 7(4), 464–469. <https://doi.org/10.1021/acschemneuro.6b00043>
- Durrant, D. M., Ghosh, S., & Klein, R. S. (2016b). The Olfactory Bulb: An Immunosensory Effector Organ during Neurotropic Viral Infections. *ACS Chemical Neuroscience*, 7(4), 464–469. <https://doi.org/10.1021/acschemneuro.6b00043>
- Epstein, A. (2015). Why and How Epstein-Barr Virus Was Discovered 50 Years Ago. In C. Münz (Ed.), *Epstein Barr Virus Volume 1: One Herpes Virus: Many Diseases* (pp. 3–15). Springer International Publishing. https://doi.org/10.1007/978-3-319-22822-8_1
- Erickson, M. A., & Banks, W. A. (2019). Age-Associated Changes in the Immune System and Blood–Brain Barrier Functions. *International Journal of Molecular Sciences*, 20(7). <https://doi.org/10.3390/ijms20071632>
- Ew, H., & N, S. (2020). Lymphotropic Viruses: Chronic Inflammation and Induction of Cancers. *Biology*, 9(11). <https://doi.org/10.3390/biology9110390>
- Farrell, H. E., Lawler, C., Tan, C. S. E., MacDonald, K., Bruce, K., Mach, M., Davis-Poynter, N., & Stevenson, P. G. (2016). Murine Cytomegalovirus Exploits Olfaction To Enter New Hosts. *MBio*, 7(2). <https://doi.org/10.1128/mBio.00251-16>
- Farrell, P. J. (2015). Epstein–Barr Virus Strain Variation. In C. Münz (Ed.), *Epstein Barr Virus Volume 1: One Herpes Virus: Many Diseases* (pp. 45–69). Springer International Publishing. https://doi.org/10.1007/978-3-319-22822-8_4
- Fields Virology | R2 Digital Library*. (n.d.-a). Retrieved November 17, 2018, from <https://www-r2library-com.libproxy.uncg.edu/resource/detail/1451105630/ch0061s3383>

Fields Virology | R2 Digital Library. (n.d.-b). Retrieved November 22, 2018, from <https://www-r2library-com.libproxy.uncg.edu/resource/detail/1451105630/ch0061s3345>

Ford, C. P. (2014). The Role of D2-Autoreceptors in Regulating Dopamine Neuron Activity and Transmission. *Neuroscience*, 282, 13–22.

<https://doi.org/10.1016/j.neuroscience.2014.01.025>

Gargouri, B., Nasr, R., ben Mansour, R., Lassoued, S., Mseddi, M., Attia, H., El Feki, A. el F., & Van Pelt, J. (2011). Reactive Oxygen Species Production and Antioxidant Enzyme Expression after Epstein–Barr Virus Lytic Cycle Induction in Raji Cell Line. *Biological Trace Element Research*, 144(1), 1449–1457. <https://doi.org/10.1007/s12011-011-9135-5>

Gargouri, B., Van Pelt, J., El Feki, A. E. F., Attia, H., & Lassoued, S. (2009). Induction of Epstein-Barr virus (EBV) lytic cycle in vitro causes oxidative stress in lymphoblastoid B cell lines. *Molecular and Cellular Biochemistry*, 324(1), 55–63.

<https://doi.org/10.1007/s11010-008-9984-1>

Gate, D., Saligrama, N., Leventhal, O., Yang, A. C., Unger, M. S., Middeldorp, J., Chen, K., Lehallier, B., Channappa, D., De Los Santos, M. B., McBride, A., Pluvinage, J., Elahi, F., Tam, G. K.-Y., Kim, Y., Greicius, M., Wagner, A. D., Aigner, L., Galasko, D. R., ... Wyss-Coray, T. (2020). Clonally expanded CD8 T cells patrol the cerebrospinal fluid in Alzheimer's disease. *Nature*, 577(7790), 399–404. <https://doi.org/10.1038/s41586-019-1895-7>

Gate, D., Saligrama, N., Leventhal, O., Yang, A. C., Unger, M. S., Middeldorp, J., Chen, K., Lehallier, B., Channappa, D., Santos, M. B. D. L., McBride, A., Pluvinage, J., Elahi, F., Tam, G. K.-Y., Kim, Y., Greicius, M., Wagner, A. D., Aigner, L., Galasko, D. R., ... Wyss-Coray, T. (2020). Clonally expanded CD8 T cells patrol the cerebrospinal fluid in

- Alzheimer's disease. *Nature*, 577(7790), 399–404. <https://doi.org/10.1038/s41586-019-1895-7>
- Granato, M., Santarelli, R., Farina, A., Gonnella, R., Lotti, L. V., Faggioni, A., & Cirone, M. (2014). Epstein-Barr Virus Blocks the Autophagic Flux and Appropriates the Autophagic Machinery To Enhance Viral Replication. *Journal of Virology*, 88(21), 12715–12726. <https://doi.org/10.1128/JVI.02199-14>
- Gros Lambert, M., & Py, B. F. (2018). Spotlight on the NLRP3 inflammasome pathway. *Journal of Inflammation Research*, 11, 359–374. <https://doi.org/10.2147/JIR.S141220>
- Guan, J., Lu, Z., & Zhou, Q. (2012). Reversible parkinsonism due to involvement of substantia nigra in Epstein-Barr virus encephalitis. *Movement Disorders*, 27(1), 156–157. <https://doi.org/10.1002/mds.23935>
- Harris, S. A., & Harris, E. A. (2015). Herpes Simplex Virus Type 1 and Other Pathogens are Key Causative Factors in Sporadic Alzheimer's Disease. *Journal of Alzheimer's Disease: JAD*, 48(2), 319–353. <https://doi.org/10.3233/JAD-142853>
- Hassani, A., Corboy, J. R., Al-Salam, S., & Khan, G. (2018). Epstein-Barr virus is present in the brain of most cases of multiple sclerosis and may engage more than just B cells. *PLoS One; San Francisco*, 13(2), e0192109. <http://dx.doi.org/10.1371/journal.pone.0192109>
- Hassani, A., Reguraman, N., Shehab, S., & Khan, G. (2021). Primary Peripheral Epstein-Barr Virus Infection Can Lead to CNS Infection and Neuroinflammation in a Rabbit Model: Implications for Multiple Sclerosis Pathogenesis. *Frontiers in Immunology*, 12, 764937. <https://doi.org/10.3389/fimmu.2021.764937>
- Hung, C.-H., Chen, L.-W., Wang, W.-H., Chang, P.-J., Chiu, Y.-F., Hung, C.-C., Lin, Y.-J., Liou, J.-Y., Tsai, W.-J., Hung, C.-L., & Liu, S.-T. (2014). Regulation of Autophagic Activation by Rta of Epstein-Barr Virus via the Extracellular Signal-Regulated Kinase Pathway. *Journal of Virology*, 88(20), 12133–12145. <https://doi.org/10.1128/JVI.02033-14>

- lizasa, H., Nanbo, A., Nishikawa, J., Jinushi, M., & Yoshiyama, H. (2012). Epstein-Barr Virus (EBV)-associated Gastric Carcinoma. *Viruses*, 4(12), 3420–3439.
<https://doi.org/10.3390/v4123420>
- Jangra, S., Yuen, K.-S., Botelho, M. G., & Jin, D.-Y. (2019). Epstein–Barr Virus and Innate Immunity: Friends or Foes? *Microorganisms*, 7(6), 183.
<https://doi.org/10.3390/microorganisms7060183>
- Jha, H. C., Mehta, D., Lu, J., El-Naccache, D., Shukla, S. K., Kovacsics, C., Kolson, D., & Robertson, E. S. (2015). Gammaherpesvirus Infection of Human Neuronal Cells. *MBio*, 6(6), e01844-15. <https://doi.org/10.1128/mBio.01844-15>
- Jha, H. C., Pei, Y., & Robertson, E. S. (2016). Epstein–Barr Virus: Diseases Linked to Infection and Transformation. *Frontiers in Microbiology*, 7.
<https://www.frontiersin.org/article/10.3389/fmicb.2016.01602>
- Johansen, T., & Lamark, T. (2011). Selective autophagy mediated by autophagic adapter proteins. *Autophagy*, 7(3), 279–296. <https://doi.org/10.4161/auto.7.3.14487>
- Johansson, P., Jansson, A., Rüetschi, U., & Rymo, L. (2010). The p38 Signaling Pathway Upregulates Expression of the Epstein-Barr Virus LMP1 Oncogene. *Journal of Virology*, 84(6), 2787–2797. <https://doi.org/10.1128/JVI.01052-09>
- Kelley, N., Jeltema, D., Duan, Y., & He, Y. (2019). The NLRP3 Inflammasome: An Overview of Mechanisms of Activation and Regulation. *International Journal of Molecular Sciences*, 20(13), 3328. <https://doi.org/10.3390/ijms20133328>
- Kim, G. H., Kim, J. E., Rhie, S. J., & Yoon, S. (2015). The Role of Oxidative Stress in Neurodegenerative Diseases. *Experimental Neurobiology*, 24(4), 325–340.
<https://doi.org/10.5607/en.2015.24.4.325>
- Kim, S. Y., Choe, K.-W., Park, S., Yoon, D., Ock, C.-Y., Hong, S. W., & Heo, J. Y. (2016). Mild form of Guillain-Barré syndrome in a patient with primary Epstein-Barr virus infection.

The Korean Journal of Internal Medicine, 31(6), 1191–1193.

<https://doi.org/10.3904/kjim.2015.033>

Kimura, T., Jain, A., Choi, S. W., Mandell, M. A., Schroder, K., Johansen, T., & Deretic, V. (2015). TRIM-mediated precision autophagy targets cytoplasmic regulators of innate immunity. *Journal of Cell Biology*, 210(6), 973–989.

<https://doi.org/10.1083/jcb.201503023>

Kimura, T., Mandell, M., & Deretic, V. (2016). Precision autophagy directed by receptor regulators – emerging examples within the TRIM family. *Journal of Cell Science*, 129(5), 881–891. <https://doi.org/10.1242/jcs.163758>

Klionsky, D. J., Abdelmohsen, K., Abe, A., Abedin, M. J., Abeliovich, H., Acevedo Arozena, A., Adachi, H., Adams, C. M., Adams, P. D., Adeli, K., Adhietty, P. J., Adler, S. G., Agam, G., Agarwal, R., Aghi, M. K., Agnello, M., Agostinis, P., Aguilar, P. V., Aguirre-Ghiso, J., ... Zughair, S. M. (2016). Guidelines for the use and interpretation of assays for monitoring autophagy (3rd edition). *Autophagy*, 12(1), 1–222.

<https://doi.org/10.1080/15548627.2015.1100356>

Koganti, S., Clark, C., Zhi, J., Li, X., Chen, E. I., Chakraborty, S., Hill, E. R., & Bhaduri-McIntosh, S. (2015). Cellular STAT3 Functions via PCBP2 To Restrain Epstein-Barr Virus Lytic Activation in B Lymphocytes. *Journal of Virology*, 89(9), 5002–5011.

<https://doi.org/10.1128/JVI.00121-15>

Korecka, J. A., Kesteren, R. E. van, Blaas, E., Spitzer, S. O., Kamstra, J. H., Smit, A. B., Swaab, D. F., Verhaagen, J., & Bossers, K. (2013). Phenotypic Characterization of Retinoic Acid Differentiated SH-SY5Y Cells by Transcriptional Profiling. *PLOS ONE*, 8(5), e63862. <https://doi.org/10.1371/journal.pone.0063862>

- Kovalevich, J., & Langford, D. (2013). Considerations for the use of SH-SY5Y neuroblastoma cells in neurobiology. *Methods in Molecular Biology (Clifton, N.J.)*, 1078, 9–21.
https://doi.org/10.1007/978-1-62703-640-5_2
- Koyuncu, O. O., Hogue, I. B., & Enquist, L. W. (2013). Virus Infections in the Nervous System. *Cell Host & Microbe*, 13(4), 379–393. <https://doi.org/10.1016/j.chom.2013.03.010>
- Kramarow, E. A., & Tejada-Vera, B. (2019). Dementia Mortality in the United States, 2000-2017. *National Vital Statistics Reports: From the Centers for Disease Control and Prevention, National Center for Health Statistics, National Vital Statistics System*, 68(2), 1–29.
- LaJeunesse, D. R., Brooks, K., & Adamson, A. L. (2005). Epstein–Barr virus immediate-early proteins BZLF1 and BRLF1 alter mitochondrial morphology during lytic replication. *Biochemical and Biophysical Research Communications*, 333(2), 438–442.
<https://doi.org/10.1016/j.bbrc.2005.05.120>
- Lan, A., Chen, J., Zhao, Y., Chai, Z., & Hu, Y. (2017). MTOR Signaling in Parkinson’s Disease. *NeuroMolecular Medicine*, 19(1), 1–10. <https://doi.org/10.1007/s12017-016-8417-7>
- Lane, C. A., Hardy, J., & Schott, J. M. (2018). Alzheimer’s disease. *European Journal of Neurology*, 25(1), 59–70. <https://doi.org/10.1111/ene.13439>
- Langston, J. W. (n.d.). The MPTP Story. *Journal of Parkinson’s Disease*, 7(Suppl 1), S11–S22.
<https://doi.org/10.3233/JPD-179006>
- Lee, Y.-H., Chiu, Y.-F., Wang, W.-H., Chang, L.-K., & Liu, S.-T. 2008. (n.d.). Activation of the ERK signal transduction pathway by Epstein–Barr virus immediate-early protein Rta. *Journal of General Virology*, 89(10), 2437–2446.
<https://doi.org/10.1099/vir.0.2008/003897-0>
- Lewy Body—An overview | ScienceDirect Topics*. (n.d.). Retrieved March 18, 2019, from <https://www.sciencedirect.com/topics/neuroscience/lewy-body>

- Li, X., & Bhaduri-McIntosh, S. (2016). A Central Role for STAT3 in Gammaherpesvirus-Life Cycle and -Diseases. *Frontiers in Microbiology*, 7, 1052.
<https://doi.org/10.3389/fmicb.2016.01052>
- Liang, J., Wang, Q., Li, J.-Q., Guo, T., & Yu, D. (2020). Long non-coding RNA MEG3 promotes cerebral ischemia-reperfusion injury through increasing pyroptosis by targeting miR-485/AIM2 axis. *Experimental Neurology*, 325, 113139.
<https://doi.org/10.1016/j.expneurol.2019.113139>
- Liu, Q., Zhang, D., Hu, D., Zhou, X., & Zhou, Y. (2018). The role of mitochondria in NLRP3 inflammasome activation. *Molecular Immunology*, 103, 115–124.
<https://doi.org/10.1016/j.molimm.2018.09.010>
- Liu, X., Tang, J., Wang, M., Ma, Q., & Wang, Y. (2013). Visual Detection and Evaluation of Latent and Lytic Gene Expression during Epstein-Barr Virus Infection Using One-Step Reverse Transcription Loop-Mediated Isothermal Amplification. *International Journal of Molecular Sciences*, 14(12), 23922–23940. <https://doi.org/10.3390/ijms141223922>
- Lopes, F. M., Schröder, R., da Frota, M. L. C., Zanotto-Filho, A., Müller, C. B., Pires, A. S., Meurer, R. T., Colpo, G. D., Gelain, D. P., Kapczinski, F., Moreira, J. C. F., Fernandes, M. da C., & Klamt, F. (2010). Comparison between proliferative and neuron-like SH-SY5Y cells as an in vitro model for Parkinson disease studies. *Brain Research*, 1337, 85–94. <https://doi.org/10.1016/j.brainres.2010.03.102>
- Louveau, A., Herz, J., Alme, M. N., Salvador, A. F., Dong, M. Q., Viar, K. E., Herod, G., Knopp, J., Setliff, J., Lupi, A. L., Mesquita, S. D., Frost, E. L., Gaultier, A., Harris, T. H., Cao, R., Hu, S., Lukens, J. R., Smirnov, I., Overall, C. C., ... Kipnis, J. (2018). CNS lymphatic drainage and neuroinflammation are regulated by meningeal lymphatic vasculature. *Nature Neuroscience*, 21(10), 1380–1391. <https://doi.org/10.1038/s41593-018-0227-9>

- Louveau, A., Smirnov, I., Keyes, T. J., Eccles, J. D., Rouhani, S. J., Peske, J. D., Derecki, N. C., Castle, D., Mandell, J. W., Kevin, S. L., Harris, T. H., & Kipnis, J. (2015). Structural and functional features of central nervous system lymphatics. *Nature*, *523*(7560), 337–341. <https://doi.org/10.1038/nature14432>
- Luo, J., Manning, B. D., & Cantley, L. C. (2003). Targeting the PI3K-Akt pathway in human cancer: Rationale and promise. *Cancer Cell*, *4*(4), 257–262. [https://doi.org/10.1016/S1535-6108\(03\)00248-4](https://doi.org/10.1016/S1535-6108(03)00248-4)
- Luo, Y., Liu, Y., Wang, C., & Gan, R. (2021). Signaling pathways of EBV-induced oncogenesis. *Cancer Cell International*, *21*(1), 93. <https://doi.org/10.1186/s12935-021-01793-3>
- MacAskill, A. F., & Kittler, J. T. (2010). Control of mitochondrial transport and localization in neurons. *Trends in Cell Biology*, *20*(2), 102–112. <https://doi.org/10.1016/j.tcb.2009.11.002>
- Maiti, P., Manna, J., & Dunbar, G. L. (2017). Current understanding of the molecular mechanisms in Parkinson's disease: Targets for potential treatments. *Translational Neurodegeneration*, *6*, 28. <https://doi.org/10.1186/s40035-017-0099-z>
- Mangold, C. A., & Szpara, M. L. (2019). Persistent Infection with Herpes Simplex Virus 1 and Alzheimer's Disease-A Call to Study How Variability in Both Virus and Host may Impact Disease. *Viruses*, *11*(10). <https://doi.org/10.3390/v11100966>
- Martinez, O. M. (2010). The Biology of Epstein—Barr Virus and Posttransplant Lymphoproliferative Disease. In V. R. Dharnidharka, M. Green, & S. A. Webber (Eds.), *Post-Transplant Lymphoproliferative Disorders* (pp. 29–43). Springer Berlin Heidelberg. https://doi.org/10.1007/978-3-642-01653-0_4
- Menet, A., Speth, C., Larcher, C., Proding, W. M., Schwendinger, M. G., Chan, P., Jäger, M., Schwarzmann, F., Recheis, H., Fontaine, M., & Dierich, M. P. (1999). Epstein-Barr Virus Infection of Human Astrocyte Cell Lines. *Journal of Virology*, *73*(9), 7722–7733.

- Modified Hirt Procedure for Rapid Purification of Extrachromosomal DNA from Mammalian Cells.* (n.d.). <https://doi.org/10.2144/98245bm14>
- Montani, M. S. G., Santarelli, R., Granato, M., Gonnella, R., Torrisi, M. R., Faggioni, A., & Cirone, M. (2019). EBV reduces autophagy, intracellular ROS and mitochondria to impair monocyte survival and differentiation. *Autophagy*, *15*(4), 652–667.
<https://doi.org/10.1080/15548627.2018.1536530>
- Moreno, M. A., Or-Geva, N., Aftab, B. T., Khanna, R., Croze, E., Steinman, L., & Han, M. H. (2018). Molecular signature of Epstein-Barr virus infection in MS brain lesions. *Neurology® Neuroimmunology & Neuroinflammation*, *5*(4).
<https://doi.org/10.1212/NXI.0000000000000466>
- Murakami, Y., Ito, M., & Ohsawa, I. (2017). Molecular hydrogen protects against oxidative stress-induced SH-SY5Y neuroblastoma cell death through the process of mitohormesis. *PLoS ONE*, *12*(5). <https://doi.org/10.1371/journal.pone.0176992>
- Neurodegenerative Diseases.* (n.d.). National Institute of Environmental Health Sciences. Retrieved February 3, 2020, from <https://www.niehs.nih.gov/research/supported/health/neurodegenerative/index.cfm>
- Pan, X., Kaminga, A. C., Wen, S. W., Wu, X., Acheampong, K., & Liu, A. (2019). Dopamine and Dopamine Receptors in Alzheimer's Disease: A Systematic Review and Network Meta-Analysis. *Frontiers in Aging Neuroscience*, *11*.
<https://www.frontiersin.org/article/10.3389/fnagi.2019.00175>
- Parzych, K. R., & Klionsky, D. J. (2014). An Overview of Autophagy: Morphology, Mechanism, and Regulation. *Antioxidants & Redox Signaling*, *20*(3), 460–473.
<https://doi.org/10.1089/ars.2013.5371>

- Pedneault, L., Katz, B. Z., & Miller, G. (1992). Detection of Epstein-Barr virus in the brain by the polymerase chain reaction. *Annals of Neurology*, 32(2), 184–192.
<https://doi.org/10.1002/ana.410320210>
- Peluffo, H., González, P., Arís, A., Acarin, L., Saura, J., Villaverde, A., Castellano, B., & González, B. (2007). RGD domains neuroprotect the immature brain by a glial-dependent mechanism. *Annals of Neurology*, 62(3), 251–261.
<https://doi.org/10.1002/ana.21170>
- Pender, M. P. (2011). The Essential Role of Epstein-Barr Virus in the Pathogenesis of Multiple Sclerosis. *The Neuroscientist*, 17(4), 351–367.
<https://doi.org/10.1177/1073858410381531>
- Pezzini, F., Bettinetti, L., Leva, F. D., Bianchi, M., Zoratti, E., Carrozzo, R., Santorelli, F. M., Delledonne, M., Lalowski, M., & Simonati, A. (2017). Transcriptomic Profiling Discloses Molecular and Cellular Events Related to Neuronal Differentiation in SH-SY5Y Neuroblastoma Cells. *Cellular and Molecular Neurobiology*, 37(4), 665–682.
<https://doi.org/10.1007/s10571-016-0403-y>
- Raab-Traub, N. (2015). Nasopharyngeal Carcinoma: An Evolving Role for the Epstein–Barr Virus. In C. Münz (Ed.), *Epstein Barr Virus Volume 1: One Herpes Virus: Many Diseases* (pp. 339–363). Springer International Publishing. https://doi.org/10.1007/978-3-319-22822-8_14
- Ray, P. D., Huang, B.-W., & Tsuji, Y. (2012). Reactive oxygen species (ROS) homeostasis and redox regulation in cellular signaling. *Cellular Signalling*, 24(5), 981–990.
<https://doi.org/10.1016/j.cellsig.2012.01.008>
- Rcom-H'cheo-Gauthier, A. N., Meedeniya, A. C. B., & Pountney, D. L. (2017). Calcipotriol inhibits α -synuclein aggregation in SH-SY5Y neuroblastoma cells by a Calbindin-D28k-

- dependent mechanism. *Journal of Neurochemistry*, 141(2), 263–274.
<https://doi.org/10.1111/jnc.13971>
- Riel, D. van, Verdijk, R., & Kuiken, T. (2015). The olfactory nerve: A shortcut for influenza and other viral diseases into the central nervous system. *The Journal of Pathology*, 235(2), 277–287. <https://doi.org/10.1002/path.4461>
- Rietdijk, C. D., Perez-Pardo, P., Garssen, J., van Wezel, R. J. A., & Kraneveld, A. D. (2017). Exploring Braak's Hypothesis of Parkinson's Disease. *Frontiers in Neurology*, 8.
<https://doi.org/10.3389/fneur.2017.00037>
- Ringheim, G. E., & Conant, K. (2004). Neurodegenerative disease and the neuroimmune axis (Alzheimer's and Parkinson's disease, and viral infections). *Journal of Neuroimmunology*, 147(1), 43–49. <https://doi.org/10.1016/j.jneuroim.2003.10.013>
- Rivero-Ríos, P., Madero-Pérez, J., Fernández, B., & Hilfiker, S. (2016). Targeting the Autophagy/Lysosomal Degradation Pathway in Parkinson's Disease. *Current Neuropharmacology*, 14(3), 238–249.
- Roselli, F., Russo, I., Fraddosio, A., Aniello, M. S., Mari, M. D., Lamberti, P., Livrea, P., & Defazio, G. (2006). Reversible Parkinsonian syndrome associated with anti-neuronal antibodies in acute EBV encephalitis: A case report. *Parkinsonism & Related Disorders*, 12(4), 257–260. <https://doi.org/10.1016/j.parkreldis.2005.11.004>
- Schieber, M., & Chandel, N. S. (2014). ROS Function in Redox Signaling and Oxidative Stress. *Current Biology*, 24(10), R453–R462. <https://doi.org/10.1016/j.cub.2014.03.034>
- Sherer, T. B., Betarbet, R., & Greenamyre, J. T. (2002). Environment, Mitochondria, and Parkinson's Disease. *The Neuroscientist*, 8(3), 192–197.
<https://doi.org/10.1177/1073858402008003004>
- Shim, S.-M., Cheon, H.-S., Jo, C., Koh, Y. H., Song, J., & Jeon, J.-P. (2017). Elevated Epstein-Barr Virus Antibody Level is Associated with Cognitive Decline in the Korean Elderly.

- Journal of Alzheimer's Disease: JAD*, 55(1), 293–301. <https://doi.org/10.3233/JAD-160563>
- Shintani, T., & Klionsky, D. J. (2004). Autophagy in Health and Disease: A Double-Edged Sword. *Science (New York, N.Y.)*, 306(5698), 990–995.
<https://doi.org/10.1126/science.1099993>
- Shiple, M. M., Mangold, C. A., Kony, C. V., & Szpara, M. L. (2017). Differentiated Human SH-SY5Y Cells Provide a Reductionist Model of Herpes Simplex Virus 1 Neurotropism. *Journal of Virology*, 91(23). <https://doi.org/10.1128/JVI.00958-17>
- Shiple, M. M., Mangold, C. A., & Szpara, M. L. (2016). Differentiation of the SH-SY5Y Human Neuroblastoma Cell Line. *Journal of Visualized Experiments : JoVE*, 108.
<https://doi.org/10.3791/53193>
- Singh, H., Koury, J., & Kaul, M. (2021). Innate Immune Sensing of Viruses and Its Consequences for the Central Nervous System. *Viruses*, 13(2), 170.
<https://doi.org/10.3390/v13020170>
- Sochocka, M., Zwolińska, K., & Leszek, J. (2017). The Infectious Etiology of Alzheimer's Disease. *Current Neuropharmacology*, 15(7), 996–1009.
<https://doi.org/10.2174/1570159X15666170313122937>
- Soldan, S. S., & Lieberman, P. M. (2020). Epstein-Barr virus infection in the development of neurological disorders. *Drug Discovery Today: Disease Models*.
<https://doi.org/10.1016/j.ddmod.2020.01.001>
- Speck, P., & Longnecker, R. (1999). Epstein-Barr virus (EBV) infection visualized by EGFP expression demonstrates dependence on known mediators of EBV entry. *Archives of Virology*, 144(6), 1123–1137. <https://doi.org/10.1007/s007050050574>
- Statistics*. (2017, October 13). Parkinson's Foundation.
<http://www.parkinson.org/Understanding-Parkinsons/Causes-and-Statistics/Statistics>

- Stephenson, J., Nutma, E., van der Valk, P., & Amor, S. (2018). Inflammation in CNS neurodegenerative diseases. *Immunology*, *154*(2), 204–219.
<https://doi.org/10.1111/imm.12922>
- Storch, A., Kaftan, A., Burkhardt, K., & Schwarz, J. (2000). 6-Hydroxydopamine toxicity towards human SH-SY5Y dopaminergic neuroblastoma cells: Independent of mitochondrial energy metabolism. *Journal of Neural Transmission*, *107*(3), 0281–0293.
<https://doi.org/10.1007/s007020050023>
- Thorley-Lawson, D. A. (2015). EBV Persistence—Introducing the Virus. In C. Münz (Ed.), *Epstein Barr Virus Volume 1: One Herpes Virus: Many Diseases* (pp. 151–209). Springer International Publishing. https://doi.org/10.1007/978-3-319-22822-8_8
- Torii, Y., Kawada, J., Murata, T., Yoshiyama, H., Kimura, H., & Ito, Y. (2017). Epstein-Barr virus infection-induced inflammasome activation in human monocytes. *PLOS ONE*, *12*(4), e0175053. <https://doi.org/10.1371/journal.pone.0175053>
- Tugizov, S., Herrera, R., Veluppillai, P., Greenspan, J., Greenspan, D., & Palefsky, J. M. (2007). Epstein-Barr Virus (EBV)-Infected Monocytes Facilitate Dissemination of EBV within the Oral Mucosal Epithelium. *Journal of Virology*, *81*(11), 5484–5496.
<https://doi.org/10.1128/JVI.00171-07>
- van der Merwe, C., van Dyk, H. C., Engelbrecht, L., van der Westhuizen, F. H., Kinnear, C., Loos, B., & Barden, S. (2017). Curcumin Rescues a PINK1 Knock Down SH-SY5Y Cellular Model of Parkinson's Disease from Mitochondrial Dysfunction and Cell Death. *Molecular Neurobiology*, *54*(4), 2752–2762. <https://doi.org/10.1007/s12035-016-9843-0>
- Volpicelli-Daley, L. A., Luk, K. C., Patel, T. P., Tanik, S. A., Riddle, D. M., Stieber, A., Meaney, D. F., Trojanowski, J. Q., & Lee, V. M.-Y. (2011). Exogenous α -Synuclein Fibrils Induce Lewy Body Pathology Leading to Synaptic Dysfunction and Neuron Death. *Neuron*, *72*(1), 57–71. <https://doi.org/10.1016/j.neuron.2011.08.033>

- Wang, Y., Branicky, R., Noë, A., & Hekimi, S. (2018). Superoxide dismutases: Dual roles in controlling ROS damage and regulating ROS signaling. *The Journal of Cell Biology*, 217(6), 1915–1928. <https://doi.org/10.1083/jcb.201708007>
- Warren-Gash, C., Forbes, H. J., Williamson, E., Breuer, J., Hayward, A. C., Mavrodaris, A., Ridha, B. H., Rossor, M. N., Thomas, S. L., & Smeeth, L. (2019). Human herpesvirus infections and dementia or mild cognitive impairment: A systematic review and meta-analysis. *Scientific Reports*, 9(1), 1–10. <https://doi.org/10.1038/s41598-019-41218-w>
- White, M. R., Kandel, R., Tripathi, S., Condon, D., Qi, L., Taubenberger, J., & Hartshorn, K. L. (2014). Alzheimer's associated β -amyloid protein inhibits influenza A virus and modulates viral interactions with phagocytes. *PloS One*, 9(7), e101364. <https://doi.org/10.1371/journal.pone.0101364>
- Woulfe, J., Gray, M. T., Ganesh, M. S., & Middeldorp, J. M. (2016). Human serum antibodies against EBV latent membrane protein 1 cross-react with α -synuclein. *Neurology - Neuroimmunology Neuroinflammation*, 3(4), e239. <https://doi.org/10.1212/NXI.0000000000000239>
- Woulfe, J. M., Gray, M. T., Gray, D. A., Munoz, D. G., & Middeldorp, J. M. (2014). Hypothesis: A role for EBV-induced molecular mimicry in Parkinson's disease. *Parkinsonism & Related Disorders*, 20(7), 685–694. <https://doi.org/10.1016/j.parkreldis.2014.02.031>
- Xie, H., Hu, L., & Li, G. (2010). SH-SY5Y human neuroblastoma cell line: in vitro cell model of dopaminergic neurons in Parkinson's disease. *Chinese Medical Journal*, 123(8), 1086–1092. <https://doi.org/10.3760/cma.j.issn.0366-6999.2010.08.021>
- Yan, M. H., Wang, X., & Zhu, X. (2013). Mitochondrial defects and oxidative stress in Alzheimer disease and Parkinson disease. *Free Radical Biology & Medicine*, 62, 90–101. <https://doi.org/10.1016/j.freeradbiomed.2012.11.014>

- Young, L. S., Arrand, J. R., & Murray, P. G. (2007). EBV gene expression and regulation. In A. Arvin, G. Campadelli-Fiume, E. Mocarski, P. S. Moore, B. Roizman, R. Whitley, & K. Yamanishi (Eds.), *Human Herpesviruses: Biology, Therapy, and Immunoprophylaxis*. Cambridge University Press. <http://www.ncbi.nlm.nih.gov/books/NBK47431/>
- Yuan, J., Cahir-McFarland, E., Zhao, B., & Kieff, E. (2006). Virus and Cell RNAs Expressed during Epstein-Barr Virus Replication. *Journal of Virology*, *80*(5), 2548–2565. <https://doi.org/10.1128/JVI.80.5.2548-2565.2006>
- Zhao, C., & Zhao, W. (2020). NLRP3 Inflammasome—A Key Player in Antiviral Responses. *Frontiers in Immunology*, *11*, 211. <https://doi.org/10.3389/fimmu.2020.00211>
- Zhao, Y., Hu, X., Liu, Y., Dong, S., Wen, Z., He, W., Zhang, S., Huang, Q., & Shi, M. (2017). ROS signaling under metabolic stress: Cross-talk between AMPK and AKT pathway. *Molecular Cancer*, *16*(1), 79. <https://doi.org/10.1186/s12943-017-0648-1>
- Zorov, D. B., Juhaszova, M., & Sollott, S. J. (2014). Mitochondrial Reactive Oxygen Species (ROS) and ROS-Induced ROS Release. *Physiological Reviews*, *94*(3), 909–950. <https://doi.org/10.1152/physrev.00026.2013>
- Zorova, L. D., Popkov, V. A., Plotnikov, E. Y., Silachev, D. N., Pevzner, I. B., Jankauskas, S. S., Babenko, V. A., Zorov, S. D., Balakireva, A. V., Juhaszova, M., Sollott, S. J., & Zorov, D. B. (2018). Mitochondrial membrane potential. *Analytical Biochemistry*, *552*, 50–59. <https://doi.org/10.1016/j.ab.2017.07.009>